



Technische Universität München

Lehrstuhl für Entwicklungsgenetik

Translational strategies to address Parkinson's disease

Marina Theodorou

Vollständiger Abdruck der von der Fakultät Wissenschaftszentrum Weihenstephan für Ernährung, Landnutzung und Umwelt der Technischen Universität München zur Erlangung des akademischen Grades eines

Doktors den Naturwissenschaften

genehmigten Dissertation.

Vorsitzender: Univ.-Prof. Dr. K. Schneitz

Prüfer der Dissertation: 1. Univ.-Prof. Dr. W. Wurst

2. Univ.-Prof. A. Schnieke, PhD

Die Dissertation wurde am 06.05.2015 bei der Technischen Universität München eingereicht und durch die Fakultät Wissenschaftszentrum Weihenstephan für Ernährung, Landnutzung und Umwelt am 16.09.2015 angenommen.

Table of contents

Table of contents.....	2
1. Abstract	6
2. Introduction.....	8
2.1 Neurodegenerative diseases	8
2.2 Parkinson’s disease.....	9
2.3 Dopaminergic neurons: development and function	10
2.4 Risk factors & mechanisms of Parkinson’s disease pathogenesis.....	16
2.5 Current therapeutic approaches	18
2.6 Future therapeutic directions.....	21
2.6.1 Programming: Directed differentiation of embryonic stem cells to dopaminergic neurons.....	22
2.6.2 Pluripotency reprogramming: Conversion of induced pluripotent stem cells to dopaminergic neurons	25
2.6.3 In vitro lineage reprogramming: Conversion of somatic cells to dopaminergic neurons.....	25
2.7 In vivo lineage reprogramming: Conversion of somatic cells to neurons	29
3. Aim of the study	31
4. Results	32
4.1 In vitro programming of embryonic stem cells to dopaminergic neurons.....	32
4.1.1 Transcription factor combinations for directed differentiation of embryonic stem cells to dopaminergic neurons	32
4.1.2 Recombinase-mediated cassette exchange in the <i>Sox1</i> locus for the generation of genetically engineered embryonic stem cells	34
4.1.3 Induction of the <i>Sox1</i> promoter and the downstream transcription factors.....	39
4.1.4 Neuronal differentiation protocols for in vitro conversion of the <i>Sox1</i> targeted embryonic stem cell lines to dopaminergic neurons	42
4.1.4.1 Monolayer neuronal differentiation protocol with retinoic acid.....	42
4.1.4.2 Embryoid body-based neuronal differentiation protocol with retinoic acid ..	44
4.1.4.3 Monolayer neuronal differentiation protocol without retinoic acid and with the supplementation of forskolin.....	46
4.2 In vivo reprogramming to dopaminergic neurons	48
4.2.1 Targeting the <i>Rosa26</i> locus in murine embryonic stem cells.....	49
4.2.2 MLN and MLNPTe induction in vitro	53
4.2.3 Generation of a <i>Rosa26</i> ^{CAG:MLN/+} knock-in mouse line	61

4.2.4	In vivo reprogramming in different tissues	63
4.2.4.1	Expression of MLN in midbrain and hindbrain regions	63
4.2.4.2	Controlled expression of MLN in astrocytes	67
4.2.4.3	Controlled expression of MLN in pericytes	73
4.2.4.4	Expression of MLN in neuronal progenitors.....	80
4.2.4.5	Expression of MLN in all tissues	83
4.2.5	In vitro activation and reprogramming potential of <i>Rosa26</i> ^{CAG:MLN/+} mouse embryonic fibroblasts.....	83
4.2.6	MLN expression induces endoplasmic-reticulum stress and the unfolded protein response	85
4.2.7	Brain injury does not influence the activation and reprogramming potential of the CAG MLN transgene in vivo	93
5.	Discussion	95
5.1	Targeting vectors versus viral infection for the overexpression of multiple genes	96
5.2	Differentiation of embryonic stem cells by targeted overexpression of transcription factors.....	97
5.2.1	Recombinase-mediated cassette exchange in the <i>Sox1</i> locus for targeted overexpression creates an artificially inducible system	98
5.2.2	<i>Ngn2</i> and <i>Lmx1b</i> simultaneous overexpression generates dopaminergic neurons from embryonic stem cells	98
5.2.3	How can the differentiation efficiency be improved?.....	100
5.2.4	Differentiation of embryonic stem cells by targeted overexpression of transcription factors: concluding remarks	102
5.3	In vivo reprogramming to dopaminergic neurons	102
5.3.1	Utilization of a genetic mouse model for conditional overexpression of three reprogramming TFs	103
5.3.2	Technical limitations of the reprogramming in the <i>Rosa26</i> ^{CAG:MLN/+} mouse line ..	105
5.3.3	Biological limitations of reprogramming in the <i>Rosa26</i> ^{CAG:MLN/+} mouse line	109
5.3.4	In vivo reprogramming to dopaminergic neurons: how can future strategies be improved?.....	111
5.3.5	In vivo reprogramming to dopaminergic neurons: concluding remarks.....	113
6.	Materials and Methods	114
6.1	Molecular biology	114
6.1.1	Genomic DNA isolation.....	114
6.1.1.1	NaOH extraction	114
6.1.1.2	Extraction using the Promega Wizard genomic DNA purification kit.....	114

6.1.1.3 Phenol-Chloroform extraction	114
6.1.2 Plasmid DNA isolation	115
6.1.2.1 Small scale plasmid DNA isolation (Mini Prep).....	115
6.1.2.2 Large scale plasmid DNA isolation (Maxi Prep).....	115
6.1.2.3 Plasmid DNA isolation from yeast cells	115
6.1.3 DNA extraction from agarose gel	116
6.1.4 Polymerase Chain Reaction	116
6.1.4.1 Short PCR for genotyping of cells or mice	116
6.1.4.2 Long Range PCR for genotyping of cells or mice	117
6.1.4.3 Bacterial/Yeast colony PCR.....	118
6.1.5 Southern blotting	118
6.1.6 Restriction digests	119
6.1.7 Agarose gel electrophoresis	119
6.1.8 Molecular cloning	120
6.1.8.1 Cloning with DNA ligase	120
6.1.8.2 In-Fusion cloning	120
6.1.8.3 Yeast cloning and transformation	120
6.1.9 Bacterial transformation	121
6.1.9.1 Transformation of chemical competent bacteria	121
6.1.9.2 Transformation of electrocompetent bacteria	121
6.1.10 DNA sequencing	122
6.1.10.1 Big Dye DNA sequencing	122
6.1.10.2 DNA sequencing by GATC Biotech.....	123
6.1.11 In vitro Cre-mediated recombination.....	123
6.1.12 RNA extraction.....	123
6.1.13 Reverse transcription	123
6.1.14 Primer design for quantitative PCR analysis.....	123
6.1.15 Quantitative Real Time PCR.....	124
6.1.16 Western blotting	124
6.1.17 Luciferase assays	125
6.2 Cellular biology	125
6.2.1 Cell culture.....	125
6.2.1.1 Embryonic stem cell culture	125
6.2.1.2 Isolation and cell culture of primary mouse embryonic fibroblasts	126

6.2.1.3 Freezing and thawing of cells	127
6.2.1.4 Metaphase chromosome counting	127
6.2.2 Transfection	128
6.2.2.1 Electroporation	128
6.2.2.2 Lipofection	128
6.2.2.3 Nucleofection	128
6.2.3 Neuronal differentiation and reprogramming	129
6.2.3.1 Monolayer neuronal differentiation	129
6.2.3.2 EB-based neuronal differentiation	129
6.2.3.3 In vitro reprogramming of mouse embryonic fibroblasts	129
6.2.4 Immunocytochemistry	130
6.2.5 Flow cytometry	130
6.3 Histology	131
6.3.1 Whole body perfusion fixation of mice	131
6.3.2 Cryosectioning	131
6.3.3 Hematoxylin-Eosin staining	131
6.3.4 TUNEL assay	132
6.3.5 Immunohistochemistry	132
6.4 Mouse genetics and colony maintenance	132
6.4.1 Blastocyst injections and embryo transfer	132
6.4.2 Generation of the <i>Rosa26</i> ^{CAG:MLN/+} mouse line	133
6.4.3 Mouse facility	133
6.4.4 Stab wound lesion	133
6.5 Statistical analysis	134
6.6 Materials	134
6.7 Equipment	137
6.8 Buffers, media, solutions	138
6.9 Antibodies	141
6.10 Primers & other sequences	142
7. Literature	149
8. Acknowledgements	183

1. Abstract

Parkinson's disease is one of the major neurodegenerative disorders. The main hallmark of the disease is the death of midbrain dopaminergic neurons in the substantia nigra. The replenishment of these lost neurons has long been attempted mainly by the differentiation of pluripotent stem cells. Quite recently a new method was developed, the direct reprogramming of somatic cells to dopaminergic neurons.

In this study both methods were applied for the *in vitro* as well as the *in vivo* generation of dopaminergic neurons. Ectopic expression of transcription factors involved in the normal development of dopaminergic neurons was intended to specifically guide their formation.

Mouse embryonic stem cells were engineered to express various transcription factor combinations under the control of the endogenous Sox1 promoter and were differentiated *in vitro*. Out of all the combinations tested, the NGN2 and LMX1B combination was the most potent in generating dopaminergic neurons. The observed differentiation efficiency could be improved by the addition of forskolin. The applied differentiation protocol was successful; however we suggest that it may be further improved by the implementation of additional factors, in order to better maintain the differentiating dopaminergic neurons and increase the differentiation efficiency.

For the *in vivo* reprogramming, a Rosa26 knock-in mouse line was generated to conditionally drive MASH1, LMX1A and NURR1 polycistronic expression under the control of a CAG promoter in various cell types/tissues. Unfortunately, *in vivo* reprogramming was not observed in any of the cell types/tissues tested. In some instances adult neurogenesis was abolished, while constant overexpression starting from early embryonic stages led to fetal or neonatal lethality. This was attributed to cell death caused by uncleaved forms of the polycistronic sequence of transcription factors. The polycistronic cassette overexpression triggered apoptosis via endoplasmic reticulum stress. This highlights the importance of considering limitations of

Abstract

the current overexpressing strategies. The in vivo system described here could constitute a valuable tool for in vivo reprogramming to dopaminergic neurons that provides essential information for optimal reprogramming conditions. However, exploring alternatives for optimal overexpression of reprogramming factors in vivo is critical in order for reprogramming attempts to be successful, while future designs should be implemented with additional factors for increased reprogramming efficiencies.

2. Introduction

2.1 Neurodegenerative diseases

The term *neurodegeneration* describes the neuronal death observed in the central nervous system (Jellinger, 2001). Neurodegenerative diseases are common, affecting people of different ages, although most frequently elderly individuals (Hindle, 2010). Some of the most prominent neurodegenerative disorders include Alzheimer's (AD), Parkinson's (PD), Amyotrophic lateral sclerosis (ALS) and Huntington's disease. The factors that lead to neurodegeneration have partially been described, yet the pathogenic etiology of many of these diseases is largely unknown. Therefore, understanding a neurodegenerative disease is a major challenge. Two of the main characteristics of such disorders are 1) progressive development and 2) irreversible neuronal death. Due to lack of understanding of the mechanistic details characterizing neurodegeneration, current treatment schemes only focus on delaying the process and providing symptomatic relief (Young, 2009).

The increase in human life expectancy contributes to the frequent occurrence of neurodegenerative diseases. The increased frequency combined with the fact that there is no available cure raise public concern. Unfortunately, neurodegeneration is diagnosed when it has already progressed to a significant degree. Studying the mechanism by which neurodegenerative diseases occur is thus of pivotal importance and will potentially provide novel therapeutic approaches.

Here, I discuss the history and etiology of PD in order to shed light on the difficulty of its characterization. Moreover, I provide an overview of the current therapeutic schemes, as well as novel methodologies that could be used for developing neuroprotective strategies. Lastly, I focus on innovative approaches for the replenishment of the dying neurons that give hope for treatment to PD patients.

2.2 Parkinson's disease

Parkinson's disease was first described in 1817 by James Parkinson as the "Shaking Palsy". Tremor-related disorders had already been mentioned before (in 1680 and 1768); however James Parkinson was the first one to characterize this as a syndrome of the nervous system (Hurwitz, 2014). The term "Parkinson's disease" was introduced by Jean-Martin Charcot in 1872, who distinguished the disorder from other related diseases with similar symptoms. Gowers in 1888 highlighted the higher prevalence of the disease in the male population. Richer introduced the first images of PD patients and together with Meige, described in more detail the clinical features of the disease (1895). However, no connection to the neurologic etiology had been made until Brissaud reported that PD patients exhibit defects in the substantia nigra, a dark staining deep region of the part of the brain proximal to the hypothalamus (midbrain). Until 1953, there was no complete evidence for the role of midbrain defects in the disease. After the role of midbrain was demonstrated by Greenfield and Bosanquet (Greenfield and Bosanquet, 1953), the PD clinical picture developed further with the introduction of the staging system characterizing the progression of the disease by Hoehn and Yahr in 1967 (Goetz, 2011).

PD is the second most common neurodegenerative disorder after AD (Bertram and Tanzi, 2005). Around 1% of the human population, mainly over the age of 65, is suffering from PD, either the familial (15%) or the sporadic form (85%) (Longo et al., 2013). The major hallmark of the disease is the death of the dopaminergic (DA) neurons in the substantia nigra pars compacta (SNc) of the midbrain, often accompanied by the formation of Lewy bodies. These are structures consisting of aggregated proteins, usually α -synuclein, which is a gene frequently linked with PD (Spillantini et al., 1997).

PD symptoms are mainly movement-related. Tremor, the most prominent symptom, is the trembling of arms, legs and head, which is accompanied by stiffness (rigidity). The latter is also responsible for a frequently observed "mask-like" appearance, characterized by the lack of facial or body gestures, giving the impression of a still image. The patients

display difficulties in initiating or preventing movement and generally move slower (bradykinesia), while they also exhibit shuffling gait and disability in maintaining balance (postural instability) (Jankovic, 2008).

Apart from motor-related symptoms, people experience non-motor symptoms as well, which vary among patients. Olfactory impairment and mood disorders are among the earliest non-motor symptoms observed. Other such symptoms that occur are autonomic dysfunction, weight imbalances, depression, dementia, sensory and sleep difficulties, etc. (Jankovic, 2008).

The diagnosis of PD is usually given after almost 50-60% of all the DA neurons of the SNc have already died, at the time point when the symptoms start to be apparent. Nevertheless, the progression of the disease begins much earlier (Ross et al., 2004). Unfortunately, there is still no way to diagnose PD at this early stage, when treatment would perhaps be more feasible. This fact hampers circumstances in the battle against PD.

2.3 Dopaminergic neurons: development and function

The midbrain is formed as the middle part of the neural tube (mesencephalon). During ectoderm development, the ventral midbrain is generated as coordinated by several signaling pathways. Among these are the Wnt (Wingless-related integration site) and the Shh (Sonic hedgehog) signaling pathways, the interplay between which contribute to the pattern of the whole structure. The constant interaction between these signaling molecules and other genes, in particular transcription factors (TFs), specify the neural precursors to become DA neurons (Hegarty et al., 2013) (Figure 1). Overall, the spatio-temporal expression pattern of all the genes involved in the generation of the ventral DA neurons provides the coordinates for the exact dorso-ventral and anterior-posterior positioning of the new neuronal population. An overview of the roles of some of these genes related to DA neuronal development will next be addressed.

En1 (Engrailed 1)

EN1 expression starts early in embryonic development (around embryonic day 8 [E8]) and is maintained throughout adulthood (Albéri et al., 2004). Apart from other regions (e.g. ectoderm of limbs, spinal cord), it is broadly expressed in the mid-hindbrain intersection, where it is also implicated in the survival of the developing midbrain DA neurons (Wurst, Auerbach, & Joyner, 1994). The *En1* deletion has been associated with PD features, including DA neuronal degeneration and motor symptoms (Sgadò et al., 2006; Veenvliet et al., 2013; Wurst et al., 1994).

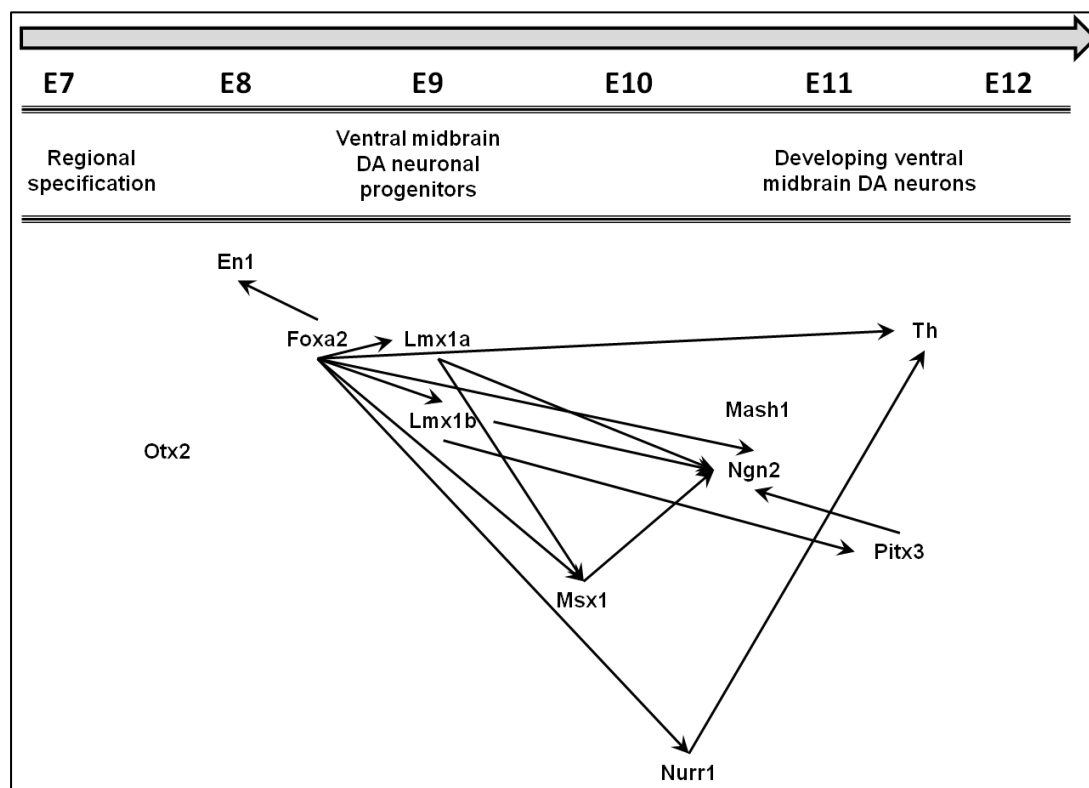


Figure 1: Gene interactions that orchestrate the dopaminergic neurons' development in the ventral midbrain from E7 until E12. Transcription factors which are involved in the differentiation, regional specification and terminal differentiation of dopaminergic neural progenitor cells are intertwined and define the molecular identity of the mature ventral midbrain dopaminergic neuronal population.

E7-E12: Embryonic day 7-12

Foxa2 (Forkhead box A2)

This gene encodes a TF which, often in cooperation with FOXA1, is involved in both induction and maintenance of the DA phenotype (Ferri et al., 2007; Metzakopian et al., 2012; Stott et al., 2013). It has been shown that both genes induce (*En1, Lmx1a, Lmx1b, Msx1, Ngn2, Nurr1*) and inhibit (*Nkx2.2, Megane*) the expression of important genes for the DA neuronal development by directly binding on the promoters of some of them, favoring thus the development of DA neurons over the neighboring GABAergic neurons (Ferri et al., 2007; Lin et al., 2009; Metzakopian et al., 2012). Overexpression of FOXA2 in neural precursor cells (Lee et al., 2010) or ESCs (Chung et al., 2009) together with other DA-specific genes resulted in the generation of functional midbrain DA neurons. By directly regulating the expression of the tyrosine hydroxylase (TH), an enzyme involved in dopamine synthesis (Lin et al., 2009), FOXA2 is of pivotal importance for the acquisition of a mature midbrain DA neuronal phenotype.

Lmx1a (LIM homebox transcription factor 1, alpha)

Lmx1a is a gene required already from the early stages of DA neuronal differentiation (Cai et al., 2009) and is required for the proliferation and specification of DA neurons (Yan et al., 2011). By regulating the expression of genes implicated in cell cycle, it orchestrates the exit of the cell cycle, determining when DA neurons should terminally differentiate (Yan et al., 2011). It has overlapping functions with *Lmx1b*, which in some degree, compensates *Lmx1a*'s role (Chung et al., 2009; Yan et al., 2011). When overexpressed in ESCs, it regulates the expression of all the DA-specific molecules required for the generation of midbrain DA neurons (Cai et al., 2009). Together with *Lmx1b* it acts synergistically with *Foxa1* and *Foxa2* (Lin et al., 2009).

Lmx1b (LIM homebox transcription factor 1, beta)

Lmx1b, apart from its essential role in the development of other neuronal types (Deng et al., 2011), is also important in the initial stages of the differentiation of DA neurons. More specifically, it regulates the expression of *Pitx3*, a gene characteristic of ventral midbrain DA neurons (Smidt et al., 2000). *Lmx1b* cooperates with *Lmx1a* and other essential DA-specific genes (Chung et al., 2009; Lin et al., 2009; Yan et al., 2011).

Mash1 (Ascl1, Achaete-Scute family bHLH transcription factor 1)

Mash1 encodes a proneural basic helix-loop-helix (bHLH) transcription factor, which is expressed in the ventricular zone together with NGN1 and NGN2 (Kele et al., 2006). However it cannot instruct DA neuronal development without the contribution of other DA-specific genes (Park et al., 2006; Parras et al., 2002). It has been shown that, when expressed together with *Nurr1*, it is involved in the determination of mature and functional midbrain DA neurons (Park et al., 2006).

Msx1 (Msh homebox 1)

Msx1 is often considered as one of the various DA-specific genes (Andersson et al., 2006a). It has also been reported to contribute to fates other than the neuronal (Roybon et al., 2008). However, it regulates the expression of *Ngn2* and is activated by *Lmx1a* (Andersson et al., 2006a). Both of these genes are key players in the formation of midbrain DA neurons, a fact which is indicative of its essential role in the DA neuronal development. Moreover, by repressing Nkx6.1, it inhibits the development of motor neurons over the also ventral DA neurons (Andersson et al., 2006a).

Ngn2 (Neurogenin 2)

Ngn2 encodes another bHLH proneural TF, which is known as neuronal activator, required for early and late development of midbrain DA neurons, although only in combination with other DA determinants (Andersson et al., 2007). Its expression has been shown to be closely related and activated by LMX1A, LMX1B, FOXA1, FOXA2, as well as PITX3, by direct binding of the latter (Hong et al., 2014; Yan et al., 2011). Deletion of *Ngn2* results in defective ventral midbrain only in regard to the DA neuronal population, which gets diminished (Andersson et al., 2006b).

Nurr1 (Nr4a2, Nuclear receptor subfamily 4, group a, member 2)

Nurr1 is an essential gene in the DA neuronal development. Partial deletion of the *Nurr1* genomic sequence leads to neuronal degeneration, more specifically reduced numbers of DA neurons, as well as reduced dopamine levels (Kadkhodaei et al., 2009). Mice completely lacking both alleles of the gene die at postnatal day 1 (P1), while heterozygous mice exhibit sensitivity in toxins related to PD and reduced dopamine release (Le et al., 1999; Zetterström et al., 1997). These defects are connected with failure to obtain fully differentiated and mature DA neurons, which is indicative of *Nurr1*'s essential role in the final stages of their development (Saucedo-Cardenas et al., 1998; Witta et al., 2000). In addition, NURR1 directly binds and activates the promoter of *Th* (Kim et al., 2003b) and there is evidence that it also regulates the expression of the dopamine transporter (*DAT*) (Sacchetti et al., 2001), two genes that are characteristic of mature midbrain DA neurons. *NURR1* has been directly connected with PD, in the form of protein levels (Le et al., 2008), or a genetic polymorphism (Zheng et al., 2003).

Otx2 (Orthodenticle homebox 2)

Otx2 is expressed along the anterior-posterior axis of the ventral midbrain (Omodei et al., 2008), where it plays an important role in defining the

neuronal subtype to be generated (Vernay et al., 2005). By repressing *Nkx2.2* (Puelles et al., 2004), it favors the development of midbrain DA neurons over serotonergic neurons (Omodei et al., 2008; Puelles et al., 2004). Its essential contribution in DA neuronal development is demonstrated by the fact that DA precursor cells that lack the *Otx2* gene, fail to activate vital genes for their maturity (i.e. *Lmx1a*, *Msx1*, *Ngn2*, *Mash1*) and never become post-mitotic, fully differentiated DA neurons (Omodei et al., 2008). Apart from its developmental contribution, it has also been shown that *Otx2* protects against PD-related neurotoxins, implying a role in toxin-dependent neurodegeneration (Di Salvio et al., 2010).

Pitx3 (Paired-Like Homeobox 3)

Pitx3 is a gene connected with the survival of the ventral midbrain DA neurons, especially the population of the substantia nigra DA neurons (Luk et al., 2013; van den Munckhof, 2003; Nunes et al., 2003). It has been shown that *Nurr1* closely interacts with and is dependent on *Pitx3* in order to activate the DA phenotype (Jacobs et al., 2009). *Pitx3* has a substantial role in midbrain DA development, revealed by the fact that it directly binds on the promoter of the *Th* gene, defining thus the DA neuronal population (Lebel et al., 2001).

The ventral DA neurons consist of three different subtypes, the A8, A9 and A10. The neuronal subtype affected in PD is the A9, the DA neurons of the SNc. The mature A9 midbrain DA neurons express PITX3 and G-protein-gated inwardly rectifying potassium channel 2 (GIRK2) (Reyes et al., 2012), as well as other DA neuronal markers, i.e. TH, DAT, vesicular monoamine transporter 2 (VMAT2), aldehyde dehydrogenase (ALDH), aromatic l-amino acid decarboxylase (AADC) (Meiser et al., 2013; Qi et al., 2008). They normally project to the striatum, where they release a neurotransmitter called dopamine and control voluntary movement. They respond to new stimuli, but not to repeated ones, except for the cases where reward is following and are

thus implicated in addictive behaviors. Sleep and memory activities are also connected with their function (Ueno et al., 2012).

2.4 Risk factors & mechanisms of Parkinson's disease pathogenesis

PD is the result of genetic predisposition and/or environmental factors (Pan-Montojo and Reichmann, 2014). Their effect is gradual, usually of late onset and often combined, which makes therapy complicated.

Many genes have been linked to the pathogenesis of PD, among which the *PARK* genes have been extensively studied by several research groups (Andres-Mateos et al., 2007; Greene et al., 2005; Plun-Favreau et al., 2007; Shiba-Fukushima et al., 2014) (Table 1). Mutations or deletions of these genes are often responsible for various forms of the disease and can be either dominant (e.g. *LRRK2*) (Park et al., 2013) or recessive (e.g. *DJ-1*) (Lopez and Sidransky, 2010).

Locus	Inheritance	Chromosome	Gene	Name of protein	Protein function
PARK1	AD	4q21-23	<i>SNCA</i>	α -synuclein	Synaptic protein
PARK2	AR	6q25.2-q27	<i>PRKN</i>	Parkin	Ubiquitin-protein ligase
PARK3	AD	2q13	<i>SPR?</i>	Aldo-keto reductase?	Unknown
PARK4	AD	4q21-23	<i>SNCA</i>	α -synuclein	Excess of α -synuclein protein
PARK5	AD	4p14	<i>UCHL1</i>	UCHL-1	Hydrolyze small C-terminal adducts of ubiquitin
PARK6	AR	1p36-p35	<i>PINK1</i>	PINK1	Mitochondrial kinase
PARK7	AR	1p36	<i>DJ-1</i>	DJ-1	Oxidative stress protection
PARK8	AD	12p11-q13	<i>LRRK2</i>	LRRK2	Multiple function by several domains
PARK9	AR	1p36	<i>ATP13A2</i>	ATPase type 13A2	Lysosomal protein
PARK11	AD	2q37.1	<i>GIGYF2?</i>	GRB10 interacting GYF protein 2	Unknown
PARK13	AD?	2p12	<i>OMI/HTRA2</i>	HtrA serine peptidase 2	Serine protease +
PARK14	AR	22q13.1	<i>PLA2G6</i>	A2 phospholipase	Phospholipid remodelling +
PARK15	AR	22q12-q13	<i>FBXO7</i>	F-box protein 7	Phosphorylation dependent ubiquitination

Table 1: Genetic loci implicated in PD (modified from Chung, 2010). The gene name and protein function, as well as chromosomal location and inheritance are also summarized. AD: autosomal dominant, AR: autosomal recessive

Apart from the genetic factors, environmental toxins have also been reported to contribute to the observed PD neurodegeneration (Goldman, 2014; Pan-Montojo and Reichmann, 2014). Maneb, rotenone, paraquat are some of the toxins widely used in pesticides, insecticides and herbicides.

Long and frequent exposure to these toxins can boost a series of unknown molecular events, affecting the mitochondrial function, the processing of oxidized molecules and the protein degradation system of the cell (Malkus et al., 2009).

Little is known about the exact mechanisms that are involved in the pathogenesis of PD, yet a common feature of neurodegeneration is oxidative stress. Throughout life the cells perform a considerable amount of biochemical reactions (metabolism), which result in the generation of reactive oxygen species. In healthy state, antioxidant mechanisms of the cells undertake their removal. In the disease state however, the antioxidant machinery may be impaired, leading to the accumulation of these toxic by-products, which eventually damage DNA, proteins and lipids (Dias et al., 2014).

In the case of PD, oxidative stress can be triggered by mutations in *PARK* genes (e.g. *DJ-1*, *PINK1*, *Parkin*, *LRRK2*, *α -Synuclein*) which are associated with mitochondria (Lesage and Brice, 2009; Malkus et al., 2009). Apart from genes though, most neurotoxins also contribute to several oxidative modifications, which result in the accumulation of toxic products in the dopaminergic cells with detrimental effects on their survival (Goldman, 2014; Malkus et al., 2009).

The DA neurons exhibit a *selective neuronal vulnerability* (SNV) in PD due to the oxidation of dopamine, the characteristic neurotransmitter of this type of neurons. This oxidation results in toxic molecules, like 6-OHDA, with deleterious effects to the neurons. The A9 subtype is more sensitive than the other DA subtypes of the substantia nigra. This could be due to differential gene expression profile of the different subtypes (Wang and Michaelis, 2010). It has been reported that genes which are highly expressed in the A9 subtype, e.g. *GIRK2*, can contribute to the increased vulnerability. By controlling the membrane potential, *GIRK2* may expose the A9 DA neurons to extrinsic toxicity, while the other subtypes lacking *GIRK2* exhibit resistance (Chung et al., 2005a). It is therefore possible that the differential gene expression can

contribute to differential response of the neurons to internal and external toxic stimuli.

Most oxidative defects caused by the genetic background and/or environmental factors trigger mitochondrial dysfunction and vice versa (Lin and Beal, 2006). The main mechanisms by which the mitochondria are affected are by inhibition of the mitochondrial respiratory chain and by the microtubule organization which is related to mitochondrial migration, fission and fusion. The major antioxidant system of the cell, the mitochondria, is thus impaired and DA neurons are restricted to rely on the degradation system (ubiquitin-proteasome system and autophagy-lysosome pathway) to get rid of hazardous by-products. However, the fast accumulation of these toxic products, together with aging, as is usually the case for PD patients, make the procedure of eliminating the harmful molecules not effective enough. The protein degradation machinery is either overloaded or impaired, a situation which deteriorates even further the harmful state of the cellular environment (McNaught et al., 2001). All the above-mentioned defects, alone or in combination, affect the function of the DA neurons and eventually lead to cell death.

2.5 Current therapeutic approaches

The DA neurons become susceptible to cell death in PD. The dopamine levels in the striatum decrease correspondingly, affecting motor control, as well as cognitive features (e.g. learning, memory, attention) (Fearnley and Lees, 1991; Gröger et al., 2014).

The first treatment for PD, dating back to its first description by Parkinson, focused on the clinical picture and aimed for the amelioration of the tremor. Once the pathology behind the disease was connected with the midbrain and more specifically with the substantia nigra, the first anticholinergic drugs were developed to control the balance between the cholinergic and dopaminergic system. These drugs were often combined by Charcot with other medications which were later known to compensate

dopamine's function. However, the need for more effective drugs was increasing. Charcot introduced brain vibration as a therapeutic in 1892. Gowers instead used Indian hemp and opium, drugs that are nowadays known to be connected with the DA system and motor control. The lack of dopamine in the striatum of PD patients, as well as its implication in controlling movement were reported much later by Carlsson et al. (in 1958), Sano et al. (in 1959) and Bertler and Rosengred (in 1959) (Goetz, 2011). From that period on, it became possible to develop focused treatments.

The currently available treatment schemes still cannot cure the disease or prevent neurodegeneration; however they can differentially control the symptoms. To date, there are several therapeutic approaches applied, including pharmacological and non-pharmacological procedures (Rascol et al., 2003; Tarazi et al., 2014) (Table 2).

Drugs	Dopaminergic medications	L-Dopa
		Dopamine agonists (apomorphine, bromocriptine, cabergoline, dihydroergocriptine, lisuride, pergolide, priribedil, pramipexole, ropinirole)
		MAO-B inhibitors (selegiline)
	Nondopaminergic medications	COMT inhibitors (entacapone, tolcapone)
		Antiglutamate (amantadine)
Surgery	Anticholinergic (benztropine, biperiden, orybenadrin, procyclidine, trihexyphenidyl)	
	Lesion (thalamotomy, pallidotomy, subthalamotomy)	
Restorative	Deep brain stimulation (thalamus, pallidum, subthalamus nucleus)	
	Transplantation, trophic factors [GDNF], stem cells, gene therapies	
Rehabilitation	Physical therapy	
	Occupational therapy	
	Speech therapy	

Table 2: Current therapeutic interventions to treat the motor features of PD (modified from Rascol et al., 2003). MAO-B: Monoamine oxidase B, GDNF: Glial cell-derived neurotrophic factor

Among the pharmacological treatments, the administration of L-Dopa (levodopa), a precursor of dopamine, is the de facto standard and provides the most effective relief, yet accompanied by additional side effects. Although

it diminishes some of the motor symptoms, it exacerbates several non-motor PD features (e.g. cognition problems, hallucinations) (Friedman, 2010). Nevertheless, it is less expensive than the dopamine agonists which are also commonly used with similar to L-Dopa effects. Due to its short half life in the brain, L-Dopa is often co-administered with COMT (Catechol-O-methyltransferase) inhibitors, which prolong L-Dopa's action in increasing the dopamine levels, thus more effectively eliminating the symptoms (Connolly and Lang, 2014).

There are also non-dopaminergic treatments available, such as anticholinergic and antiglutamate drugs. The decrease in the dopamine levels is often accompanied by an increase in the levels of other neurotransmitters, like acetylcholine and glutamate, which tend to create tremor and uncontrolled movement. The administration of anticholinergic and antiglutamate drugs assists to the restoration of the balance between the different neurotransmitters in the brain, thus better controlling the movement (Stayte and Vissel, 2014).

Apart from the pharmacological treatment, patients often benefit from the deep brain stimulation, a procedure which creates an artificial brain pacemaker that controls nerve cells' stimulation. This is usually performed in patients whose symptoms cannot be controlled with L-Dopa and who experience various side effects (e.g. hypotension, arrhythmias, anxiety, hallucinations). However, the deep brain stimulation requires high expertise and expensive equipment (Chen et al., 2013).

Several trials for fetal nigral transplantations have been performed (Hauser et al., 1999; Kordower and Brundin, 2009; Olanow et al., 2003). The grafts were generally not rejected and integrated successfully, while the graft-derived DA neurons survived and performed their function normally. However, there was no improvement in the motor symptoms (Olanow et al., 2003) and occasionally the grafts were also affected by the disease (Kordower and Brundin, 2009).

Regional treatments with neurotrophic factors (GDNF) have also been attempted. Infusion of GDNF in the brain of PD patients resulted in increased dopamine storage, as well higher numbers of DA neurons. The action of GDNF could not be clearly correlated with increased survival of the DA neurons or increased regeneration of their axonal projections (Gill et al., 2003). However, the technical hurdles associated with infusing GDNF in the brain and the restricted regional diffusion of the drug limits its application.

Viral delivery was thus introduced for gene therapy in the PD field. Adeno-associated viral vectors (AAV vectors) have already been used in clinical trials for the delivery of genes like *AADC*, *TH*, *GAD* (*Glutamate decarboxylase*), as well as *GDNF* (*Glial cell-derived neurotrophic factor*) and *neurturin* (an analogue of GDNF) (Mittermeyer et al., 2012; Muramatsu et al., 2010; Richardson et al., 2011). Clinical trials based on lentiviral vectors are also developing thanks to the larger packaging capacity of these vectors compared to the AAV (Palfi et al., 2014). So far, amelioration of the motor symptoms has been observed, while the trials have generally been safe. However, there is still need for development of novel strategies for the patients to benefit more with minor side effects.

2.6 Future therapeutic directions

Given that the available treatment schemes only ameliorate symptoms and improve the patient's quality of life, current research is focusing on the replacement of the lost neurons as an ultimate solution to curing the disease (Nandy et al., 2014; Oh et al., 2014; Zhang and Su-Chun, 2010). Therefore, the development of highly efficient protocols for the generation of DA neurons is of high importance. In addition to cell replacement approaches, the generation of DA neurons in vitro may facilitate PD modeling towards a better understanding of the mechanisms underlying the disease, as well as permit large scale drug screening on the pathogenic DA neurons (Allodi and Hedlund, 2014; Badger et al., 2014; Zhao et al., 2014).

The majority of existing protocols concern the *in vitro* conversion of embryonic stem cells (ESCs) to DA neurons (Hsieh and Chiang, 2014). However, the induced pluripotent stem cell (iPSC) technology was also introduced in the field with promising results (Hartfield et al., 2014; Stanslowsky et al., 2014), which was recently followed by lineage reprogramming approaches, bypassing the pluripotent stage (Caiazzo et al., 2011; Liu et al., 2012; Pfisterer et al., 2011a) (Figure 2). These different technologies will be addressed below.

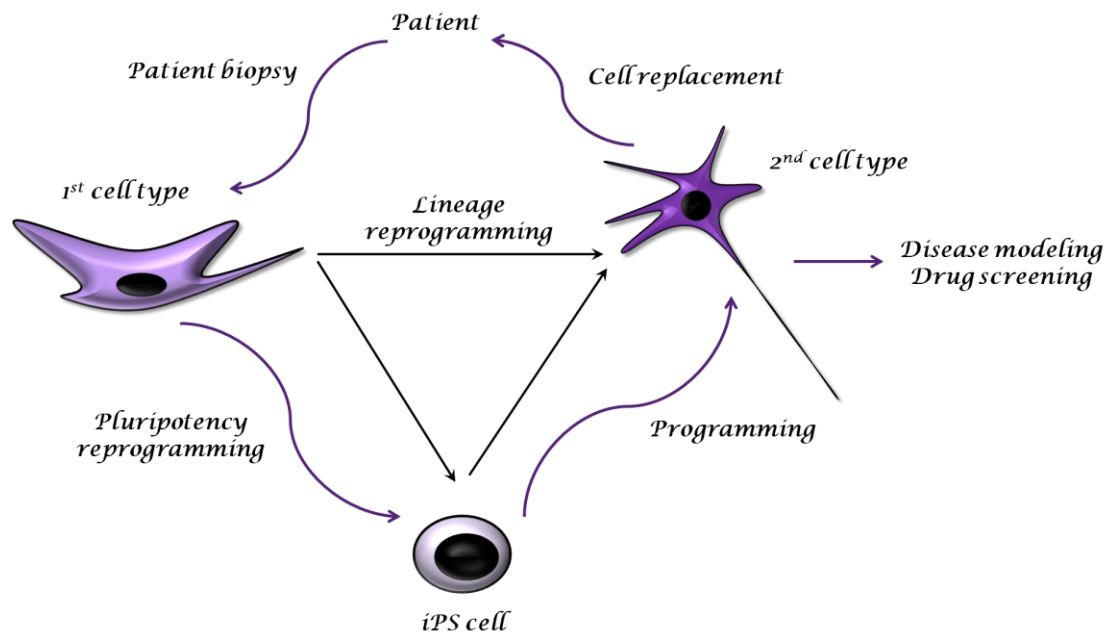


Figure 2: Manipulating cell fates for regenerative medicine of PD. The advent of pluripotency and lineage reprogramming enable disease modeling and drug screening approaches, as well as cell replacement interventions, which pave the way towards personalized medicine.

2.6.1 Programming: Directed differentiation of embryonic stem cells to dopaminergic neurons

In addition to neural precursors (Daadi and Weiss, 1999; Kim et al., 2003a; Papanikolaou et al., 2008; Shim et al., 2007; Studer et al., 2000) or neural stem cells (NSCs) (Deleidi et al., 2011; García-parra et al., 2013; Krabbe et al., 2009; Rössler et al., 2010), ESCs have extensively been used as a cell source for the generation of DA neurons. There are several existing

protocols for the differentiation of either murine (Kim et al., 2006; Lee et al., 2000; Morizane et al., 2002; Ying et al., 2003), human (Kriks et al., 2011; Sánchez-Danés et al., 2012; Zhang and Su-Chun, 2010), or primate (Kawasaki et al., 2002; Takagi et al., 2005; Yue et al., 2006) ESCs to DA neurons (Gale and Li, 2008; Kriks et al., 2011). Most of these protocols can be divided in three categories: 1) the embryoid body (EB)-based (Cho et al., 2008; Díaz and Díaz-Martínez, 2009; Lee et al., 2000), 2) the co-culture-based (Hayashi et al., 2008; Yue et al., 2006; Zeng et al., 2004) and 3) the monolayer protocols (Ying et al., 2003).

The EBs are multi-cellular, spherical structures that are formed during the differentiation of ESCs in the absence of feeder cells or coating substrates and of Leukemia Inhibitory Factor (LIF) (Desbaillets et al., 2000). Being able to give rise to cells of all germ layers (ectoderm, mesoderm and endoderm), they constitute a valuable tool in differentiation experiments. The differentiation medium is often supplemented with additional factors to specifically drive differentiation towards the cell lineage of interest (Geeta et al., 2008; Lee et al., 2000). However, limitations involving the transportation of critical differentiation factors to the inner part of the spherical formation inevitably triggers heterogeneity in the differentiating population (Kinney et al., 2011).

Alternatively, ESC differentiation is often performed in co-cultures with cell types that offer a supportive and/or nutrient environment that promotes survival and preferentially favors specific cell fate decisions (Kawasaki et al., 2002; Morizane et al., 2002). In the case of DA neurons, PA6 cells (Zeng et al., 2004), sertoli cells (Yue et al., 2006) and meningeal cells (Hayashi et al., 2008) have been co-cultivated with ESCs, among other stromal and feeder cell lines (Correia et al., 2007; Kim et al., 2006).

The third category, the monolayer differentiation protocols facilitate the monitoring of the differentiation, as cells are plated at low density on coated cell culture surfaces, without the requirement of co-cultivated cell lines and accelerate remarkably the whole procedure (Ying et al., 2003). Cells are equally exposed to all medium components and the situation resembles the

natural in vivo embryonic neural development (Abranches et al., 2009). These characteristics offer the potential for large scale DA neuronal differentiation, opening the route to in vitro molecular modeling of PD.

However, the differentiation towards the dopaminergic cell fate is not trivial and often requires additional factors. The DA neurons and their intermediate precursors are very prone to stress and cell death. Therefore, survival and/or neurotrophic factors (GDNF, TGF β) (Rolletschek et al., 2001; Zhang and Su-Chun, 2010) or growth factors (FGF2, FGF20) (Correia et al., 2008; Takagi et al., 2005; Yan et al., 2005) are often used as supplements in the differentiation media, in order to protect the developing neurons and better preserve the fully differentiated, mature neurons.

Most neuronal differentiation protocols lack reproducibility since many factors may vary (e.g. media composition, growth/neurotrophic factors etc.), hence chemical compounds were introduced in the in vitro DA neuronal development (Iacovitti et al., 2007; Kriks et al., 2011; Zhang and Su-Chun, 2010). By supplementing the differentiation media with defined chemicals, better control of the overall procedure can be achieved. While in some cases the addition of growth and/or neurotrophic factors is indispensable (Zhang and Su-Chun, 2010), chemical compounds additionally provide the benefit of incorporating molecules of essential signaling pathways naturally involved in DA neuronal development (activators of Shh and canonical Wnt signaling) (Kriks et al., 2011).

The composition of a chemically defined differentiation media, as well as all the additional components (neurotrophic/growth factors) aim to simulate the in vivo developmental environment, namely the activation or inhibition of critical signaling pathways with the subsequent transcriptional regulation that they confer (Goridis and Brunet, 1999). More specifically, the existing DA differentiation protocols intend to indirectly activate/inhibit specific TFs or signaling molecules (e.g. TCF/LEF, Shh) that play crucial roles in the induction, specification, differentiation and maintenance of DA neurons.

Along these lines, genetically engineered ESCs that overexpress key TFs were introduced in the PD research field (e.g. LMX1A, NURR1) (Cho et al., 2011; Chung et al., 2002, 2005b; Kim et al., 2006; Sánchez-Danés et al., 2012). These trials produced a high yield of DA neurons, proving the significance of individual TFs in the DA developmental process. This observation additionally provides hope for the improvement of the achieved neuronal induction efficiencies by using additional potent TFs implicated in DA neurogenesis or combinations of them.

2.6.2 Pluripotency reprogramming: Conversion of induced pluripotent stem cells to dopaminergic neurons

Conversion of ESCs to the desired cell type raises bioethical concerns, thus hampering the progress towards regenerative medicine (Gibson et al., 2012). The iPSCs were introduced as an alternative pluripotent cell source, which can be derived in large numbers from fully differentiated cells (Pu et al., 2012). The notable advantage of iPSC technology in the PD field is that the DA neurons derived from patient-derived iPSCs are derived specifically from the PD patient, hence facilitating personalized therapeutic approaches (Badger et al., 2014).

Similarly to ESCs, protocols for the conversion of iPSCs to DA neurons have already been established (Sundberg et al., 2013; Swistowski et al., 2010; Theka et al., 2013; Yoshikawa et al., 2013). Nevertheless, there are still challenges to be overcome, like the high diversity of the cell population and the frequently observed defective chromosomal status of the reprogrammed cells (Jacobs, 2014; Roessler et al., 2013).

2.6.3 In vitro lineage reprogramming: Conversion of somatic cells to dopaminergic neurons

To replace lost DA neurons in PD patients, successful transplantation approaches of neurons derived from pluripotent stem cells are required.

However, most attempts are often coupled with a major limitation, which is tumor formation (Gutierrez-Aranda et al., 2010; Li et al., 2013; Politis and Lindvall, 2012; Ron-Bigger et al., 2010; Zhao et al., 2011).

To avoid this and to make use of existing abundant cell types, several research groups applied the previously obtained knowledge from the iPSC field to reprogram somatic cells directly into the cell type of interest, bypassing the pluripotent cell stage (Buganim et al., 2012; Hendry et al., 2013; Huang et al., 2014; Ieda et al., 2010; Muraoka et al., 2014; Najm et al., 2013).

Most of the reported lineage reprogramming has been achieved with the overexpression of TFs involved in the normal development of the cell types of interest (Barzilay et al., 2009; Masip et al., 2010; Schimmang, 2013). Nonetheless, micro RNAs (miRNAs) have also recently been introduced in the field of direct reprogramming (Ambasudhan et al., 2011; Shenoy and Blelloch, 2012; Sun et al., 2010; Victor et al., 2014; Yoo et al., 2011). Both of these approaches, alone or in combination aim to simulate the *in vivo* developmental cues which determine the cell fate.

Direct reprogramming is extensively applied in neuroscience. Neurons have been obtained through the direct conversion of different starting cell types (Ambasudhan et al., 2011; Vierbuchen et al., 2010; Xue et al., 2013). In many cases it has been proven that the induced neurons are fully functional and mature (Kim et al., 2011a; Son et al., 2011; Thier et al., 2012) and transplantations in animal models showed that the cells are active and can integrate correctly (Corti et al., 2012; Han et al., 2012; Lujan et al., 2012).

Choosing an appropriate starting cell type offers advantages to the reprogramming process. Fibroblasts are easily accessible in large numbers, thus making them perhaps the most optimal starting cell type. However, their localization out of the brain perhaps limits the conversion potential, since fibroblasts and neurons have little similarities in their developmental programs. The use of brain cells could overcome this hurdle, hence facilitating the conversion. Astrocytes are supportive glial cells of the central nervous and constitute the numerically superior cell type in the brain, while they share

some epigenetic characteristics with neurons. For this reason they may provide better results in terms of ease of reprogramming (Tian et al., 2011). Nevertheless, sufficient amounts cannot be obtained that easily. Pericytes on the other hand are a relatively adequate cell source, since they cover blood vessels all over the body. The brain pericytes are of neuroectodermic origin, thus related to neurons; however the pericytes outside the brain are derived from mesoderm, which perhaps requires more lineage fate-determining factors for efficient neuronal reprogramming.

Neuronal direct reprogramming has also been introduced in the PD field. In vitro studies confirm the generation of DA neurons mainly from fibroblasts (Kim et al., 2014; Liu et al., 2012; Pfisterer et al., 2011a; Sheng et al., 2012a; Torper et al., 2013) and astrocytes (Addis et al., 2011a). Controlled ectopic lentiviral overexpression of TFs which are involved in the development of DA neurons (Figure 3) trigger reprogramming with diverse conversion efficiencies (Figure 4).

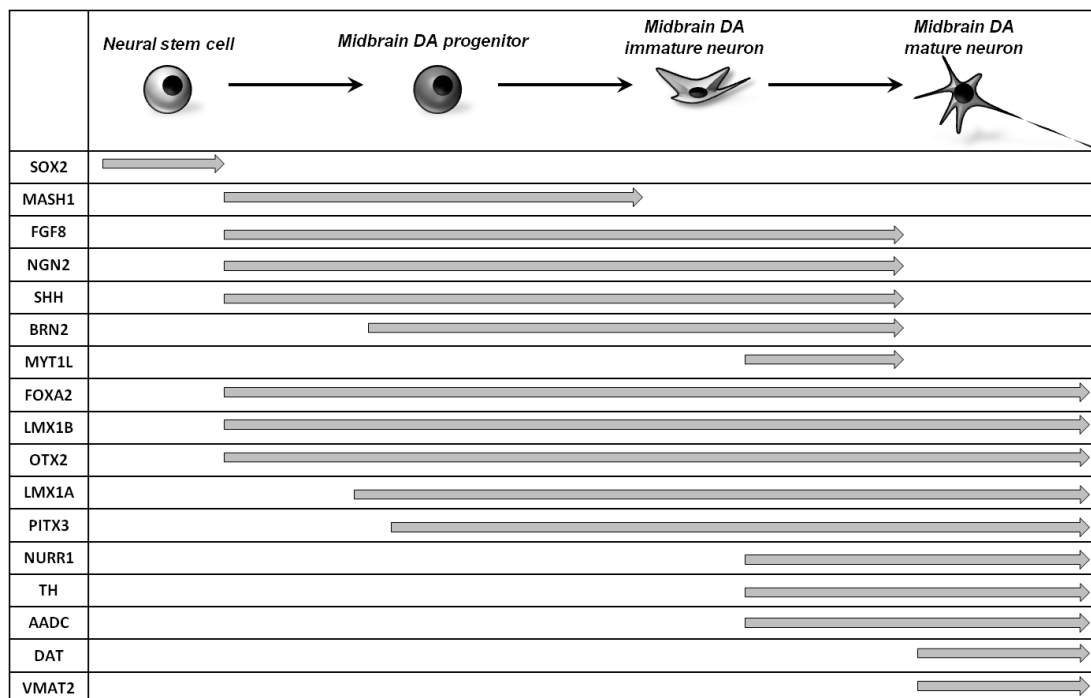


Figure 3: Signaling & regulatory proteins involved in midbrain DA neurons' development from the NSC to the mature DA neuron. The expression profile defines the stage of the DA neuronal development and determines the cell identity.

More specifically, I refer to one particular reprogramming study by Caiazzo et al. (Caiazzo et al., 2011). This group achieved one of the best conversion efficiencies of mouse embryonic fibroblasts (MEFs) to DA neurons by the viral overexpression of *Mash1*, *Lmx1a* and *Nurr1*. Each gene was cloned in a lentiviral backbone and expression was controlled by a doxycycline-dependent promoter, which allowed induction only upon doxycycline administration in the media.

The simultaneous induction of the three TFs rendered almost 20% TH-expressing neurons. Sixteen days after the initial induction, the TH-expressing neurons were also positive for other DA-specific markers, i.e. VMAT2, DAT, ALDH1A1. Although most of the obtained neurons were postmitotic and exhibited electrophysiological properties typical of DA neurons, they were still not identical, in terms of expression profile, to naturally derived DA neurons. However, when transplanted at an early reprogramming stage (4 days post-induction) in the ventricle of young mice, they could follow in vivo their transdifferentiation program and integrate successfully.

Similarly to MEFs, human fetal as well as adult fibroblasts obtained from PD patients gave similar results in vitro in this study, thus providing evidence that the application of this reprogramming strategy from mouse to human is possible.

All the above-mentioned achievements provide hope for future possibilities towards modeling PD and drug screening models, or even for transplantation of the in vitro reprogrammed cells. However, obtaining the DA neurons in situ would provide more benefits related to therapy of PD.

Introduction

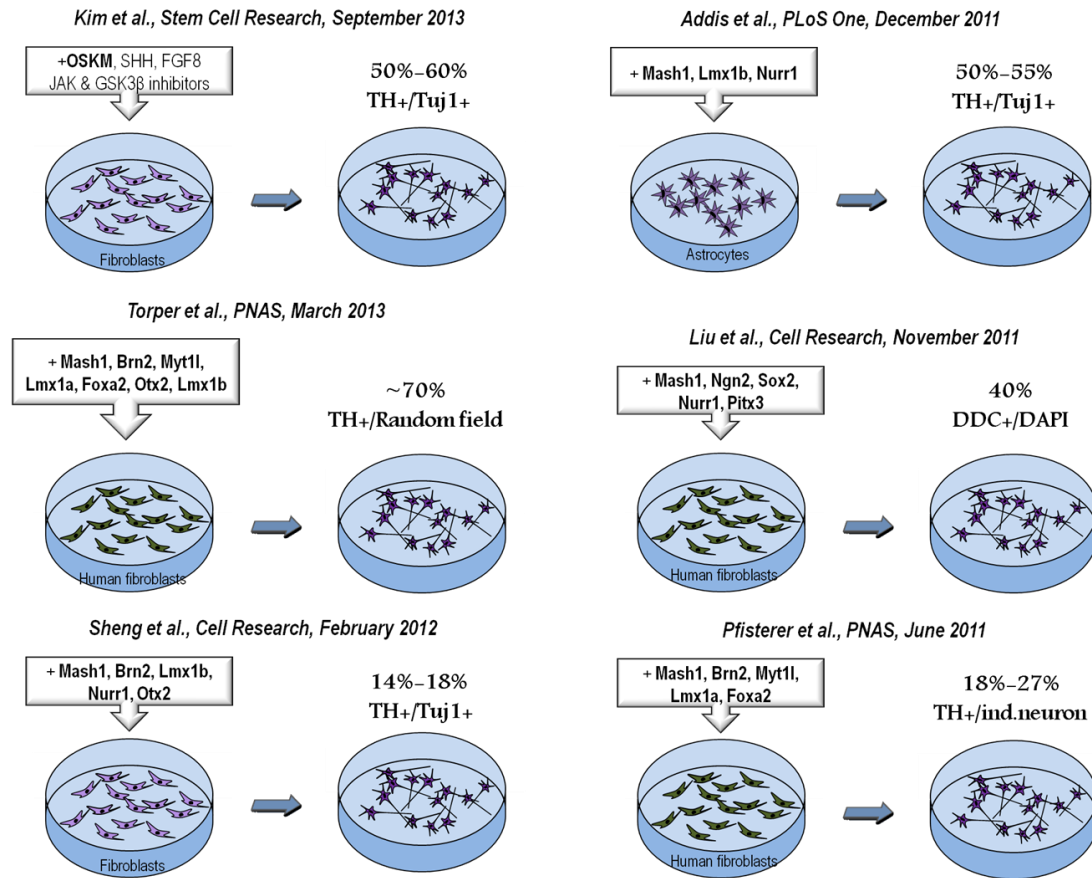


Figure 4: Literature overview of in vitro lineage reprogramming to DA neurons. Ectopic overexpression of several combinations of TFs in fibroblasts and astrocytes in vitro gives TH⁺ neurons with different efficiencies. OSKM: *Oct4*, *Sox2*, *Klf4*, *Myc*, DDC: Dopa Decarboxylase (marker of dopaminergic neurons)

2.7 In vivo lineage reprogramming: Conversion of somatic cells to neurons

In vivo reprogramming, the direct conversion of somatic cells to other lineage fates in the body, is also rapidly maturing, opening new routes towards personalized medicine. The application of reprogramming in the clinic could potentially set the foundation for the replacement of dying cells directly in the diseased area. This would eliminate several limitations, namely having to obtain large amounts of in vitro reprogrammed cells, keeping the cells healthy and stable for long periods in culture and transplant rejection (Fong et al., 2010). The ability to reprogram in vivo may thus facilitate and accelerate

cell replacement. There would be no further requirement for in vitro cultures, which, along with all its negative consequences related to chromosomal defects of the cells, allows for potentially less laborious, less time-consuming and less risky procedures. Furthermore, the reprogramming procedure may benefit from the presence of other cell types in close proximity to the cells to be reprogrammed, as the interactions between closely related cell lineages in the niche could favor the conversion.

In vivo reprogramming has already been applied in neuroscience with the hope to obtain adequate numbers of the neuronal type of interest in situ (Guo et al., 2014; Niu et al., 2013; Rouaux and Arlotta, 2013; Su et al., 2014; Torper et al., 2013) (Figure 5). This has so far been achieved by injection of viruses which express the gene/s of interest directly in the area where the conversion takes place. Although achieved for other neuronal subtypes (e.g. GABAergic, glutamatergic neurons), in vivo conversion to DA neurons still remains a challenge. It seems that there is still valuable information missing in order to simulate the developmental program of DA neurons in vivo.

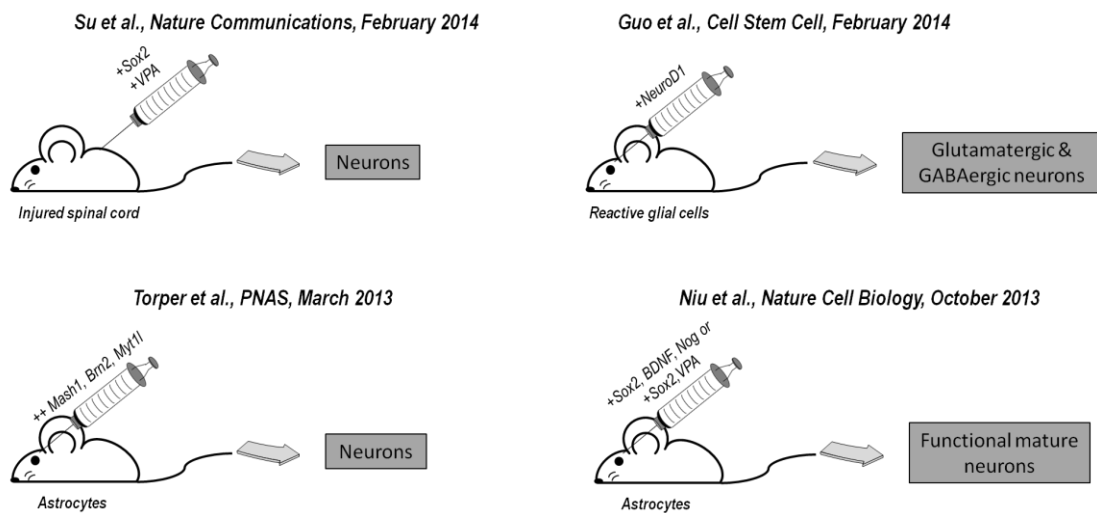


Figure 5: Literature overview of in vivo lineage reprogramming to DA neurons. Neuronal reprogramming has been achieved by viral infection in the brain or spinal cord for the overexpression of TFs and signaling molecules, supplemented in some cases with VPA treatment for histone deacetylase inhibition. VPA: Valproic acid

3. Aim of the study

According to the latest achievements mentioned above, the use of TFs involved in the specification of the DA neuronal fate provides promising results for the optimization of conversion efficiencies. Many different TFs have been used in reprogramming studies, indicating that perhaps even more potent combinations exist that could instruct more faithfully the endogenous dopaminergic phenotype and function.

In order to drive ESCs towards the dopaminergic cell fate, I constructed “molecular paths” by the overexpression of specific TFs, driving ESCs to the ectodermal precursor stage and then to the neural cell stage, to eventually acquire the dopaminergic identity. In this regard, regionally expressed TFs were proposed to act as spatio-temporal coordinates to determine the exact positional identity of the newly generated cell in the anterior-posterior and the dorso-ventral axes, specifying it as a DA neuron.

In addition, I aimed for the direct conversion of somatic cells to DA neurons *in vivo* following a similar approach. I generated a genetic mouse model for the conditional overexpression of a combination of TFs. The combination of MASH1, LMX1A and NURR1 (Caiazzo et al., 2011) was demonstrated to generate DA neurons from fibroblasts *in vitro*. A genetic approach for *in vivo* reprogramming to DA neurons has never been reported before, but would serve as a useful tool to prove, understand and optimize the reprogramming process *in vivo*. The tissue/cell type specific overexpression of these TFs and the subsequent reprogramming potential was intended to provide a proof-of-principle for *in vivo* reprogramming to DA neurons. By applying this genetic approach, I sought to identify cell types most susceptible to reprogramming, determine the optimal timing and duration of TFs' overexpression, as well as assess the conversion efficiency to DA neurons *in situ*.

4. Results

4.1 In vitro programming of embryonic stem cells to dopaminergic neurons

ESCs constitute a valuable tool for regenerative medicine (Kehat et al., 2001; Liu et al., 2000; Lumelsky et al., 2001) and screening approaches (Aubert et al., 2002; Desbordes et al., 2008; Zweigerdt et al., 2003) and have also been widely used for the generation of DA neurons (Kriks et al., 2011; Lee et al., 2000; Sánchez-Danés et al., 2012). ESCs can give rise to all germ layers, i.e. endodermal, mesodermal and ectodermal precursors.

4.1.1 Transcription factor combinations for directed differentiation of embryonic stem cells to dopaminergic neurons

In order to be driven towards the neural fate, ESCs must be directed to the ectodermal fate. SOX1 expression is connected to neural plate formation and is restricted to a narrow developmental frame which is during the neural progenitor cell stage (Abranches et al., 2009; Pevny et al., 1998). To drive ectopic expression of selected transcription factors (TFs) for a restricted period, I made use of the *Sox1* promoter, using it as a natural inducible system. This system in combination with the neuronal conditions of the medium should trigger the neuronal differentiation of ESCs.

Once the cell has already committed to the neuronal fate, TFs involved in several phases throughout the development of DA neurons should in turn specify the molecular and functional identity of a DA neuron. For my experiments, I combined TFs according to their role during DA neuronal development (neurogenic and patterning) and their regional expression, while avoiding TFs with overlapping functions (Figure 6). I generated vectors overexpressing these TFs under the endogenous *Sox1* promoter by yeast cloning, which allows the simultaneous insertion of multiple fragments in a plasmid backbone by homology.

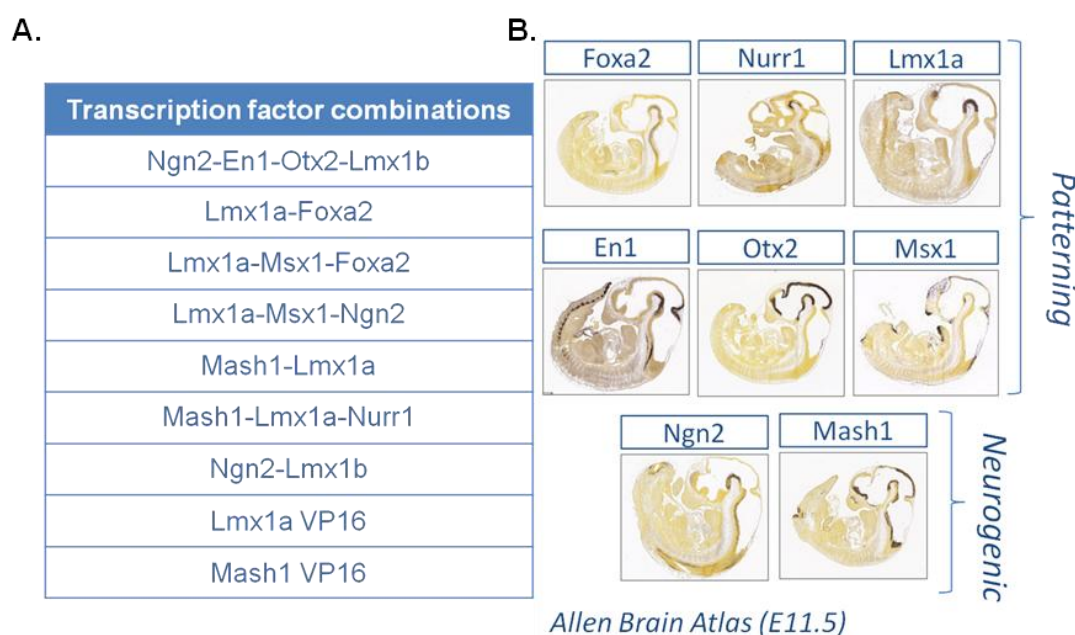


Figure 6: Neurogenic and patterning TFs involved in DA neuronal differentiation.

- A. TF combinations were designed to be ectopically expressed under the control of the Sox1 promoter for the directed differentiation of ESCs towards the DA cell fate.
- B. Expression pattern of selected patterning and neurogenic TFs at E11.5 mouse embryos (sagittal sections, images adopted from Allen Institute for Brain Science).

Most of the polycistronic combinations contain one neurogenic/proneural factor-either *Mash1* or *Ngn2* (Castro et al., 2006; Park et al., 2006), or molecules which are inducing their expression and one or more patterning TFs. In one instance, I combined *Mash1* with VP16, which is a strong transactivator (Hirai et al., 2010), with the aim to enhance *Mash1*'s neurogenic activity. The same concept was applied for *Lmx1a*. LMX1A has been proven extremely potent in converting ESCs or iPSCs to DA neurons, without the need for additional factors (Andersson et al., 2010; Hong et al., 2014; Sánchez-Danés et al., 2012). By fusing *Lmx1a* with VP16, we aimed for further improvement of its DA neuronal differentiation potential. Considering its pivotal role in the generation of DA neurons in the ventral midbrain, *Lmx1a* was a component of most of the vectors, (Cai et al., 2009; Nefzger et al., 2012). In some cases *Lmx1b* was chosen instead, a gene which is closely related to *Lmx1a* in terms of expression pattern and function (Deng et al., 2011; Yan et al., 2011).

It is noteworthy to mention that one combination of TFs differed remarkably from all the rest, namely the *Ngn2-En1-Otx2-Lmx1b* combination. It contains *Otx2*, which acts as a repressor of the hindbrain identity (Simeone et al., 2011; Vernay et al., 2005) and *En1*, a TF important for the survival of the DA neurons (Alves dos Santos and Smidt, 2011; Simon and Saueressig, 2001; Sonnier et al., 2007). These two TFs combined with *Ngn2* and *Lmx1b*, aimed for a single step reproduction of the developmental pathway of DA neurons, by inducing neurogenesis (*Ngn2*) characteristic of the ventral midbrain (*Lmx1b*), promoting the survival of the newly generated DA neurons (*En1*) and repressing neighboring neuronal types (e.g. serotonergic neurons (*Otx2*), thus providing the coordinates of the exact positional and functional identity of DA neurons.

4.1.2 Recombinase-mediated cassette exchange in the *Sox1* locus for the generation of genetically engineered embryonic stem cells

To facilitate the targeting of the various TF combinations in the *Sox1* locus I exploited the properties of the recombinase-mediated cassette exchange (RMCE) (Turan et al., 2013). During this procedure, a recombinase, in this case Cre, catalyzes the exchange of cassettes flanked by *loxP* sites between a donor plasmid and a genomic site with complementary recombinase sequences. Two heterologous *loxP* sites were utilized in each case: the *loxP257* and a reverse wild type *loxP* site. The *loxP257* is a mutated version of the wild type *loxP* site (Wong et al., 2005). Utilizing thus different *loxP* sites in opposite orientations, the risk of self-recombination was minimized and the exchange efficiency was increased (Toledo et al., 2006; Wong et al., 2005).

Specifically, the whole process encompasses two steps. Firstly, a targeting vector is integrated into the genetic locus of interest by standard homologous recombination in the ESCs. This vector consists of homology arms and a positive/negative selection cassette flanked by *loxP* sites. Secondly, an “exchange” vector carrying any of the above-mentioned TF

combinations flanked by complementary to the other vector *loxP* sites is co-transfected with a Cre-expressing plasmid into the cells generated after the first step. The Cre-expressing plasmid catalyzes the recombination of the *loxP* flanked cassettes of the genetic locus and the exchange plasmid and subsequently their exchange (Figure 7). Consequently, the generation of a series of differentially *Sox1* targeted ESC lines is significantly accelerated, avoiding repeated homologous recombination steps, which is often a hindrance to gene targeting. Moreover, following RMCE, genotyping of the obtained ESC clones is simplified dramatically with short range PCR.

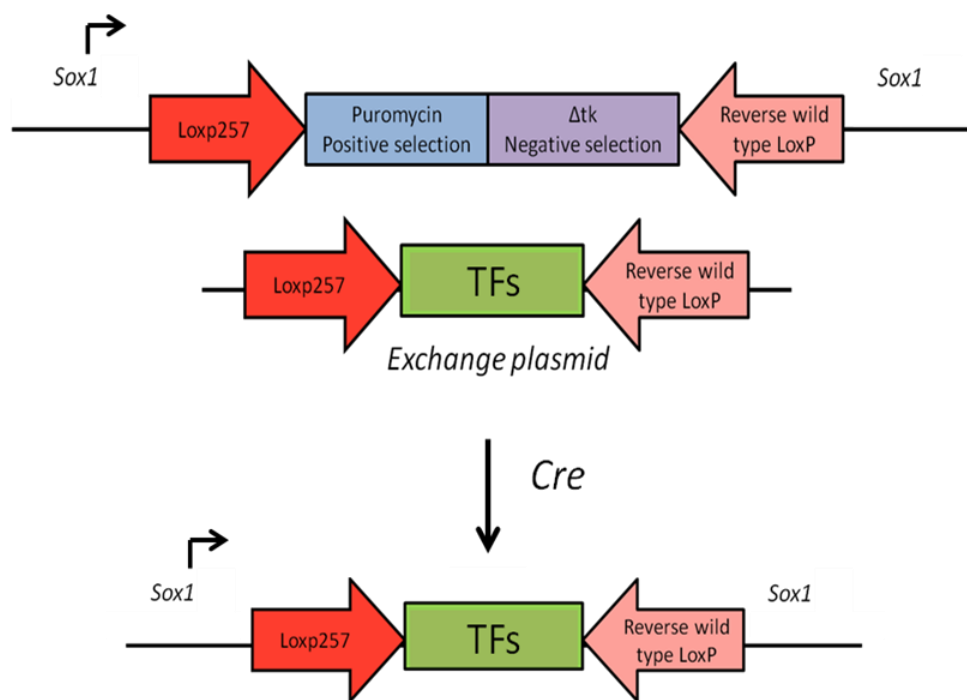


Figure 7: Recombinase-mediated cassette exchange. A construct consisting of a positive/negative selection cassette flanked by two *loxP* sites is integrated into the locus of interest (*Sox1*). Cre recombinase catalyzes the exchange of the two *loxP* flanked cassettes between the modified *Sox1* locus and the exchange plasmid which is co-transfected with Cre. Each exchange plasmid contains different polycistronic cassettes of TFs, which after Cre-mediated recombination are under the control of the *Sox1* promoter.

For the integration into the *Sox1* locus, a vector containing a 3.7 kb 5' homology arm, a 4.9 kb 3' homology arm and the *puro Δtk* cassette flanked by the *loxP257* and a reverse wild type *loxP* site was cloned and electroporated in murine ESCs. The positive clones were resistant to puromycin selection and successful 3' recombination into the *Sox1* locus was confirmed by long

range PCR (Figure 8). This step resulted in the generation of a stable ESC line (*Sox1*^{RMCE puro $\Delta tk/+$}), which serves as a valuable tool for the construction of a variety of ESC lines with different genetic modifications in the *Sox1* locus. This can be achieved by merely exchanging the *loxP*-flanked cassette, avoiding thus many homologous recombination steps.

Subsequently, each of the TF combinations mentioned above were cloned into the exchange plasmid between the two *loxP* sites. To achieve simultaneous overexpression of all TFs of a given combination, I utilized the viral T2A sequence. By the mechanism of ribosome skipping during translation, it allows the expression of consecutive genes in equimolar quantities (Donnelly et al., 2001; Kim et al., 2011b). Since many of the combinations contain more than two TFs, the use of T2A sequence was required more than once in each construct. To avoid undesirable recombination effects due to DNA sequence repeats, the primary T2A sequence was optimized with silent mutations, which nevertheless provided the same peptide sequence. To easily assess the expression of the TFs, a *myc* tag was cloned at the end of the last TF in each combination.

Each exchange plasmid was co-transfected with the pCAG-Cre-bpA plasmid in the *Sox1*^{RMCE puro $\Delta tk/+$} ESC line. The absence of the negative selection cassette provided an indication for successful cassette exchange upon Cre-mediated recombination. The negative selection cassette consists of a truncated version of the herpes simplex virus type I thymidine kinase gene (*Δtk*). When eukaryotic cells express this gene, they incorporate nucleoside analogs like ganciclovir or FIAU (Fialuridine, or 1-(2-deoxy-2-fluoro-1-D-arabinofuranosyl)-5-iodouracil) into their DNA, which eventually becomes toxic (Salomon et al., 1995). Upon successful cassette exchange, the cells became resistant to treatment with such analogs.

Results

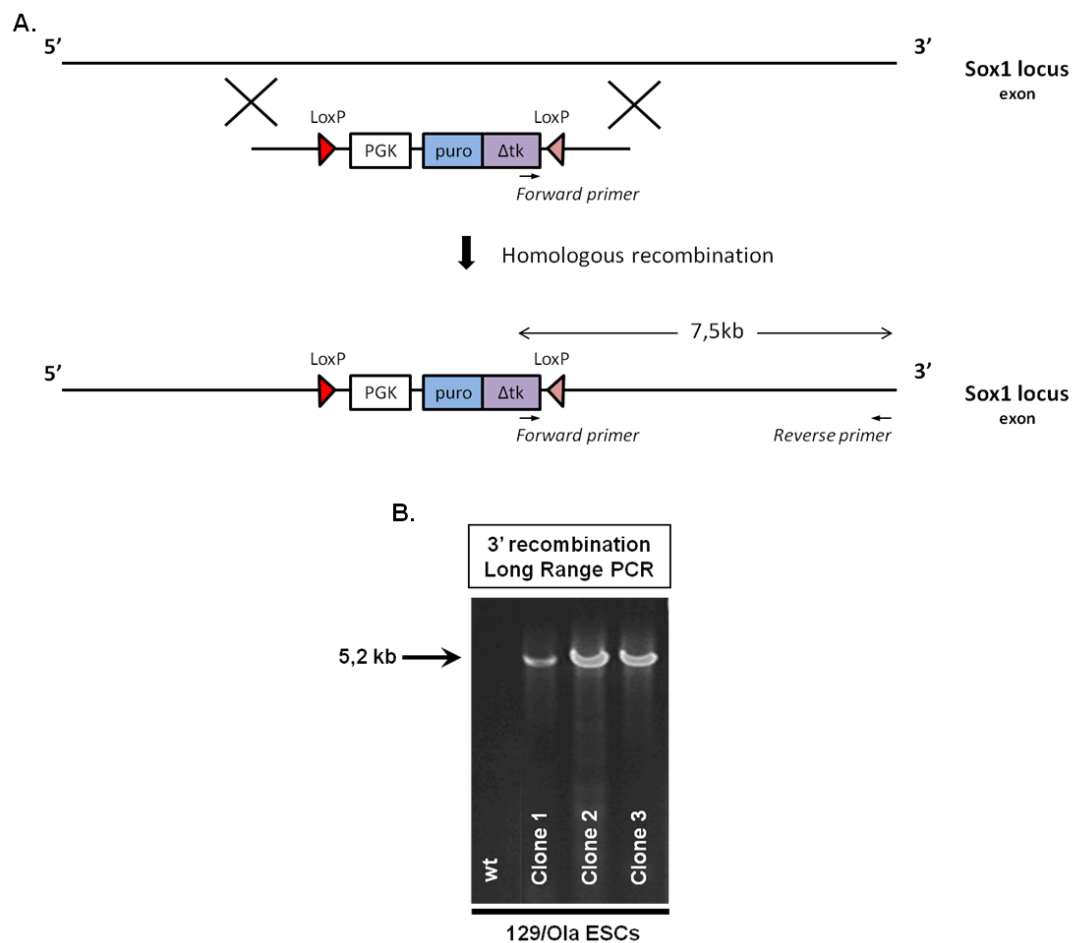


Figure 8: Targeting the *Sox1* locus for RMCE

- A. Schematic representation of homologous recombination in the *Sox1* locus (exon) of murine ESCs. The targeting plasmid was recombined in the locus with the use of 5' and 3' homology arms and the positive ESC clones were selected with puromycin treatment.
- B. Long range PCR for the analysis of 3' recombination of the RMCE targeting plasmid into the *Sox1* locus with primers depicted in (A).

puro: puromycin *N*-acetyl transferase

To determine the optimal FIAU concentration for the selection of ESC clones, I performed a kill curve, testing several FIAU concentrations on *Sox1*^{RMCE *puro* Δtk/+} and wild type ESCs. The optimal concentration was determined as indicated by the color change of phenol red, which is a pH indicator in culture medium and can be correlated with the growth rate of the cells. This was confirmed by a cell viability assay using AquaBluer (data not

shown). This is a redox indicator and is reduced by living cells with a subsequent change in fluorescence intensity. Based on these results, the optimal FIAU concentration was selected as the lowest at which almost all *Sox1*^{RMCE puro $\Delta tk/+$} die and wild type cells survive and was determined at 0.4 μ M.

The FIAU-resistant ESC clones obtained after RMCE in the *Sox1* locus were then screened for the confirmation of successful cassette exchange by PCR. The *puro Δtk* cassette was not detected in any case in the *Sox1* locus, confirming its complete removal by Cre-mediated recombination. The PCR reaction confirmed successful 5' and 3' Cre-mediated recombination of the *LF*, *Mash1 VP16*, *ML*, *NEOL* and *NL* combinations, however only 3' Cre-mediated recombination of the *LMF*, *LMN* and *Lmx1a VP16* combinations. The failure to confirm 5' recombination for these three combinations, although the ESC clones were FIAU-resistant, could be due to either inefficient exchange or PCR failure. Nevertheless, these combinations were included in further analyses. The *MLN* combination however was dismissed as unsuccessfully recombined (Figure 9).

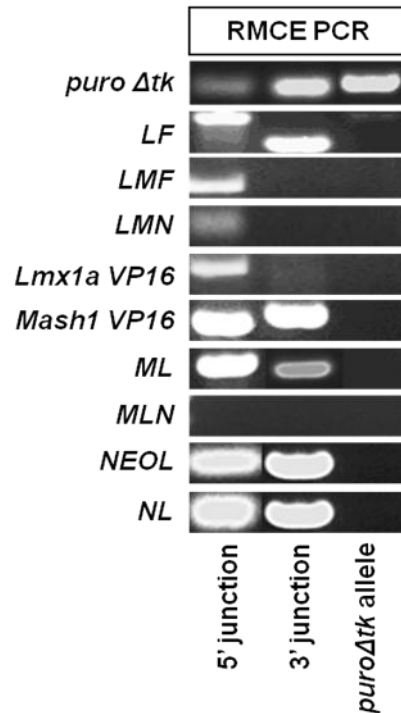


Figure 9: PCR for the analysis of RMCE. To test 5' Cre-mediated recombination a forward primer upstream of the first *loxP* site and a reverse primer specific for the first TF in each polycistronic combination were utilized. Similarly, to test 3' Cre-mediated recombination, a forward primer specific for the last TF in each case and a reverse primer downstream of the second *loxP* site were utilized.

4.1.3 Induction of the *Sox1* promoter and the downstream transcription factors

To assess the induction of expression of *Sox1* and the TFs, I performed quantitative real time PCR. Specifically, I tested the *Sox1* and *Mash1* RNA levels of the *Sox1*^{RMCE *puro* Δtk /+}, *Sox1*^{RMCE *Mash1* VP16/+} and *Sox1*^{RMCE *ML*/+} ESCs over the course of 4 days under neuronal differentiation conditions, a period during which *Sox1* is normally induced (Abranches et al., 2009; Pevny et al., 1998).

The analysis revealed significant upregulation of *Sox1* RNA levels with time in all ESC lines tested (Figure 10A), as well as significant upregulation of *Mash1* RNA levels of the *Sox1*^{RMCE *Mash1* VP16/+} and *Sox1*^{RMCE *ML*/+} ESCs (Figure 10B).

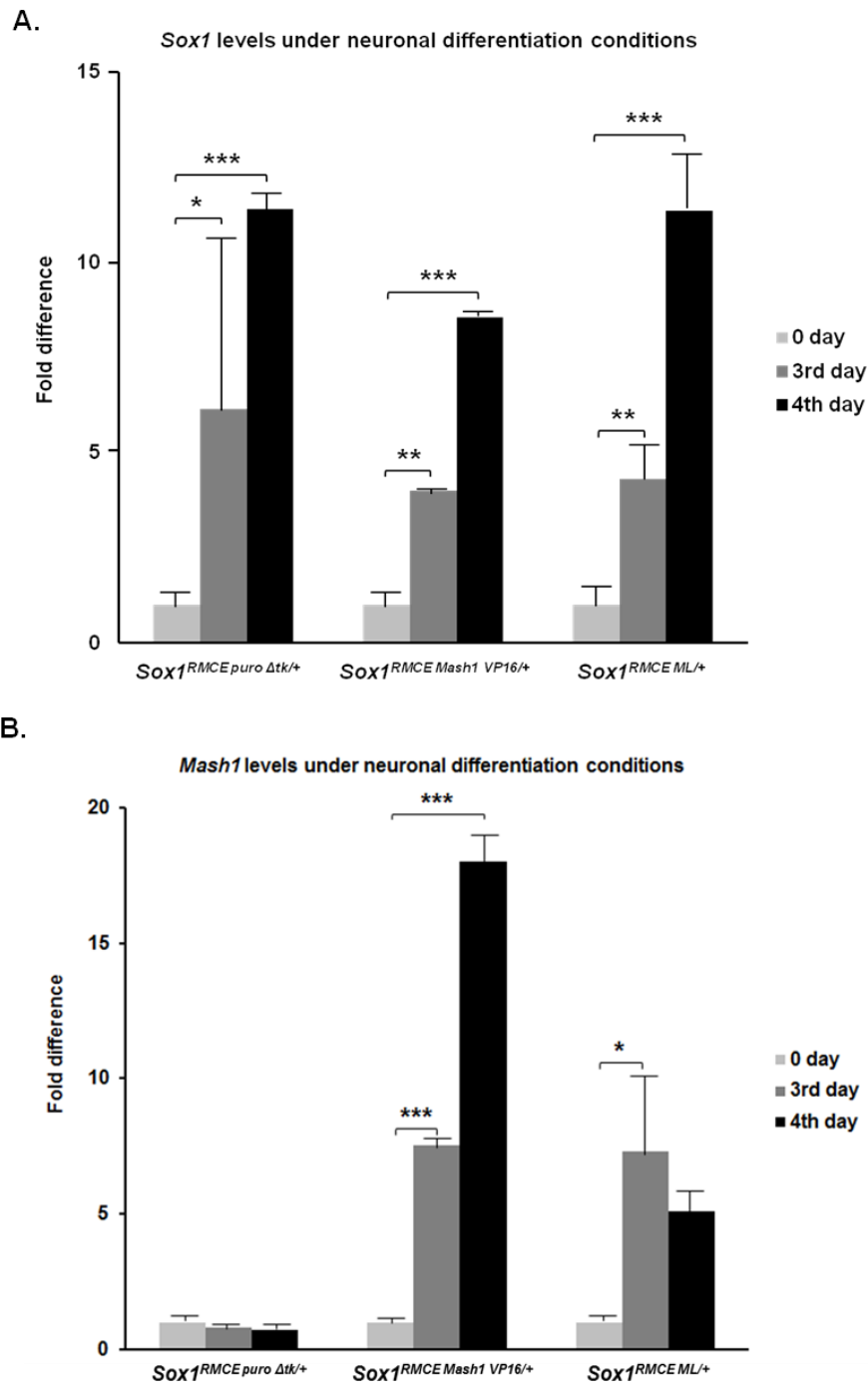


Figure 10: Upregulation of *Sox1* and *Mash1* levels under neuronal differentiation conditions. Quantitative Real time PCR depicting the RNA levels of (A) *Sox1* and (B) *Mash1* in the *Sox1^{RMCE puro Δtk/+}*, the *Sox1^{RMCE Mash1 VP16/+}* and the *Sox1^{RMCE ML/+}* ESCs after 4 days under neuronal differentiation conditions. The levels were normalized to the 0 day conditions, each of which was set to 1. Unpaired t-test, * $p \leq 0.05$, ** $p \leq 0.01$, *** $p \leq 0.0001$, $n=2$. Error bars represent mean \pm SD.

These results confirm the gradual induction of the endogenous *Sox1* gene, which showed gradual activation of its promoter and subsequently of its

Results

downstream genes (here, of *Mash1*) under the given cell culture conditions. Surprisingly though, the RNA levels of *Mash1* in the *Sox1*^{RMCE ML/+} ESCs were reduced on the 4th day, which can be attributed to possible RNA degradation.

To confirm *Sox1* and subsequent TF activation also on the protein level, I performed immunocytochemical staining. I utilized an antibody against MYC in order to detect expression of the *myc* tag cloned at the end of each combination. This would indicate expression of the upstream TFs as well. The *Sox1* targeted ESC lines were stained after 3 days in neuronal differentiation conditions. The result revealed MYC expression in all *Sox1* targeted ESC lines (Figure 11). The background signal detected in the wild type cells probably corresponds to endogenous MYC expression which is highly activated in undifferentiated ESCs (Varlakhanova et al., 2010). The *Sox1* modified ESCs however, have lost one of their *Sox1* alleles during the targeting procedure, resulting thus in a less undifferentiated state than wild type ESCs (Elkouris et al., 2011), hence exhibiting reduced MYC signal in some instances. Nevertheless, the *Sox1*^{RMCE NEOL/+} (*NEOL*) and *Sox1*^{RMCE NL/+} (*NL*) ESC lines exhibited strong MYC signal, indicating high levels of expression of the upstream TFs.

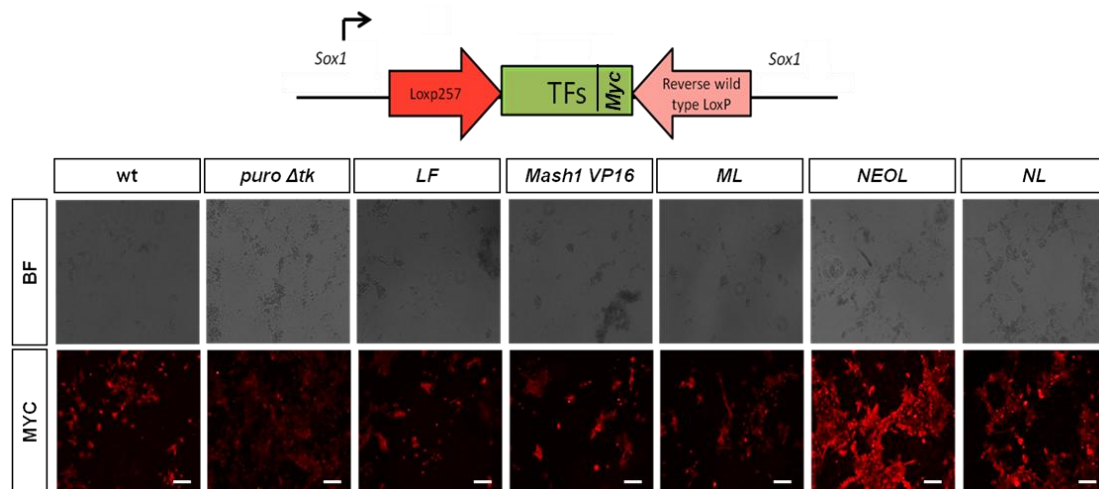


Figure 11: Expression of the MYC tag in the *Sox1* targeted ESCs. Immunocytochemical staining with an antibody against MYC of the *Sox1* targeted ESCs overexpressing different combinations of TFs. Cells were plated under neuronal differentiation conditions for 3 days.

BF: Bright field, Scale bars: 50 μ m (all pictures are the same size)

4.1.4 Neuronal differentiation protocols for in vitro conversion of the *Sox1* targeted embryonic stem cell lines to dopaminergic neurons

4.1.4.1 Monolayer neuronal differentiation protocol with retinoic acid

Having confirmed *Sox1* induction and activation of TF expression under differentiation conditions, I sought to utilize these genetic tools for the generation of DA neurons. For this purpose, I used a monolayer differentiation protocol, using N2B27 (B27 contains small amount of all-trans retinoic acid) medium (Neuronal Differentiation Medium 1, NDM1) (Ying et al., 2003) for the DA neuronal differentiation of the *Sox1* targeted ESC lines. During monolayer neuronal differentiation, the ESCs are plated at low density, deprived of serum and are guided towards ectoderm fate. The supplementation of all-trans retinoic acid (RA, also known as vitamin A acid) in the differentiation medium has been shown to enhance the neurogenic potential of ESCs (Lu et al., 2009). Therefore, I treated ESCs with all-trans RA for 3 days and let them differentiate for another 5 days, without RA administration. For the detection of DA neurons I performed immunocytochemical staining, utilizing antibodies against TUJ1 and TH (Tyrosine Hydroxylase). TUJ1 represents neural-specific beta III tubulin, therefore acts as a general neuronal marker. Tyrosine Hydroxylase catalyzes the conversion of L-Tyrosine to L-DOPA, which is a precursor to dopamine. Dopamine is the characteristic neurotransmitter of DA neurons; therefore TH expression indicates the dopaminergic identity of a neuron. This differentiation protocol generated TUJ1⁺ neurons even during early stages of the differentiation procedure (Figure 12A). However none of the TUJ1⁺ neurons was TH⁺ (Tyrosine Hydroxylase) (data not shown). This observation was confirmed by Western blotting, which additionally revealed different levels of TUJ1 protein among the ESC lines overexpressing different TF combinations (Figure 12B). The highest TUJ1 protein levels were observed when *Ngn2* and *Lmx1b* were overexpressed (*NL*), which showed a 2-fold increase compared to the wild type ESCs (data not shown). The other ESC lines displayed comparably lower TUJ1 levels, however higher than the control lines (wild type and *Sox1*^{RMCE puro Δtk/+} (hereafter called *puro Δtk*)). Exempt from this observation was the *LF* ESC line, which generated more

Results

neurons during the early stages (4 days after protocol initiation), that apparently could not survive the differentiation procedure.

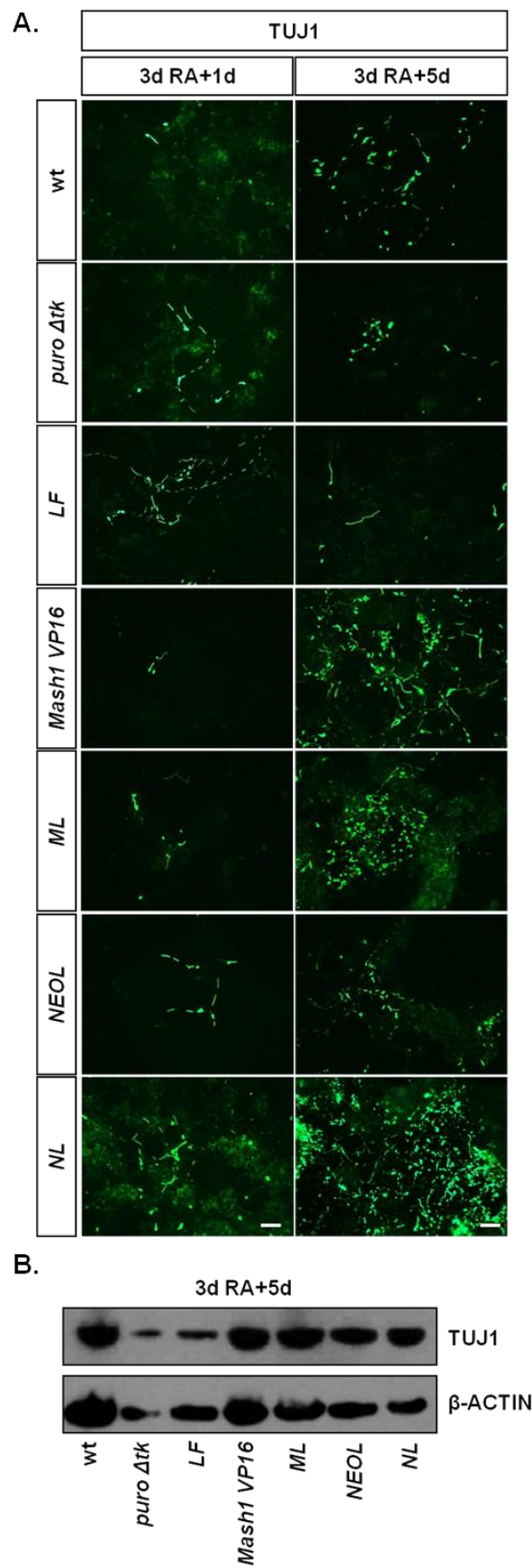


Figure 12: Neuronal differentiation of the *Sox1* targeted ESCs treated with RA in monolayer cultures

- A. Immunocytochemical staining with an antibody against TUJ1 of the different *Sox1* targeted ESC lines under neuronal differentiation conditions and treatment with RA. The staining was done at two different time points, 3+1 and 3+5 days of differentiation.
- B. Western blot depicting the expression of TUJ1 in the *Sox1* targeted ESC lines after 8 days of differentiation.

RA: Retinoic Acid, Scale bars: 50 μ m (all pictures are the same size)

4.1.4.2 Embryoid body-based neuronal differentiation protocol with retinoic acid

The conditions of the monolayer neuronal differentiation (low density, lack of serum) result in stress for the cells and therefore increased cell death is observed, which perhaps limits the number of neurons eventually obtained (Mfopou et al., 2014). To overcome those discrepancies, I applied an EB-based neuronal differentiation protocol with the addition of RA (Bibel et al., 2007). This protocol employs generation of EBs in a serum-containing medium and subsequently cultivation of dissociated EBs in N2 medium, which is later replaced by a medium closely resembling the N2B27 composition. The protocol gives rise mainly to glutamatergic and GABAergic neurons from wild type ESCs. With minimal medium (N2B27 medium throughout the differentiation of EBs) and timing modifications (reduced incubation for EB formation), together with the effect of the *Sox1* promoter and the downstream TFs, I tested whether this protocol could be used for the generation of DA neurons instead of the monolayer protocol.

Unfortunately, no DA neurons were observed after 10 or more days of differentiation, although there was an abundance of neurons formed, as shown by immunocytochemical staining against TUJ1 (Figure 13). It is noteworthy that the highest neuronal yield was obtained from the *Mash1* *VP16* and the *NL* combinations, both of which consist of a proneural TF (MASH1 and NGN2 respectively). However, almost equally high neuronal

yield was obtained from the wild type and the *puro Δtk* ESCs. This observation may be due to two reasons. Firstly, due to the fact that the wild type cells retain their pluripotency to a bigger extent than the *Sox1* targeted ESC lines (loss of one *Sox1* allele) (Elkouris et al., 2011), being thus able to give rise to a broader range of neuronal populations. Secondly it is possible that the overexpression of the selected TFs in combination with the severe differentiation conditions (no serum or growth factors supporting survival) resulted in increased stress and subsequently death of the ESCs or newly formed neurons.

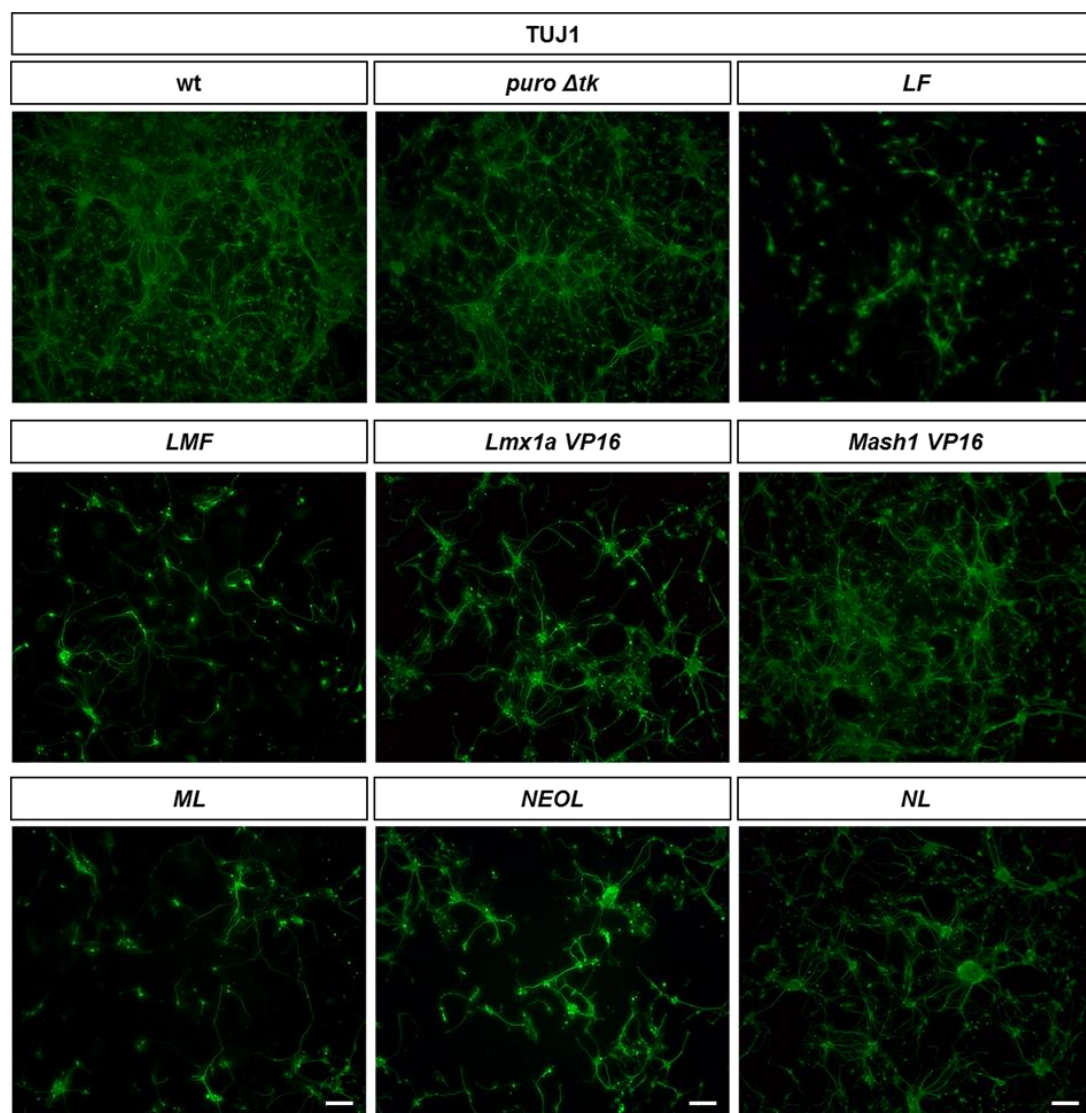


Figure 13: EB-based neuronal differentiation of the *Sox1* targeted ESCs treated with RA (modified from Bibel et al.). Immunocytochemical staining with an antibody against TUJ1 of the different *Sox1* targeted ESC lines under neuronal differentiation conditions and treatment with RA. Scale bars: 50 μ m (all pictures are the same size)

4.1.4.3 Monolayer neuronal differentiation protocol without retinoic acid and with the supplementation of forskolin

RA, apart from its neuronal promoting effect, supports the differentiation of radial glial cells too (Bibel et al., 2007), hampering thus the generation of neurons (Cooper et al., 2010). To test whether RA has an inhibitory effect in the generation of DA neurons and to improve the differentiation efficiency, it was excluded from further DA neuronal differentiation attempts. To completely eliminate its effect, the B27 reagent (with RA) was replaced by B27 without RA. Yet, once again, the dissociated EBs could not give rise to TH⁺ neurons (data not shown). This prompted me to leave out the EB stage, since these aggregates constitute heterogeneous cell populations, which can give rise to all three germ layers. Instead, modifying the previously applied monolayer neuronal differentiation protocol in a way to prevent cell loss during the procedure and to selectively eliminate cell populations other than ectoderm would exclude heterogeneity.

One important modification was the medium composition. Except for the B27 replacement (without RA), ascorbic acid (also known as vitamin C), which promotes cell survival, was also included (Jetti and Raghuvver, 2014) and N2, which has similar to B27 composition, was excluded. Moreover, I investigated for additional molecules that further promote survival and neurogenesis. Among these, I mainly focused on dorsomorphin and forskolin. Dorsomorphin is a known BMP signaling inhibitor (Yu et al., 2009). It has been demonstrated that expression of BMPs in the SVZ of adult mice hampers neurogenesis, while favouring gliogenesis instead (Lim et al., 2000). Taking these observations into consideration, I hypothesized that dorsomorphin may promote neurogenesis. Forskolin induces the synthesis of cyclic AMP (cAMP), which results in activation of the cAMP responsive element binding protein (CREB) (Michel and Agid, 2002). After being phosphorylated, CREB activates the expression of *Bcl-2* (Wilson et al., 1996), a gene implicated in promoting the survival of neuronal populations by preventing apoptosis (Dubois-Dauphin, 1994; Farlie and Dringen, 1995). CREB is also an activator of CBP and p300, both of which proteins result in

transcriptional activation by recruiting the RNA polymerase II and by interacting with histone acetyltransferases (Yuan and Gambee, 2001). Forskolin has previously been shown to protect and promote the differentiation of DA neurons (Paldino et al., 2014). Therefore, the supplementation of forskolin in the differentiation medium aimed for increased neuronal yield (Li et al., 2000). To test their effect on the differentiation of the *Sox1* targeted ESC lines, I supplemented the modified neuronal differentiation medium (Neuronal Differentiation Medium 2, NDM2) with either of these. For this experiment, I used the *NL* ESC line, which in all neuronal differentiation protocols tested, yielded the best neuronal differentiation potential compared to all the others.

The addition of forskolin in the modified medium (NDM2) resulted in high TUJ1 and TH fluorescence intensity in differentiated *NL* ESCs as measured with a fluorescence reader after immunocytochemical staining with antibodies against TUJ1 and TH. It was higher than the one observed when dorsomorphin was supplemented, or when either of them was supplemented in the previously used neuronal differentiation medium (N2B27, NDM1) (data not shown).

However, the yield of TH⁺ neurons obtained with the addition of forskolin was not as high as expected using the genetically modified ESCs (Figure 14). Theoretically every cell that passes through a neuroectodermal phase (expresses SOX1) should overexpress the selected TFs under the *Sox1* locus and should be driven towards the DA neuronal fate. Therefore, a differentiation efficiency of up to 100% was expected. Unfortunately, the obtained TH⁺ neurons were very few. The differentiation efficiency could not be further improved to compete the efficiencies achieved by published protocols, where growth factors or essential signaling molecules are supplemented (Kriks et al., 2011; Lee et al., 2000), while the few TH⁺ neurons were not adequate to pursue in vitro modeling of PD and drug screening approaches.

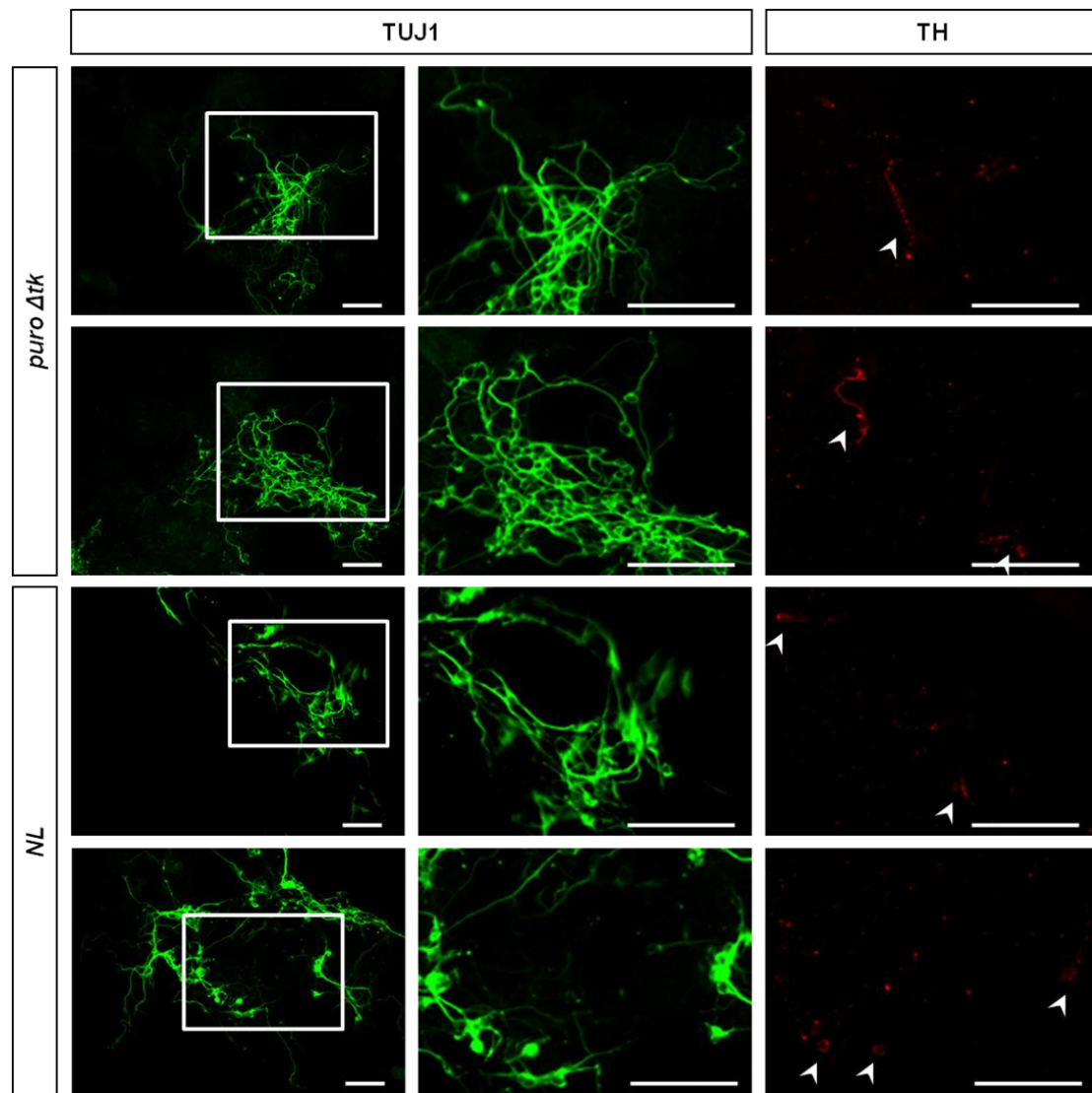


Figure 14: Neuronal differentiation of the *Sox1* targeted ESCs treated with forskolin in monolayer cultures. Immunocytochemical staining with antibodies against TUJ1 and TH of the control (*puro Δtk*) and *NL* ESC lines under neuronal differentiation conditions and treatment with forskolin. The second and third columns provide a higher magnification of the first column. The arrows indicate TH⁺ neurons. Scale bars: 50 μm

4.2 In vivo reprogramming to dopaminergic neurons

Somatic cells have recently been used as a cell source for the generation of DA neurons in vitro. My goal was to trigger the conversion of somatic cells to DA neurons in vivo. Caiazzo et al. reported in 2011 the generation of DA neurons starting from fibroblasts in vitro with the overexpression of three TFs, namely MASH1, LMX1A and NURR1 (Caiazzo

et al., 2011). These are three of several TFs, involved in neurogenesis (MASH1 (Kele et al., 2006)) and DA neuronal development (LMX1A (Cai et al., 2009; Yan et al., 2011), NURR1 (Kadkhodaei et al., 2009; Saucedo-Cardenas et al., 1998)). Fibroblasts were infected by viruses overexpressing each of the three TFs upon addition of doxycycline in the culture medium. After 2-3 weeks under neuronal differentiation conditions, the fibroblasts were converted into neurons expressing TH, as well as other DA neuronal markers, such as ALDH1A1 and DAT. These neurons were also functional as confirmed by their electrophysiological properties. However, none of the neurons expressed PITX3, a TF characteristic of the ventral midbrain identity of the DA neurons. I utilized the same combination of TFs to specifically drive cell fate towards the DA pathway *in vivo*. To enhance the conversion efficiency and to ensure the ventral midbrain identity of the newly generated neurons (characteristic of the DA neurons of the SNc), I also included PITX3 in the above-mentioned combination as a second and potentially improved reprogramming strategy.

The strategy for *in vivo* reprogramming relied on the generation of two Rosa26 mouse lines, each conditionally overexpressing a polycistronic combination of the selected TFs in specific cell types/tissues. This approach was intended to provide a proof-of-principle of *in vivo* reprogramming to DA neurons, as well as useful knowledge for the optimal reprogramming conditions. The major goals were to identify the optimal cell type to be converted, as well as the duration and timing of the overexpression of the selected TFs.

4.2.1 Targeting the *Rosa26* locus in murine embryonic stem cells

The combination of *Mash1*, *Lmx1a* and *Nurr1* was cloned in a *Ai9 Rosa26* targeting construct (Madisen et al., 2010), utilizing viral 2A peptides (Donnelly et al., 2001; Kim et al., 2011b), which are common elements of polycistronic vectors (Carey et al., 2009; Daniels et al., 2014; Lin et al., 2013; Shao et al., 2009). The vector contains a *loxP*-flanked cassette, consisting of

3 copies of the SV40 polyadenylation signal (poly(A)) (“stop” cassette). The “stop” cassette lies upstream of the coding sequence. Consequently, MLN expression driven by the strong CAG promoter can only be activated upon Cre-mediated recombination of the “stop” cassette. The *Ai9 CAG MLN* vector was targeted to the *Rosa26* locus of murine ESCs by homologous recombination (Figure 15A). ESC clones were treated with G418 to select for recombinant clones. To confirm successful integration in the locus, clonal ESC genomic DNA, before and after the targeting, was digested with *PvuII*. The different bands generated were detected in a Southern blot using a 5' probe (Figure 15B). The 6.5 kb band corresponded to the recombined *MLN* allele in the 5' *Rosa26* locus, while the smaller 5.8 kb band corresponded to the wild type *Rosa26* allele. Long range PCR was performed for the analysis of the 3' recombination (Figure 15C). Together the genotyping analyses revealed successful homologous recombination in the *Rosa26* locus, creating heterozygous *Rosa26*^{CAG:MLN/+} targeted ESC clones. Two clones were subsequently selected for chromosome counting. The normal chromosome count in mice is 40 (2n). These clones exhibited high percentage of normal chromosome numbers (97% for clone 1, 73% for clone 2) (Figure 15D), suggesting that these ESCs clones were appropriate for blastocyst injections.

A similar procedure was followed for the second combination of genes, that of *Mash1*, *Lmx1a*, *Nurr1* and *Pitx3*. To more easily follow expression of the TFs, this polycistronic combination was implemented with *Tau eGFP* (Wernig et al., 2002). Therefore, eGFP fluorescence ensures that all upstream TFs are also expressed in equimolar quantities using the 2A viral peptides. Moreover, eGFP in this case was fused to Tau protein. Tau is expressed in neuronal processes, where it is associated with microtubules. Tau eGFP expression facilitates thus the imaging of newly generated neurons that express the TFs.

The polycistronic *Mash*, *Lmx1a*, *Nurr1*, *Pitx3* and *Tau eGFP* combination (hereafter called *MLNPTe*) was also cloned into the *Ai9 Rosa26* targeting vector (Figure 16A) and homologous recombination was confirmed by PCR for the 5' (Figure 16B) and long range PCR for the 3' site (Figure

Results

16C). One successfully recombined ESC clone exhibited normal chromosomal numbers in a high percentage (73%) (Figure 16D) and was selected for further experiments.

Once the *Rosa26*^{CAG:MLN/+} and *Rosa26*^{CAG:MLNPTe/+} ESCs were obtained, a series of in vitro experiments were performed to test for the conditional expression of the selected TFs.

Results

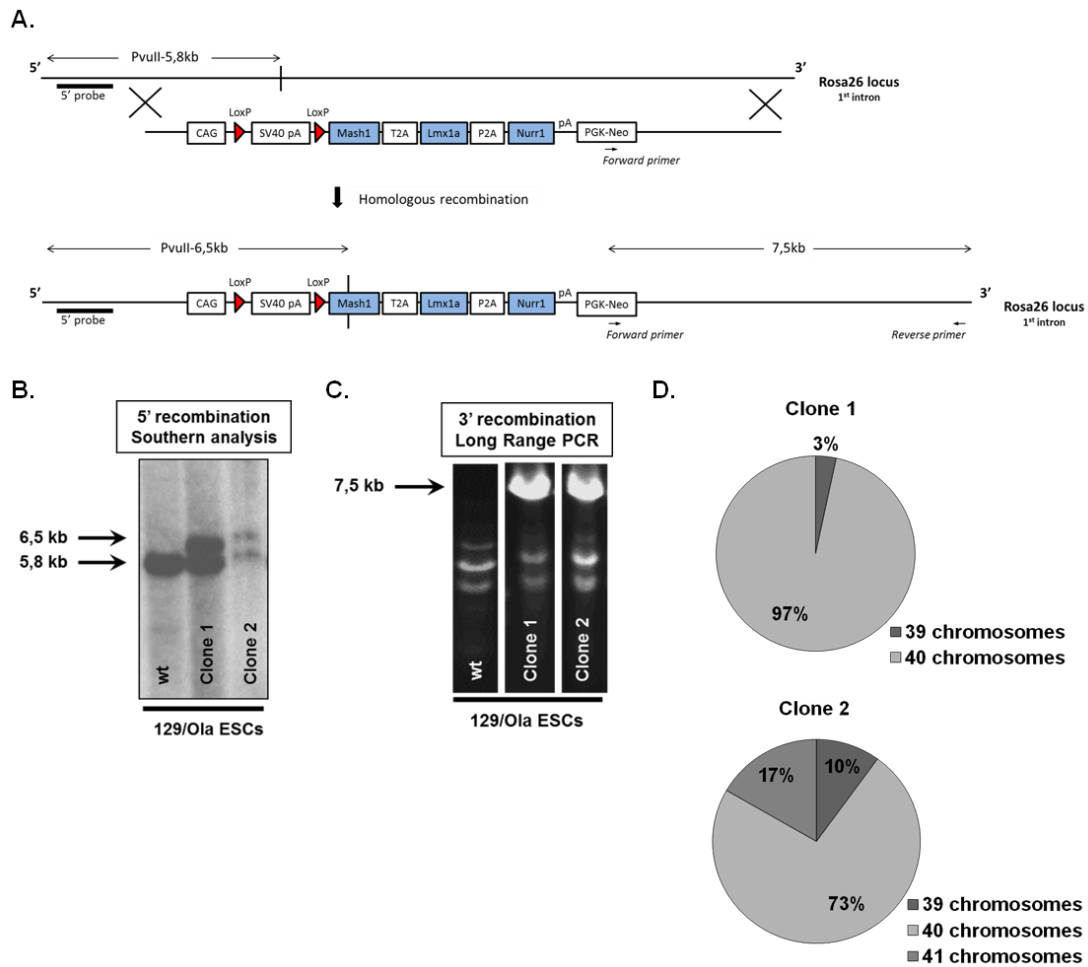


Figure 15: Targeting of *MLN* in the *Rosa26* locus

- A. Schematic representation of homologous recombination in the *Rosa26* locus. A CAG promoter-driven polycistronic vector for the conditional expression of *Mash1*, *Lmx1a* and *Nurr1* was targeted in the *Rosa26* locus by homologous recombination.
- B. Southern analysis of ESC clones for the analysis of 5' homologous recombination of the MLN expressing construct in the *Rosa26* locus. Digestion of the ESC genomic DNA with *PvuII* produced products with different sizes corresponding to the wild type (5.8 kb) and recombined allele (6.5 kb).
- C. Long range PCR for the analysis of 3' recombination of the MLN expressing construct in the *Rosa26* locus.
- D. Chromosome counting of two *Rosa26* targeted ESC clones. Metaphase chromosome spreads were prepared from the two ESC clones.
 wt: Wild type, *Neo*: neomycin phosphotransferase

Results

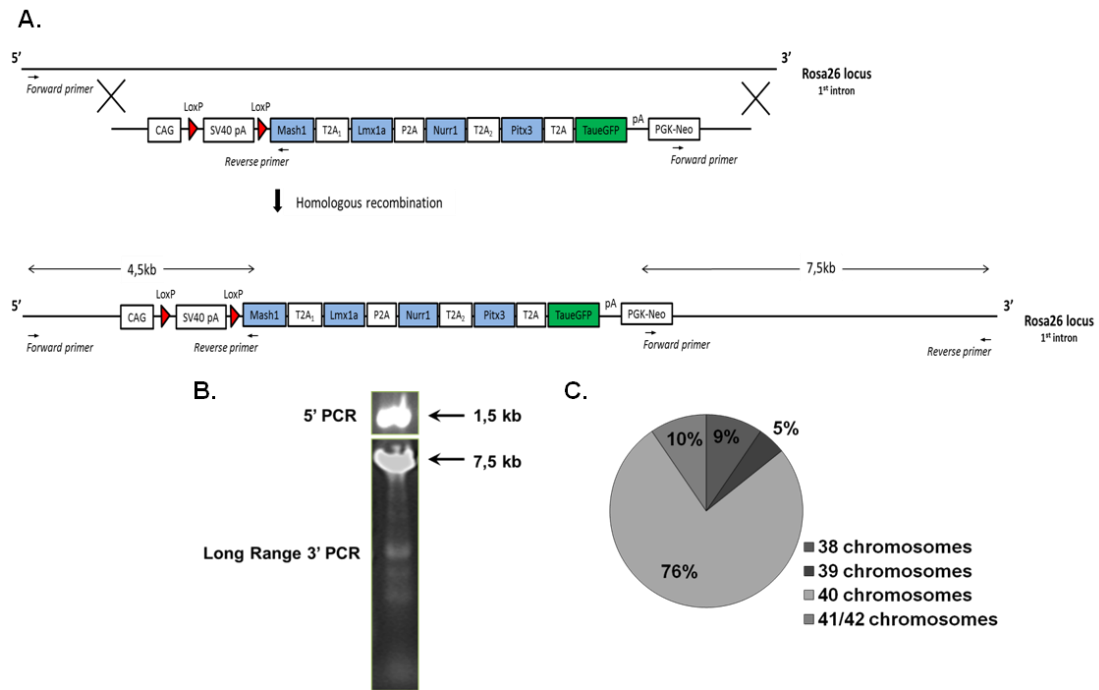


Figure 16: Targeting of *MLNPTE* in the *Rosa26* locus

- Schematic representation of homologous recombination in the *Rosa26* locus. A CAG promoter-driven polycistronic vector for the conditional expression of *Mash1*, *Lmx1a*, *Nurr1*, *Pitx3* and *TaueGFP* was targeted in the *Rosa26* locus by homologous recombination.
- PCR and long range PCR for the analysis of 5' and 3' recombination respectively of the MLNPTE expressing construct in the *Rosa26* locus.
- Chromosome counting of the *Rosa26* targeted ESC clone. Metaphase chromosome spreads were prepared from the ESC clone.

4.2.2 MLN and MLNPTE induction in vitro

The first technical question to be addressed was whether the “stop” cassette can be successfully deleted. To test this, I treated the plasmid DNA of both constructs (*Ai9 CAG MLN* and *Ai9 CAG MLNPTE*) with Cre recombinase in vitro. Treated as well as untreated (control) plasmid DNAs were then used as templates for PCR amplification of a fragment including the “stop” cassette (Figure 17A, C). The reaction provided products of two different sizes with the same primer pair, which indicated Cre-mediated

Results

recombination (recombined band) or not (non-recombined band) of the *loxP*-flanked “stop” cassette (Figure 17B, D).

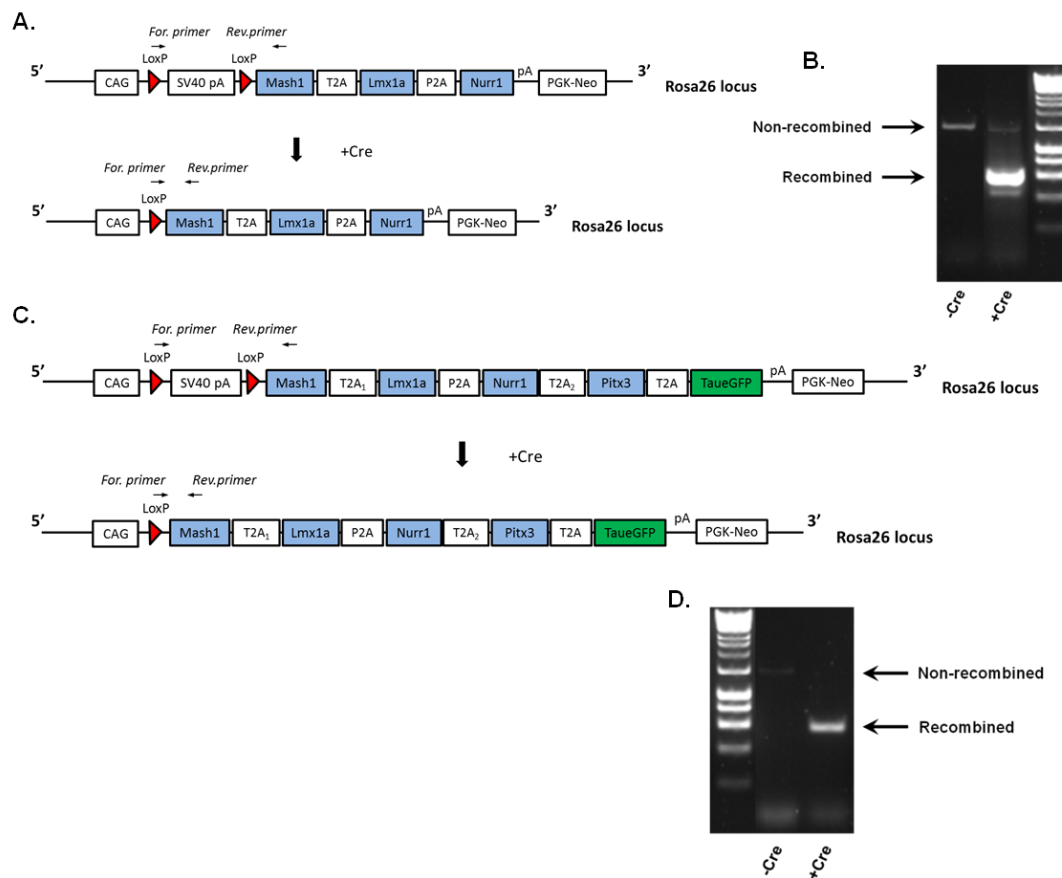


Figure 17: In vitro Cre-mediated recombination of the *MLN* and *MLNPTe* constructs

- Schematic representation of Cre-mediated recombination of the *MLN* construct.
- PCR reaction for the detection of in vitro Cre-mediated recombination of the *MLN* construct with (+Cre) and without (-Cre) the addition of Cre recombinase.
- Schematic representation of Cre-mediated recombination of the *MLNPTe* construct.
- PCR reaction for the detection of in vitro Cre-mediated recombination of the *MLNPTe* construct with (+Cre) and without (-Cre) the addition of Cre recombinase.

Following Cre-mediated recombination the expression of the downstream genes should be induced. To test whether the TFs are expressed in vitro, I transfected HEK293T cells with either the *Ai9* CAG *MLN* or the *Ai9* CAG *MLNPTe* construct, in combination with the *pCAG-Cre-bpA* construct, encoding for Cre recombinase. One day later, I performed immunocytochemical staining with antibodies against MASH1 and LMX1A in

the case of the *MLN* combination (Figure 18A) and *PITX3* in the case of the *MLNPTe* combination, while in parallel I analyzed Tau eGFP fluorescence (Figure 18B). All of these factors could be detected, albeit in low frequency, perhaps due to reduced transfection efficiency of these big constructs (McLenachan et al., 2007).

To test the functionality of the *MLN* construct in the targeted ESCs and to create a useful tool for subsequent in vitro experiments, I generated a *Rosa26^{CAG:MLN/+};CAG:MERCReMER* ESC line permanently expressing *MERCReMER*. This is a tamoxifen-inducible Cre recombinase (Seiler et al., 2008; Verrou et al., 1999). ESC clones stably transfected with *pCAG-MERCReMER* were selected with puromycin (Figure 19A).

To assess the efficiency of cassette recombination, I treated *Rosa26^{CAG:MLN/+};CAG:MERCReMER* ESCs with tamoxifen for 2 days. DNA from treated and untreated cells was isolated and utilized as template for PCR amplification of an area flanking the “stop” cassette (Figure 19A). The same primer pair provided products of different sizes, corresponding to the deleted (treated with tamoxifen) and non-deleted (untreated) version of the modified *Rosa26 CAG MLN* locus (Figure 19B). This provided the proof that *MERCReMER* can successfully mediate the deletion of the “stop” cassette upon tamoxifen administration, displaying however minor recombination even in the absence of tamoxifen (Verrou et al., 1999).

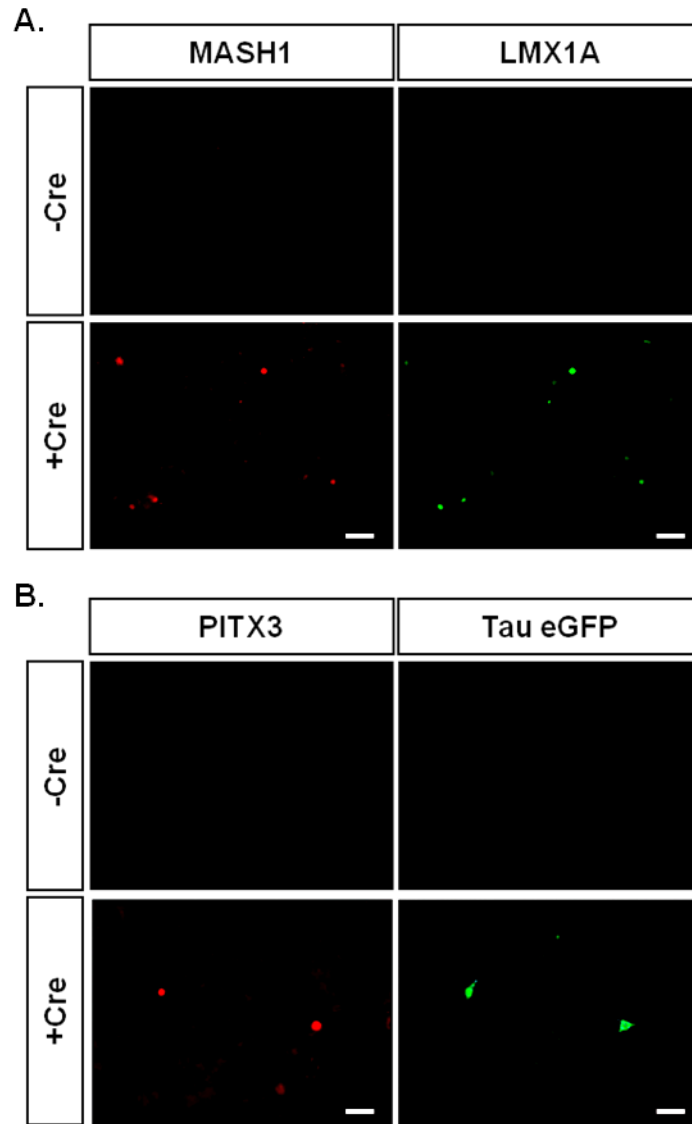


Figure 18: Induction of TFs' expression upon Cre-mediated recombination

- A. Immunocytochemical staining with antibodies against MASH1 and LMX1A of HEK293T cells transfected with the *MLN* construct with (+Cre) and without (-Cre) co-transfection of a Cre expressing plasmid.
- B. Immunocytochemical staining with an antibody against PITX3 and detection of Tau eGFP fluorescence of HEK293T cells transfected with the *MLNP_Te* construct with (+Cre) and without (-Cre) co-transfection of a Cre expressing plasmid.

Scale bars: 50 um (all pictures are the same size)

Results

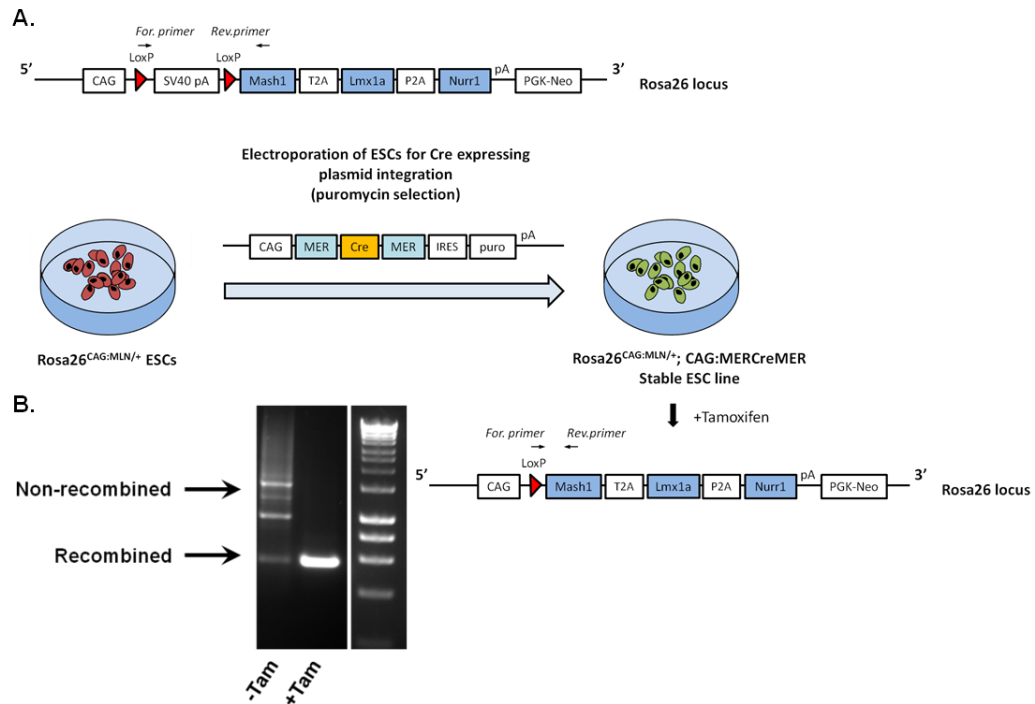


Figure 19: Generation of a conditional *MLN*-expressing ESC line

A. Schematic representation of the generation of the stable *Rosa26*^{CAG:MLN/+};*CAG:MERCReMER* stable ESC line. *Rosa26*^{CAG:MLN/+} ESC clones were electroporated with a *MERCReMER* expressing plasmid. The cells were selected with puromycin. Upon tamoxifen administration *MERCReMER* is activated and catalyzes the recombination of the “stop” cassette.

B. PCR reaction for the detection of *MERCReMER* recombination with (+Tam) and without (-Tam) tamoxifen administration.

Tam: tamoxifen

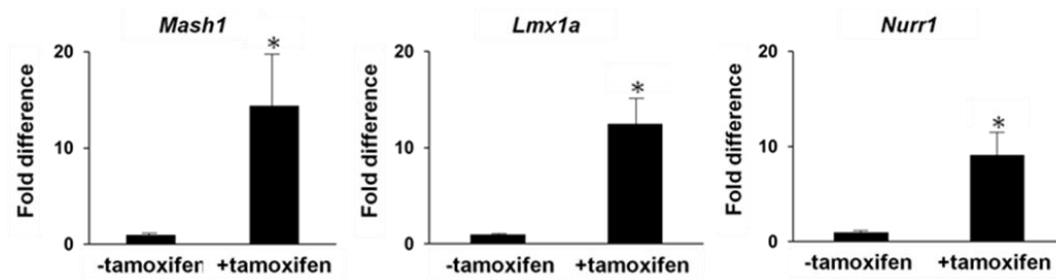
Next I sought to examine whether *MERCReMER*-mediated recombination results in *MLN* expression. I first tested the RNA levels of the three TFs before and after tamoxifen treatment. I observed a significant increase of *Mash1*, *Lmx1a* and *Nurr1* RNA levels of tamoxifen-treated cells compared to the untreated, as revealed by quantitative real time PCR (Figure 20A). This finding was confirmed on the protein level, as shown by immunocytochemical staining using antibodies against *MASH1* and *NURR1* (Figure 20B). Low levels of expression are detected without tamoxifen treatment due to the fact that *MERCReMER* can cause background recombination, as discussed above, hence resulting in weak activation of

MLN expression. To further validate these results and to quantify the cell population expressing the two TFs, I analyzed treated with tamoxifen and untreated *Rosa26^{CAG:MLN/+};CAG:MERC_{Cre}MER* ESCs by flow cytometry. The results confirmed expression of MASH1 and NURR1, which were also co-expressed in the positive ESC population (Figure 20C).

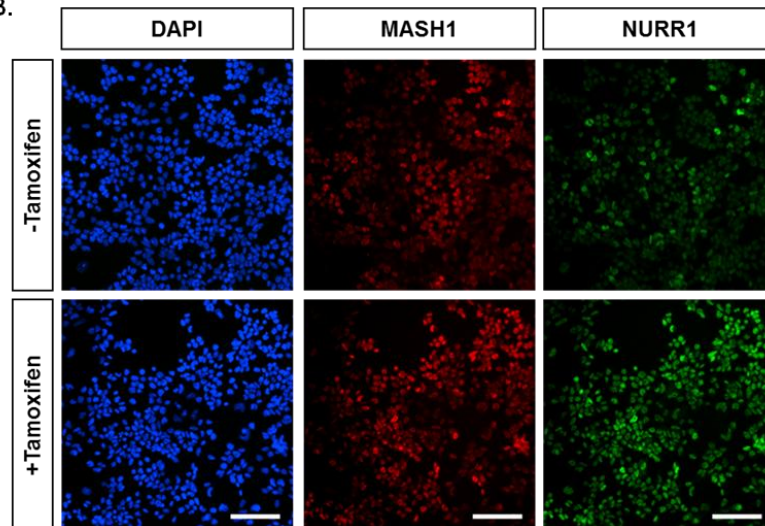
However, expression of the proteins is not necessarily indicative of the functionality of the three TFs. To prove that the TFs exhibit normal function, I utilized the same ESC line to perform luciferase assays. Luciferase reporter constructs responsive to each of the TFs (Castro et al., 2006; Jehn et al., 2014; Peng et al., 2011) were transfected in *Rosa26^{CAG:MLN/+};CAG:MERC_{Cre}MER* ESCs treated with tamoxifen. In all cases, the activity of each of MASH1, LMX1A and NURR1 was higher in the cells treated with tamoxifen compared to the untreated, confirming that the three TFs can perform normally upon induction of their expression (Figure 21).

Results

A.



B.



C.

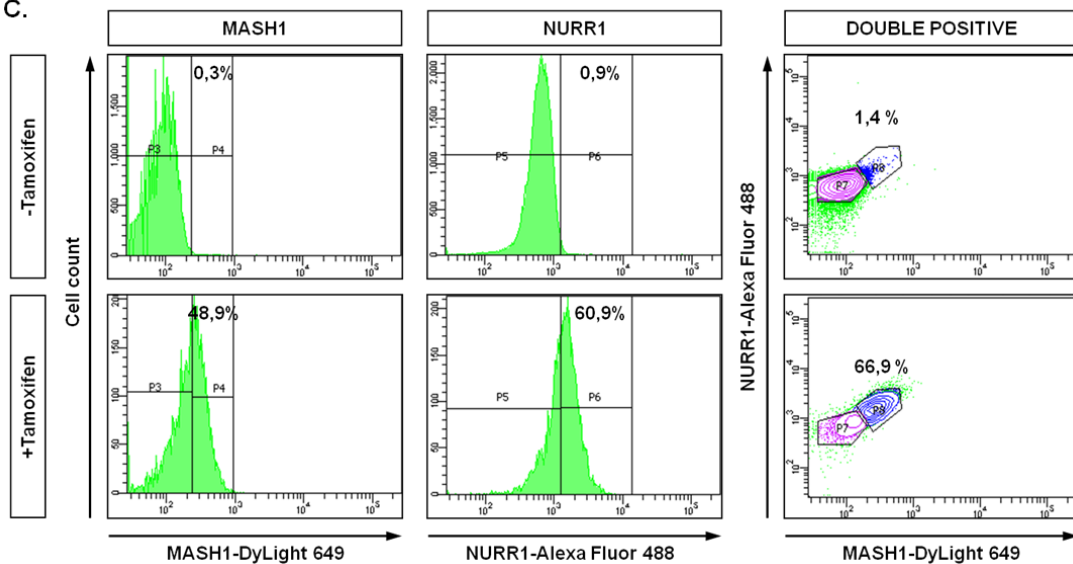


Figure 20: Induction of *MLN* expression in the *Rosa26^{CAG:MLN/+};CAG:MERCReMER* ESC line

- A. RNA levels of synthetic cDNAs *Mash1*, *Lmx1a* and *Nurr1* in the *Rosa26^{CAG:MLN/+};CAG:MERCReMER* ESC line with and without tamoxifen administration. The RNA levels were quantified by quantitative real time PCR, using the $\Delta\Delta CT$ method. The RNA levels were normalized to the “-tamoxifen” condition, which was set to 1. Unpaired t-test, * $p \leq 0.05$, $n=2$. Error bars represent mean \pm SD.

Results

B. Immunocytochemical staining with antibodies against MASH1 and NURR1 of *Rosa26^{CAG:MLN/+};CAG:MERCReMER* ESCs with and without tamoxifen administration.

C. Flow cytometry analysis with antibodies against MASH1 and NURR1 of *Rosa26^{CAG:MLN/+};CAG:MERCReMER* ESCs with and without tamoxifen administration.

Scale bars: 50 um (all pictures are the same size)

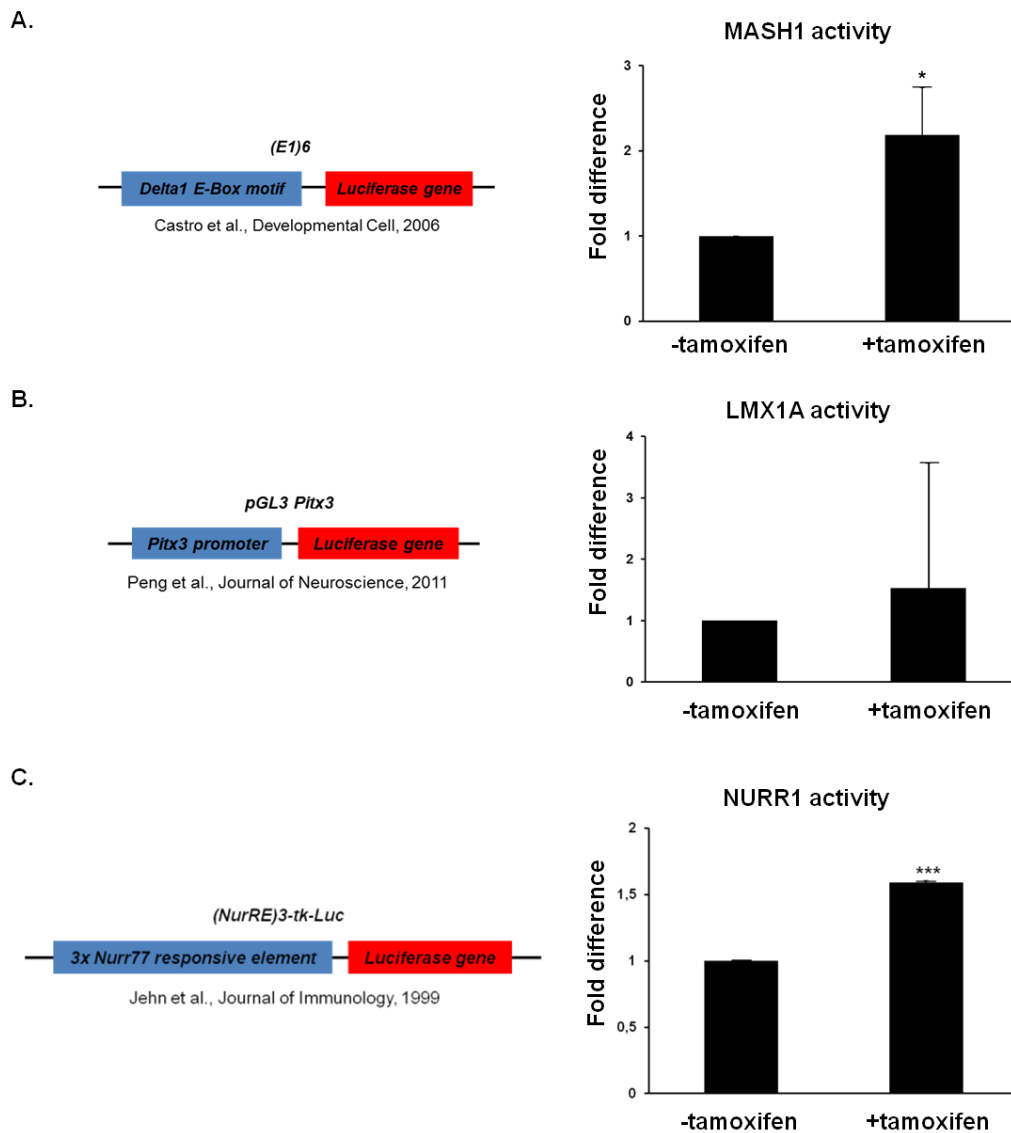


Figure 21: Activity of MASH1, LMN1A and NURR1 in the *Rosa26^{CAG:MLN/+};CAG:MERCReMER* ESC line. Luciferase reporter plasmids for MASH1 (A), LMN1A (B) and NURR1 (C) were transfected in *Rosa26^{CAG:MLN/+};CAG:MERCReMER* ESCs and the enzymatic activity was measured with (+Tam) and without (-Tam) tamoxifen administration. Unpaired t-test, *p ≤ 0.05, *** p ≤ 0,0001, n=3. Error bars represent mean ± SD.

4.2.3 Generation of a *Rosa26*^{CAG:MLN/+} knock-in mouse line

Having confirmed successful Cre-mediated recombination, induction of expression and functionality of the three TFs in vitro, I proceeded with the generation of a knock-in mouse line for the conditional overexpression of MLN in vivo. *Rosa26*^{CAG:MLN/+} ESCs were injected into BALB/c murine blastocysts, obtaining mice with a high percentage of chimerism (90%) (Figure 22A, B), exhibiting normal sperm quality (Figure 22C). To confirm that there was no leaky expression of the MLN transgene that could potentially hinder germline transmission, RNA isolated from the sperm of one of the chimeric mice was assessed for *Mash1*, *Lmx1a* and *Nurr1* expression levels, which were compared to the respective levels of *Rosa26*^{CAG:MLN/+};CAG:MERCReMER ESCs treated with tamoxifen. The result clearly confirmed no induction of the *MLN* transgene in the chimeric mouse (data not shown). After several breeding rounds with wild type mice, germline transmission was confirmed by PCR, depicting the presence of the *MLN* cassette recombined into the first intron of the *Rosa26* locus, hence generating heterozygous *Rosa26*^{CAG:MLN/+} mice (Figure 22D). The *Rosa26*^{CAG:MLNPTe/+} ESCs failed to contribute to the germline transmission, therefore further experiments concerning the *MLNPTe* construct were not pursued.

The *Rosa26*^{CAG:MLN/+} mouse line allows for the simultaneous overexpression of MLN, driven by the CAG promoter in specific cell types/tissues as instructed by expression of Cre recombinase. Therefore, a list of Cre/CreERt2 expressing mouse lines was selected for cell type/tissue specific excision of the “stop” cassette (Table 3).

Results

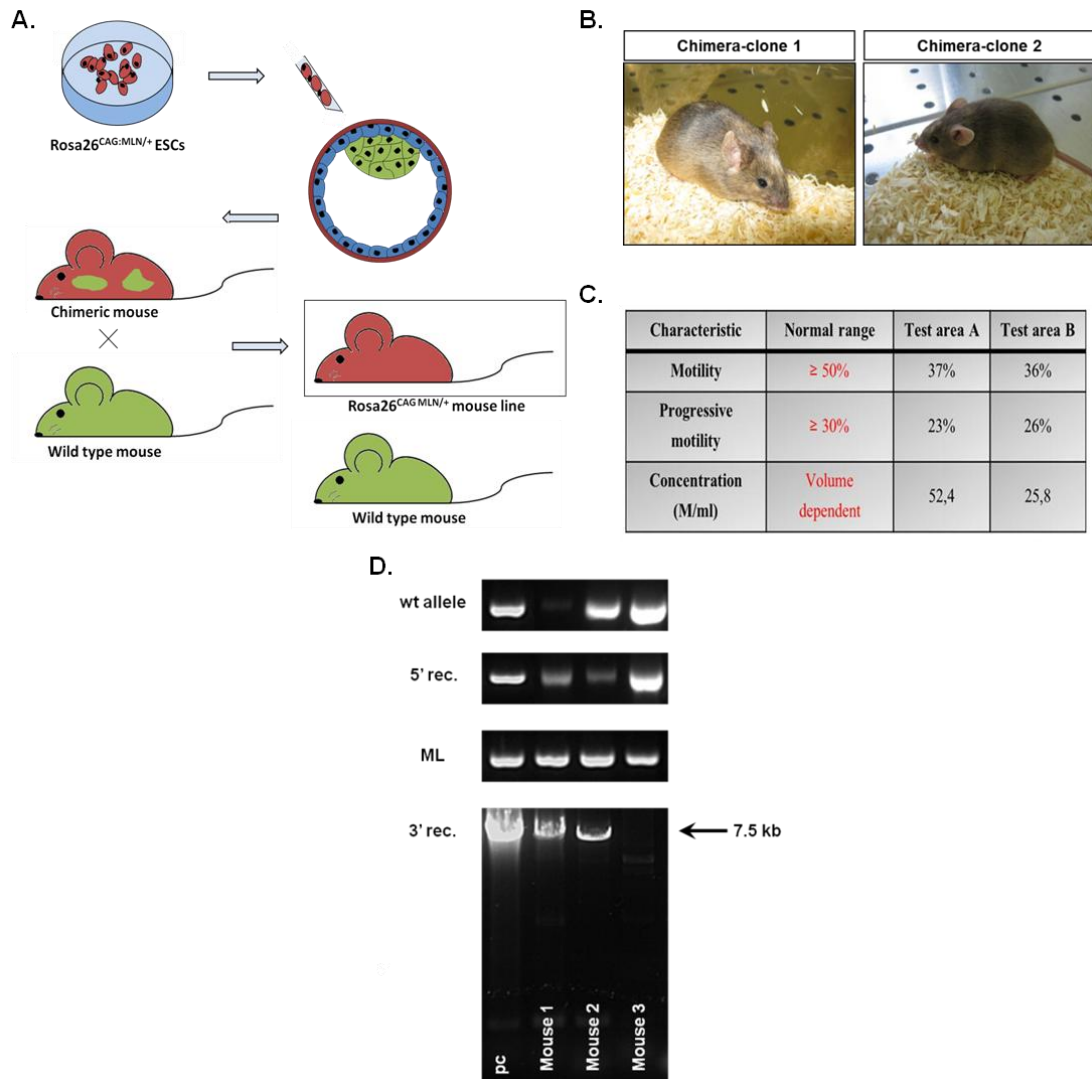


Figure 22: Generation of the *Rosa26*^{CAG:MLN/+} mouse line

- Schematic representation of the procedure from blastocyst injection to the generation of the *Rosa26*^{CAG:MLN/+} mouse line.
- Two chimeric mice generated after the injection of ESC clones 1 and 2 in blastocysts.
- Sperm quality test of a 90% chimeric mouse.
- PCR confirming germline transmission, with the 5' and 3' recombination, as well the presence of the MLN cassette in 2 of the 3 mice tested. These mice were also heterozygous for the CAG:MLN allele, as shown in the first panel of the PCR picture.

Mouse line	Tissue/Cell type	Reference
<i>En1</i> ^{Cre/+}	Ventral midbrain	Kimmelet al., 2000
<i>Glast</i> ^{CreERT2/+}	Glial cells/Astrocytes	Mori et al., 2006
<i>Nestin-Cre</i>	Dividing neurons/Neuronal precursor cells	Tronche et al., 1999
<i>Rosa26</i> ^{Cre/+}	All tissues	Soriano, 1999
<i>Tnap</i> ^{TgCreERT2/+}	Pericytes	Dellavalle et al., 2011

Table 3: Cre/CreERT2 mouse lines crossed to the *Rosa26*^{CAG:MLN/+} mouse line. Cre expression is driven by different promoters thus allowing conditional overexpression of *MLN* in different cell types/tissues.

4.2.4 In vivo reprogramming in different tissues

By crossing the *Rosa26*^{CAG:MLN/+} to mouse lines driving Cre or CreERT2 expression under specific endogenous promoters, *MLN* expression was induced in a controlled manner and in vivo reprogramming potential of specific cell types/tissues could be evaluated. Analysis of all the different cell types/tissues tested in the study is given below.

4.2.4.1 Expression of *MLN* in midbrain and hindbrain regions

The first mouse line selected to be crossed with the *Rosa26*^{CAG:MLN/+} mouse line was the *En1*^{Cre/+} (Kimmel et al., 2000). This line offered the advantage of assessing the reprogramming potential in an early and more plastic developmental stage, since *EN1* expression is induced during early embryogenesis (E8). Furthermore, *EN1* is expressed in the midbrain and hindbrain, offering thus the possibility of reprogramming a region proximal to the target cell type, i.e. the midbrain DA neurons, quality which could potentially facilitate the conversion process.

Pregnant mice were sacrificed and embryos were dissected at E13.5 to evaluate *MLN* induction and early potential reprogramming events (Figure

23A). Interestingly, some of the double heterozygous embryos (hereafter called *MLN/Cre*) exhibited lack of midbrain and hindbrain structures (Figure 23B), a feature closely resembling the phenotype observed in *En1* null mice (Wurst et al., 1994). The genotyping of the litter was performed with a primer pair also indicative of the Cre-mediated recombination as analyzed above (Figure 17) and thus successful deletion of the “stop” cassette in the double heterozygous animals was confirmed (Figure 23C).

However, immunohistochemical staining of coronal brain sections with antibodies against LMX1A and TH exhibited no ectopic LMX1A expression and subsequently no ectopic TH immunoreactivity in the areas where Cre is expressed (Figure 24). Thus, although Cre-mediated recombination is successful, MLN expression is not observed and conversion to DA neurons is not taking place. The phenotype of the double heterozygous embryos (Figure 23B) implies that MLN induction leads to some kind of defect, related to cell loss perhaps due to cell death.

To ensure that the lack of ectopic TH expression is not attributed to inadequate duration of expression of the reprogramming factors, a P0 litter was dissected. Surprisingly, none of the surviving pups were double heterozygous (*MLN/Cre*) in two examined litters, indicating that MLN expression at this early stage (E8, when EN1 is expressed) may be associated with embryonic lethality (Table 4). This observation correlates with the early postnatal lethality observed in *En1* null mice due to feeding inability (Wurst et al., 1994). Overall, the *En1^{Cre/+}* mouse line provided evidence that Cre mediated recombination occurs, which nevertheless did not result in MLN activation or subsequent reprogramming events.

Results

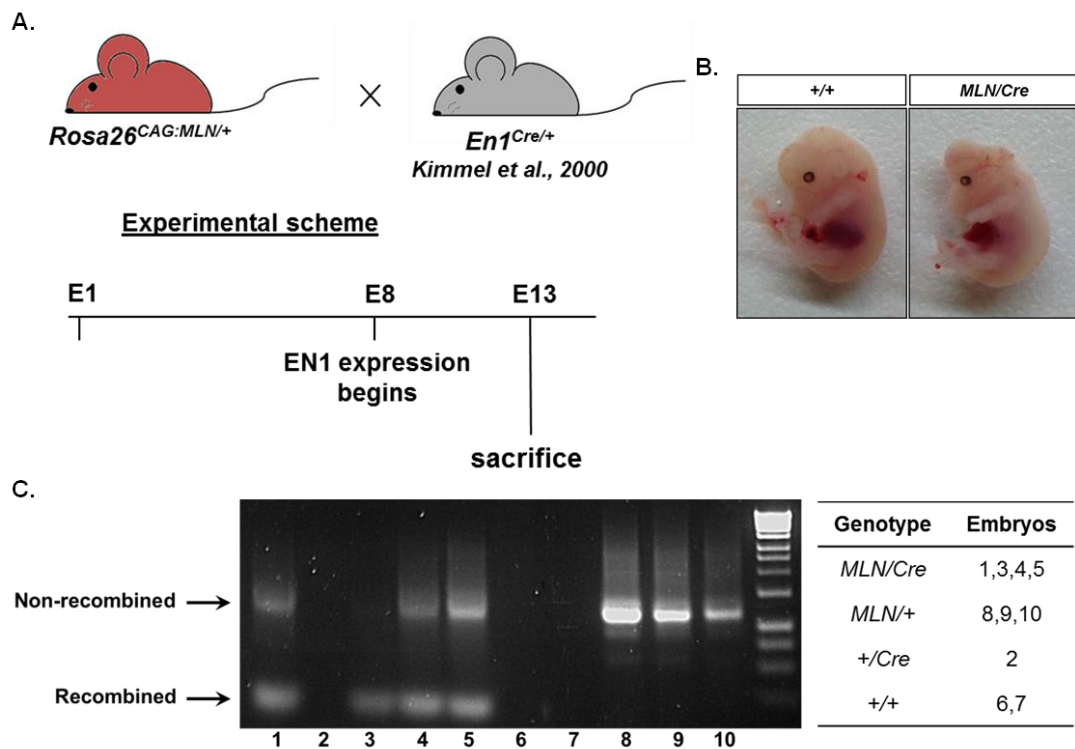


Figure 23: Breeding of *Rosa26*^{CAG:MLN/+} with *En1*^{Cre/+}

- Schematic representation of the breeding and experimental design.
- Sagittal aspect of a wild type (+/+) embryo and a double heterozygous (*MLN/Cre*) embryo at E13.5.
- PCR reaction for the genotyping of the *Rosa26*^{CAG:MLN/+};*En1*^{Cre/+} E13.5 offspring and the detection of Cre-mediated recombination of the *Rosa26*^{CAG:MLN/+} transgene in the brain.

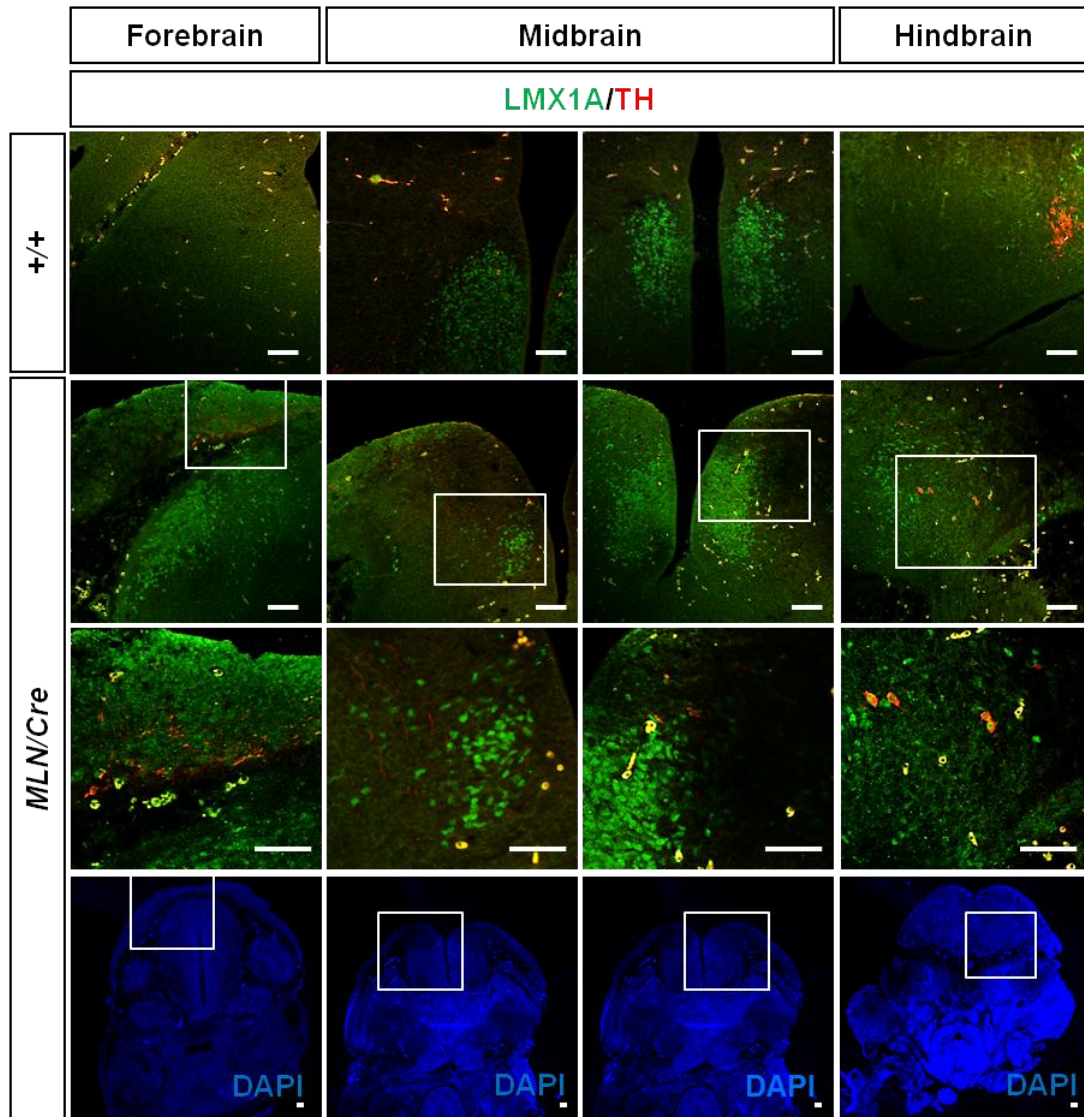


Figure 24: Ectopic MLN and TH expression are not induced in *Rosa26^{CAG:MLN/+};En1^{Cre/+}* E13.5 brains. Immunohistochemical staining with antibodies against LMX1A and TH in coronal brain sections of +/+ and *MLN/Cre* E13.5 embryos. Scale bars: 50 μ m

1 st litter		2 nd litter	
Genotype	Pups	Genotype	Pups
<i>MLN/Cre</i>	0	<i>MLN/Cre</i>	0
<i>MLN/+</i>	1	<i>MLN/+</i>	1
<i>+/Cre</i>	2	<i>+/Cre</i>	3
<i>+/+</i>	4	<i>+/+</i>	2

Table 4: Genotypes of two litters of P0 animals generated from the intercross between *Rosa26*^{CAG:MLN/+} and *En1*^{Cre/+}. The numbers in the second column of each table indicate the number of pups of the corresponding genotypes.

4.2.4.2 Controlled expression of MLN in astrocytes

Fibroblasts are so far the most widely used cell type for reprogramming towards the neuronal lineage. However, astrocytes have already been implicated in neuronal reprogramming in vitro and in vivo, being able to give rise to neuroblasts (Niu et al., 2013) or other neuronal populations (Berninger et al., 2007; Corti et al., 2012; Heinrich et al., 2010; Torper et al., 2013), including DA neurons (Addis et al., 2011b). Astrocytes are brain glial cells with a highly supportive role, providing neurons with trophic factors and protecting them against oxidative stress (Bachoo et al., 2004). They are characterized by lineage plasticity and are closely related to neurons, since they share the ectodermic origin and epigenetic memory, a fact which may facilitate their neuronal conversion, compared to fibroblasts (Tian et al., 2011).

To test whether astrocytes can be converted to DA neurons in vivo when overexpressing MLN, I crossed the *Rosa26*^{CAG:MLN/+} to the *Glast*^{CreERT2/+} mouse line (Mori et al., 2006). GLAST is expressed in astrocytes, in cells of the subgranular zone (SGZ) and the lateral ventricle, as well as in glial cells of the cerebellum (Bergmann glia) and of the retina (Müller cells) (Mori et al., 2006). By crossing the *Glast*^{CreERT2/+} to a *CAG-CAT-eGFP* transgenic mouse line (with *chloramphenicol acetyltransferase (CAT)* being flanked by *loxP*

Results

sites), a new line was generated, which displayed eGFP fluorescence upon Cre induction by tamoxifen administration (Kawamoto et al., 2000). This provided a useful tool for validating Cre-mediated recombination of the “stop” cassette in the *MLN* transgene.

PD mainly occurs in the adult period of life, therefore reprogramming of adult somatic cells to DA neurons is of utmost importance. For this reason, I was interested in converting astrocytes/glia cells in the adult stage. The littermates derived from the *Rosa26^{CAG:MLN/+};Glast^{CreERT2/+}, CAG-CAT-eGFP/+* breeding were injected with tamoxifen at P21, P23 and P25 and were sacrificed at P60, allowing a period of at least 35 days for reprogramming to take place (Figure 25A). Cre-mediated recombination was confirmed in the brain by PCR detecting the recombined and non-recombined version of the *MLN* transgene (Figure 25B).

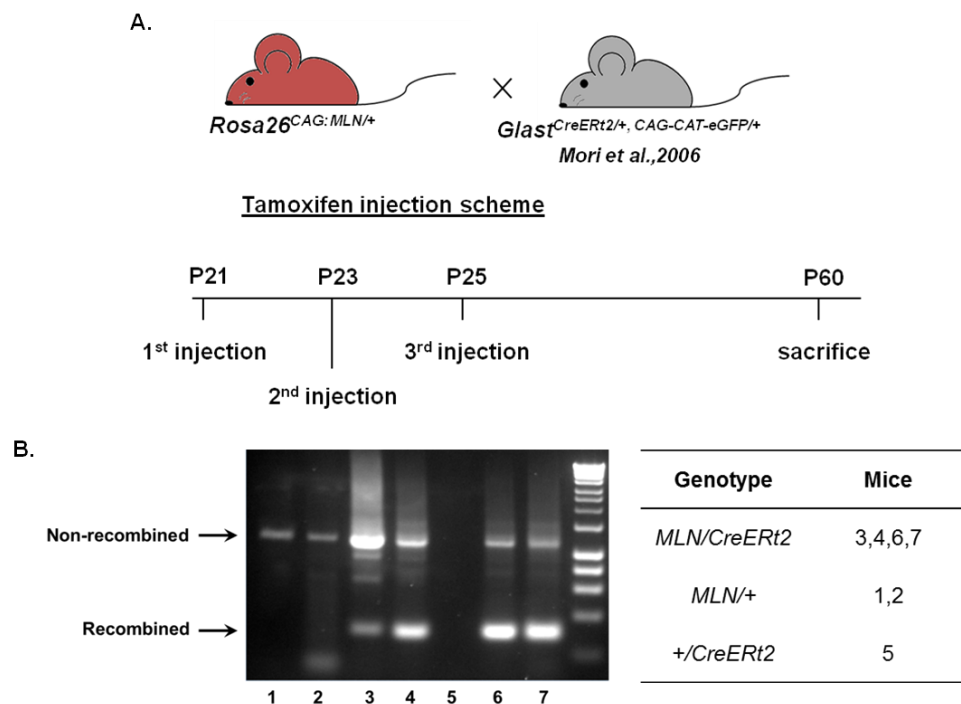


Figure 25: Breeding of *Rosa26^{CAG:MLN/+}* with *Glast^{CreERT2/+}, CAG-CAT-eGFP/+*

- A. Schematic representation of the breeding and experimental design.
- B. PCR reaction for the genotyping of the *Rosa26^{CAG:MLN/+};Glast^{CreERT2/+}, CAG-CAT-eGFP/+* P60 offspring after tamoxifen administration and the detection of CRE-mediated recombination of the *Rosa26^{CAG:MLN/+}* transgene in the brain.

However, *MLN* transgene expression was not observed in any of the GFP⁺ (Cre expressing) cells of the brain (Figure 26A). Similarly, no TH or DAT ectopic expression was detected, implying that reprogramming of astrocytes to DA neurons *in vivo* could not occur (Figure 26B). Also, general neuronal reprogramming was ruled out since there was no exogenous expression of the neuronal marker NEUN (Mullen et al., 1992) (Figure 27A). Quite remarkably though, the immunohistochemical staining of the brain sections with an antibody against DCX, a marker for newly generated neurons (Rao and Shetty, 2004), revealed absence of the DCX⁺ neurons normally residing in the dentate gyrus and olfactory bulb of the double heterozygous animals (*MLN/CreERT2*), that normally express GLAST (Figure 27B). It is likely that *MLN* overexpression was detrimental to the Cre expressing cells, which were diminished. Alternatively, *MLN* overexpression altered the molecular identity of these cells and they no longer turned on DCX. However, the complete absence of DCX protein implies inhibition of *Dcx*-driven neurogenesis and not a gradual change in the expression profile of these cells.

This outcome may be the result of prolonged expression of *MLN* (35 days). To avoid this issue, I followed the same breeding scheme, but dissected the pups at P30, only 5 days after the last tamoxifen injection (Figure 28A). The genotyping of the littermates revealed successful Cre-mediated recombination in the brain upon tamoxifen administration (Figure 28B).

However, the same outcome was observed: there is no expression of *MLN* as shown by immunohistochemical staining with antibodies against LMX1A and NURR1 (Figure 29A, B), as well as no ectopic TH expression (Figure 29C).

Overall, the breeding of the *Rosa26*^{CAG:MLN/+} to the *Glast*^{CreERT2/+} mouse line provided further evidence that the “stop” cassette can be excised by the action of Cre recombinase in the brain (astrocytes and glial cells), but failed to induce *MLN* and TH or DAT expression at both time points tested. Moreover, the line displayed absence of naturally occurring DCX⁺ neurons in highly neurogenic regions of the brain (dentate gyrus, lateral ventricle). These

results pointed to potential problems of the *MLN* transgene and the need for further investigation of other potential cell types to be reprogrammed at different developmental stages.

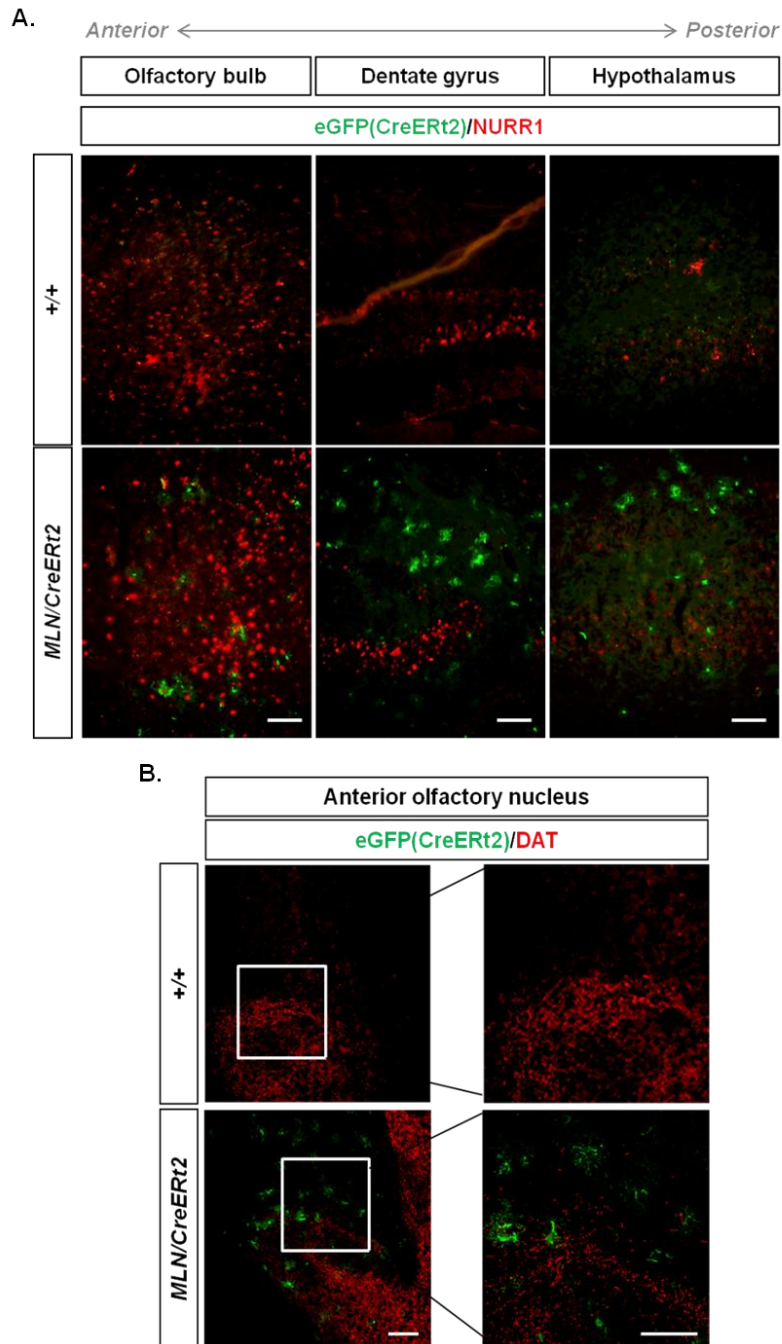


Figure 26: MLN and ectopic DAT expression are not induced in *Rosa26^{CAG:MLN/+};Glast^{CreERT2/+}, CAG-CAT-eGFP/+* P60 brains. Immunohistochemical staining with antibodies against NURR1 (A) and DAT (B) in sagittal brain sections of +/+ and *MLN/CreERT2* P60 mice. The green signal corresponds to eGFP expression, which is indicative of CreERT2 activity. Scale bars: 50 um (all pictures are the same size)

Results

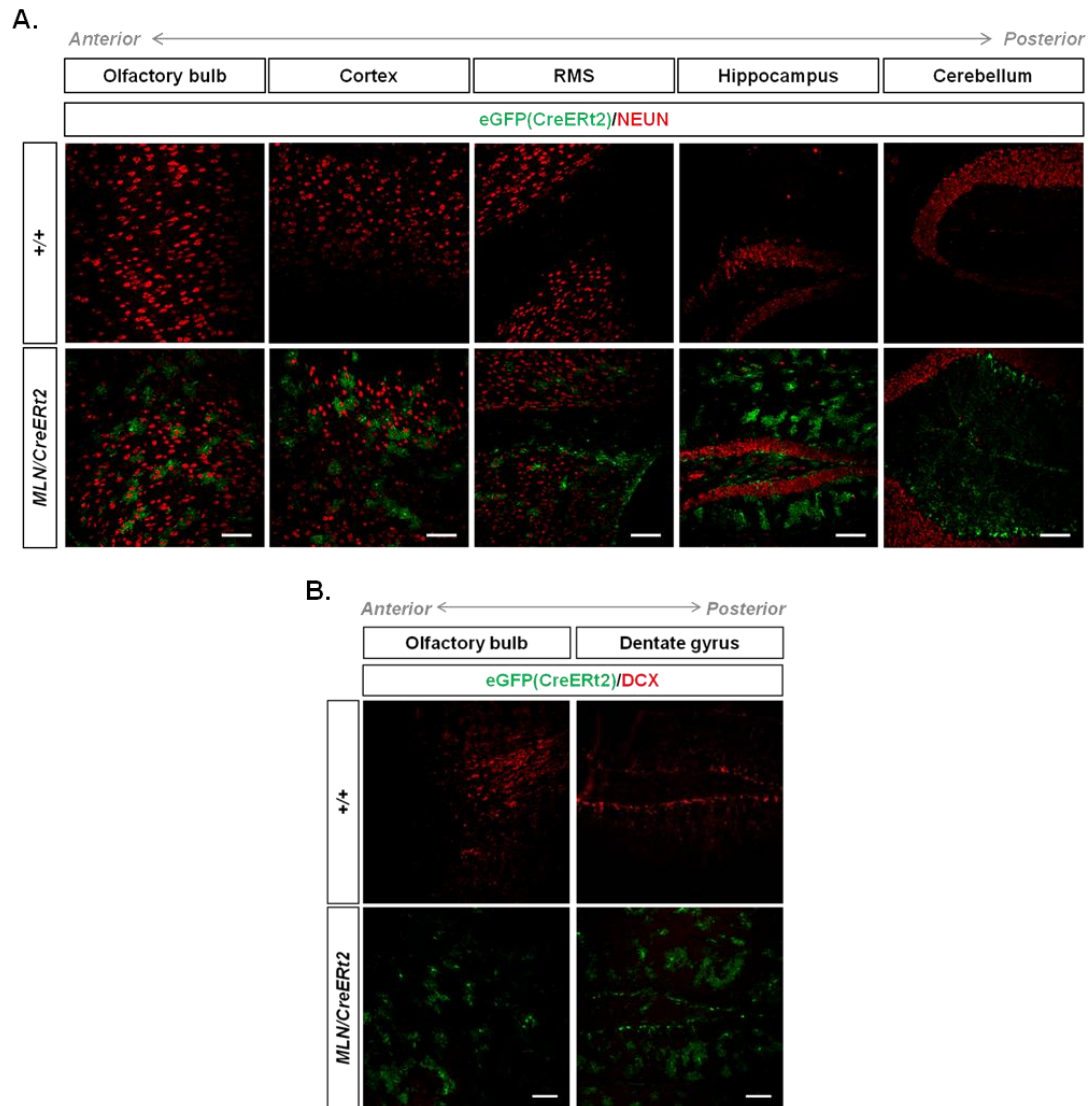


Figure 27: No ectopic NEUN but reduced DCX expression in *Rosa26^{CAG:MLN/+};Glast^{CreERT2/+}, CAG-CAT-eGFP/+* double heterozygous P60 brains. Immunohistochemical staining with antibodies against NEUN (A) and DCX (B) in sagittal brain sections of +/+ and *MLN/CreERT2* P60 mice. The green signal corresponds to eGFP expression, which is indicative of CreERT2 activity. Scale bars: 50 μ m (all pictures are the same size)

Results

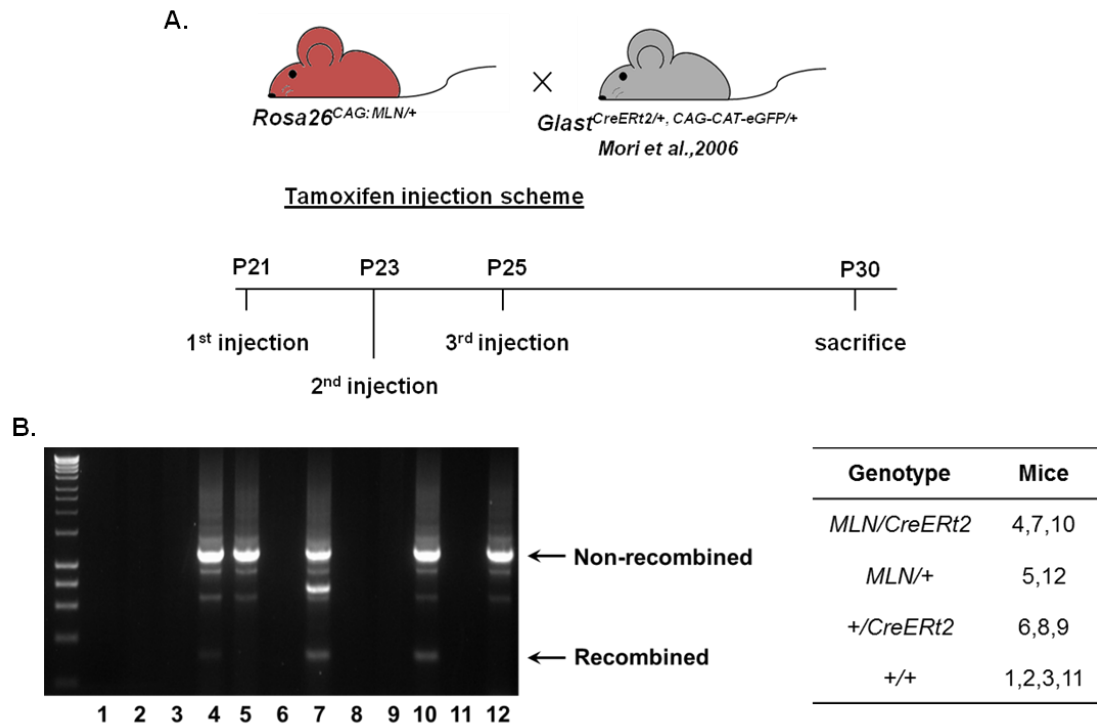


Figure 28: Breeding of *Rosa26*^{CAG:MLN/+} with *Glast*^{CreERT2/+}, CAG-CAT-eGFP/+

- A. Schematic representation of the breeding and experimental design.
- B. PCR reaction for the genotyping of the *Rosa26*^{CAG:MLN/+}; *Glast*^{CreERT2/+}, CAG-CAT-eGFP/+ P30 offspring after tamoxifen administration and the detection of CRE-mediated recombination of the *Rosa26*^{CAG:MLN/+} transgene in the brain.

Results

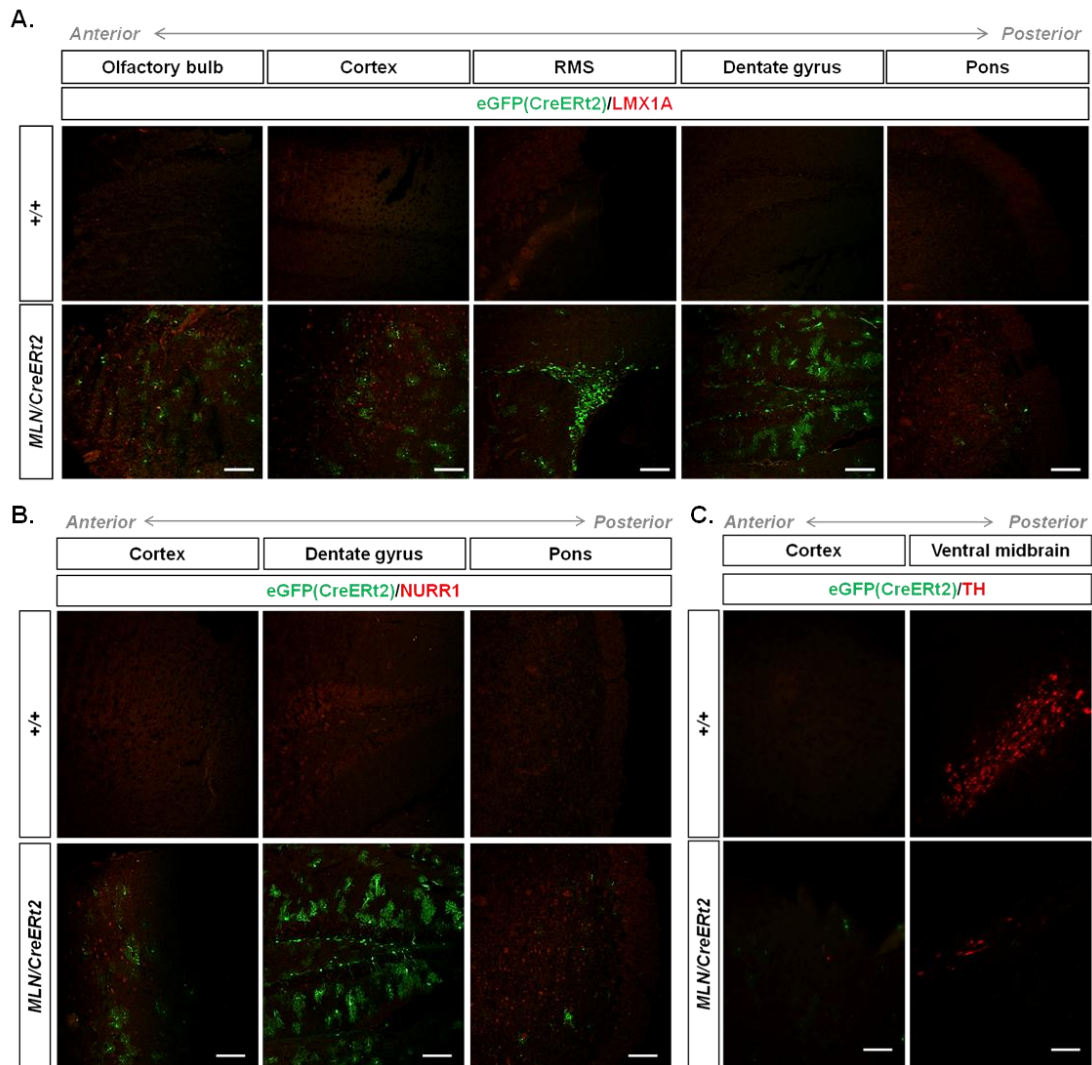


Figure 29: MLN expression is not induced in brains of *Rosa26*^{CAG:MLN/+}; *Glast*^{CreERT2/+}, *CAG-CAT-eGFP/+* P30 animals. Immunohistochemical staining with antibodies against LMX1A (A), NURR1 (B) and TH (C) in sagittal brain sections of +/+ and *MLN/CreERT2* P30 mice. The green signal corresponds to eGFP expression, which is indicative of CreERT2 activity. Scale bars: 50 μ m (all pictures are the same size)

4.2.4.3 Controlled expression of MLN in pericytes

Another cell type that has been used for neuronal reprogramming is pericytes (Karow et al., 2012). These cells are abundant in blood vessels in the brain and elsewhere in the body (liver, heart, kidney, bone), offering thus an abundant cell source for reprogramming. Since they are implicated in healing after brain injury, it could provide a suitable source for replenishing lost neurons (Nivet et al., 2013).

TNAP (tissue non-specific alkaline phosphatase), is expressed in several tissues in the body (Hotton et al., 1999) and in pericytes (Dellavalle et al., 2011). After crossing the *Tnap*^{TgCreERT2/+} to the *Rosa26*^{CAG:MLN/+} mouse line, I injected the progeny three times with tamoxifen at P21, P23 and P25 (Figure 30A). Interestingly, all double heterozygous mice (*MLN/CreERT2*) died by P26, implying that the induction of MLN expression triggered problems in essential tissues (Figure 30B).

To avoid lethality and produce mice for examination, I followed the same breeding scheme once again, however injected tamoxifen only twice (P21, P23). Nonetheless, the *MLN/CreERT2* mice already exhibited lethargy and hypokinesia. The mice were sacrificed at P25 and were subsequently analyzed for MLN expression and reprogramming potential (Figure 31).

Once again, similarly to the *Glast*^{CreERT2/+} mouse line, there was no MLN expression in the brain (Figure 32A), although there was ectopic MLN expression observed in the liver of the *MLN/CreERT2* animals, as shown by immunohistochemical staining with antibodies against the three TFs (Figure 32B). This observation indicated silencing of the *MLN* transgene in the brain, although CreERT2-mediated recombination was apparent by eGFP expression (Figure 32A).

CpG methylation is an epigenetic modification occurring in eukaryotic genomic DNA and is often associated with heterochromatin, which typically characterizes inactive genomic regions (Jaenisch and Bird, 2003; Pikaart et al., 1998; Tate and Bird, 1993). Since it is correlated with differential gene expression and to rule out or confirm a possible role in MLN expression in vivo, I performed an analysis for the detection of the methylation status of the *CAG MLN* sequence in brain and liver of these animals.

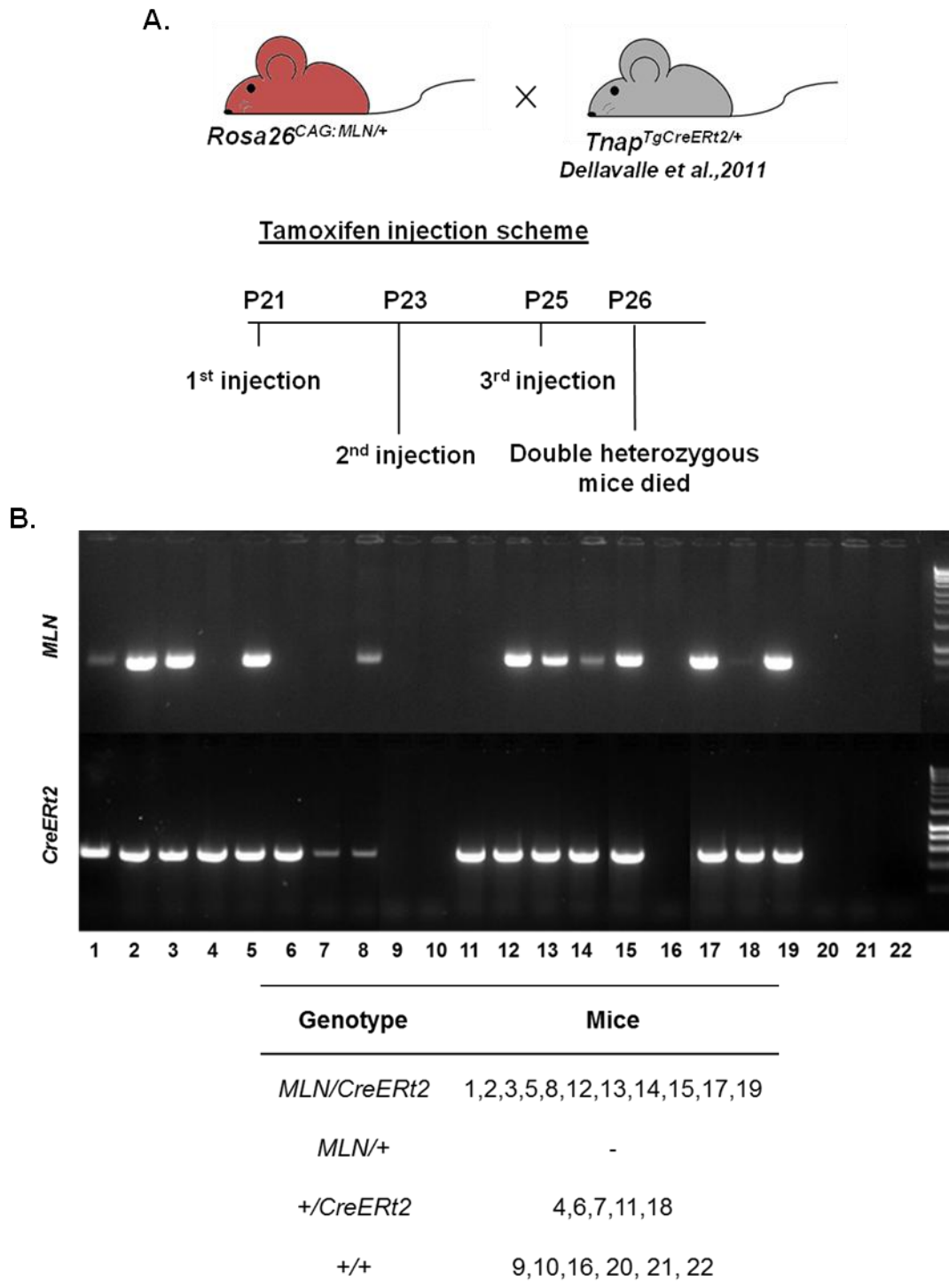


Figure 30: Breeding of *Rosa26*^{CAG:MLN/+} with *Tnap*^{TgCreERT2/+}

- A. Schematic representation of the breeding and experimental design.
- B. PCR reaction for the genotyping of the *Rosa26*^{CAG:MLN/+}; *Tnap*^{TgCreERT2/+} offspring.

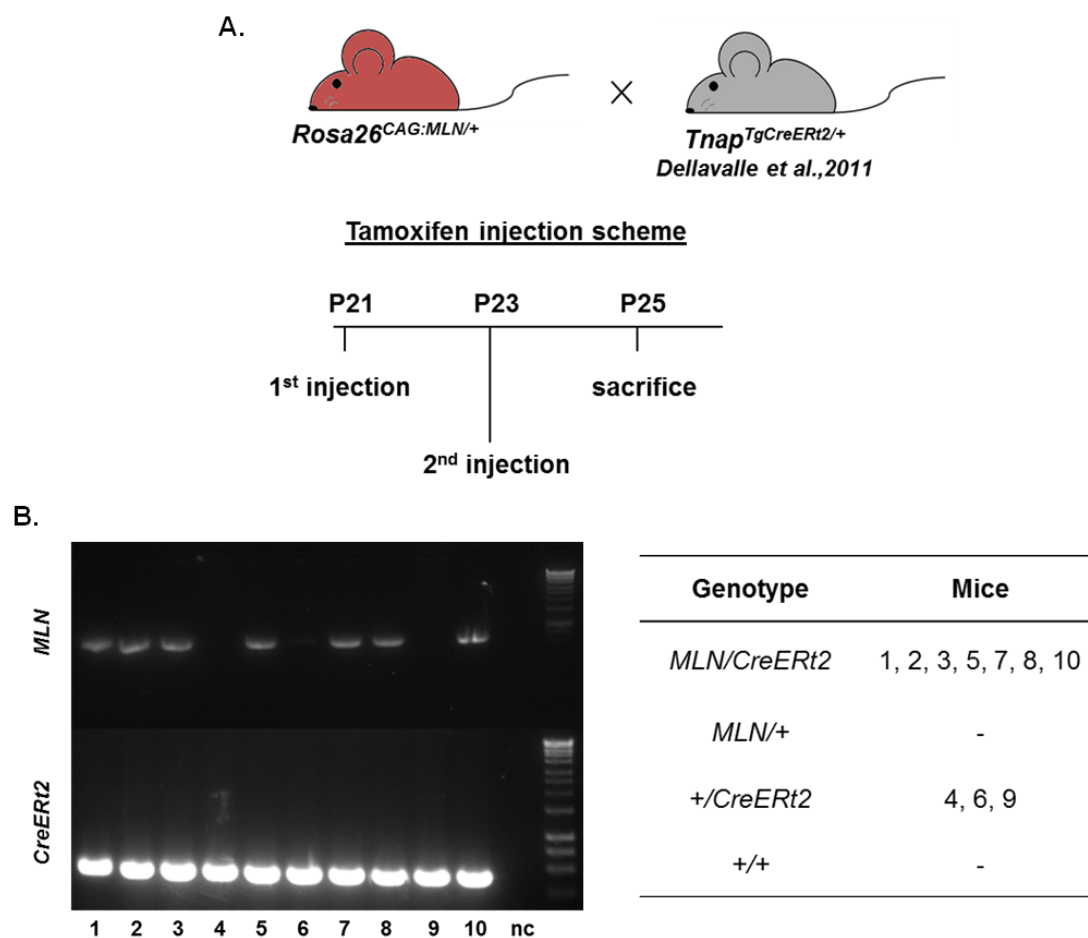


Figure 31: Breeding of *Rosa26*^{CAG:MLN/+} with *Tnap*^{TgCreERT2/+}

- A. Schematic representation of the breeding and experimental design.
- B. PCR reaction for the genotyping of the *Rosa26*^{CAG:MLN/+}; *Tnap*^{TgCreERT2/+} P25 offspring.

Several restriction enzymes can be used that exhibit differential sensitivities towards methylated genomic DNA. PCR amplification of the resulting products revealed differences in the methylation pattern of brain and liver tissue of the *MLN/CreERT2* offspring (Figure 32C). Both enzymes utilized here, *HpaII* and *MspI*, digest downstream of the first cytosine of the CCGG sequence. However, *HpaII* cannot catalyze the digestion when either of the cytosines is methylated. *MspI* on the other hand can successfully digest DNA when the internal cytosine is methylated (C $\underline{\underline{C}}$ GG), but is sensitive to the methylation of the external cytosine (C $\underline{\underline{C}}$ GG). Therefore, the presence of a PCR product after digestion with *HpaII* reveals methylated and thus undigested DNA, whereas the presence of a PCR product after digestion with

MspI, indicates methylation of the external cytosine only and thus undigested DNA (Oakeley, 1999). Using this scheme, differences in methylation patterns could be identified.

The reaction resulted in PCR products when *HpaII*-digested DNA was utilized as a template in both brain and liver for the *Mash1* and *Nurr1* sequence, but revealed differential methylation pattern of the *Mash1* sequence among the two tissues, showing methylation of the external cytosine only in the brain and not in the liver (*MspI* digestion). These results indicate that part of the *Mash1* and *Nurr1* sequences, which are GC-rich, are methylated in both tissues. More importantly, it was proven that methylation of different cytosine residues occurs in the *Mash1* sequence among different tissues. This observation implies possibly differential transcriptional regulation of the *CAG MLN* transgene among the *MLN/CreERT2* brains and livers (Figure 32C).

According to earlier results (Figure 32 A, B), MLN are expressed in the liver, but not in the brain. This is possibly a consequence of differential methylation of the *Mash1* in the brain compared to the liver. This effect could additionally be the result of methylation of the *CAG* promoter, which due to technical difficulties of amplification of this repeat-rich area, could not be assessed. However, the lack of MLN expression in the brain could also be the consequence of increased degradation of the large *MLN* transcript (around 4kb). This is a likely possibility that coincides with the observation that large transcripts are susceptible to degradation in the brain to a bigger extent than in other tissues (Zetoune et al., 2008).

Although MLN expression was induced only for a short period before sacrificing the animals (4 days from first tamoxifen injection), I analyzed if liver cells could be reprogrammed in vivo to TH⁺ neurons/cells. As expected, due to inadequate duration of the TF expression, there was no reprogramming observed (data not shown).

Taking into account the results obtained from the breeding to the *Tnap^{TgCreERT2/+}* mouse line, it is concluded that a) MLN are not expressed in

Results

the brain possibly due to differential methylation pattern of the transgene and/or potential decreased mRNA stability in the brain, b) MLN induction is most probably related to rapid death of the mice and c) there is no reprogramming to DA neurons in the liver-where MLN is expressed-4 days after the first tamoxifen injection.

Results

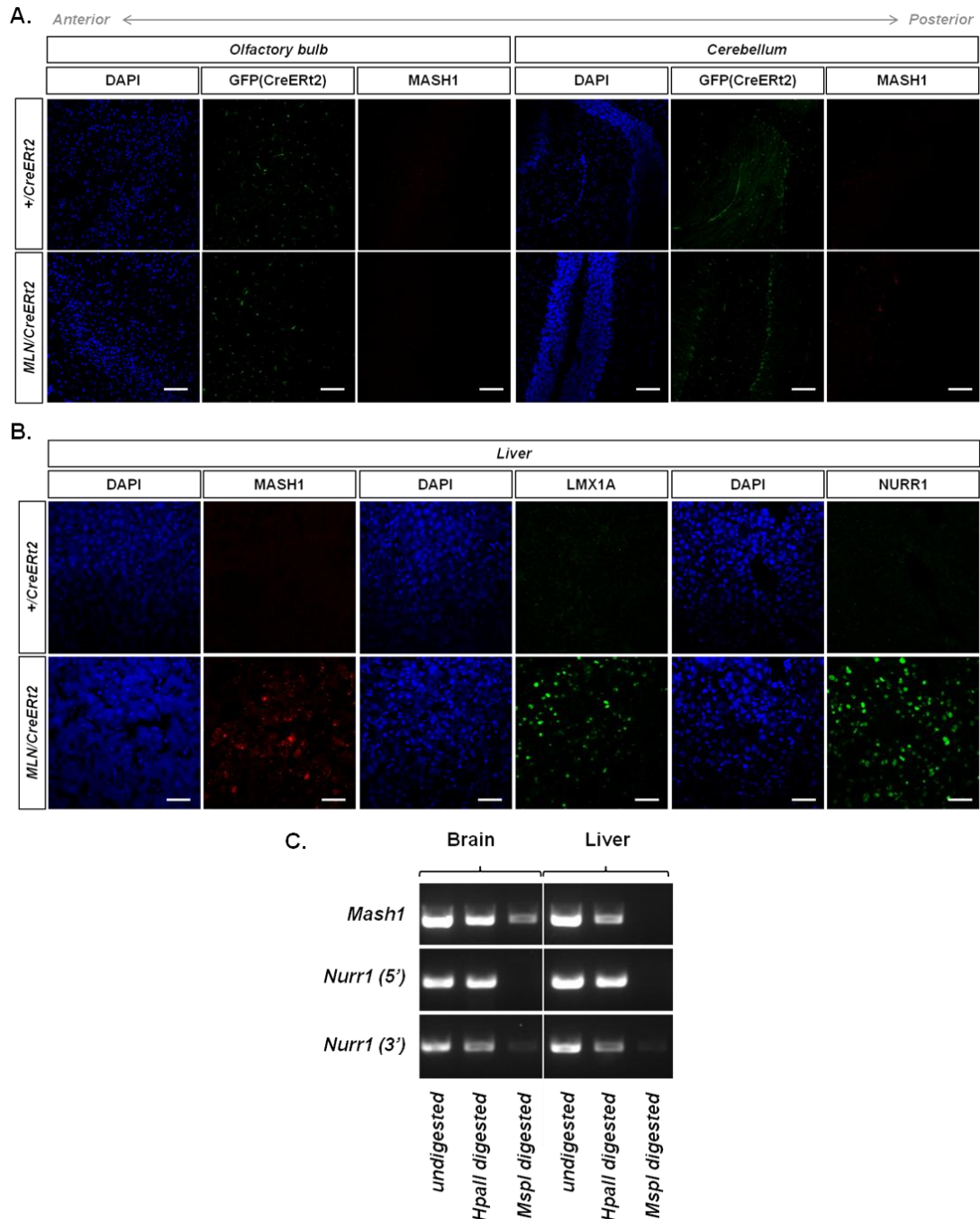


Figure 32: MLN expression is induced in livers but not in brains of *Rosa26^{CAG:MLN/+};Tnap^{TgCreERT2/+}* P25 animals

A, B. Immunohistochemical staining with antibodies against MASH1, LMX1A and NURR1 in sagittal brain sections (A) and livers (B) of +/CreERT2 and MLN/CreERT2 P25 mice. The green signal in the brain corresponds to GFP expression, which is indicative of CreERT2 activity.

C. Methylation status of *Mash1* and *Nurr1*. Brain and liver genomic DNA of MLN/CreERT2 animals were digested with *HpaII* and *MspI* and were used as templates for PCR amplification. The presence or absence of PCR products is indicative of the methylation status of the given sequences.

Scale bars: 50 μ m (all pictures are the same size)

Upon immunohistochemical staining with antibodies against the three TFs, it was noteworthy to observe that although LMX1A and NURR1 were expressed in areas where Cre catalyzed recombination of the “stop” cassette (Nestin expressing cells), ectopic MASH1 was not detected (Figure 34). This could potentially be attributed to a technical issue of the staining procedure.

However, there were no reprogramming events observed, as shown by immunohistochemical staining with an antibody against TH (Figure 34). This prompted me to check at later developmental stages, when MLN would be expressed for longer periods. At E19.5 there was still no reprogramming to DA neurons observed (data not shown). Interestingly, when I dissected pups at birth (P0), there were no double heterozygous (*MLN/Cre*) mice surviving, indicating again, as in the case of the *Rosa26^{CAG:MLN/+};En1^{Cre/+}* intercross (Table 4), embryonic lethality possibly correlated to the MLN overexpression.

Overall, the *Nestin-Cre* mouse line suggested problematic transgene expression, since not all of the TFs were detected in the CNS of the double heterozygous embryos, absence of reprogramming events and lethality at later stages upon MLN induction.

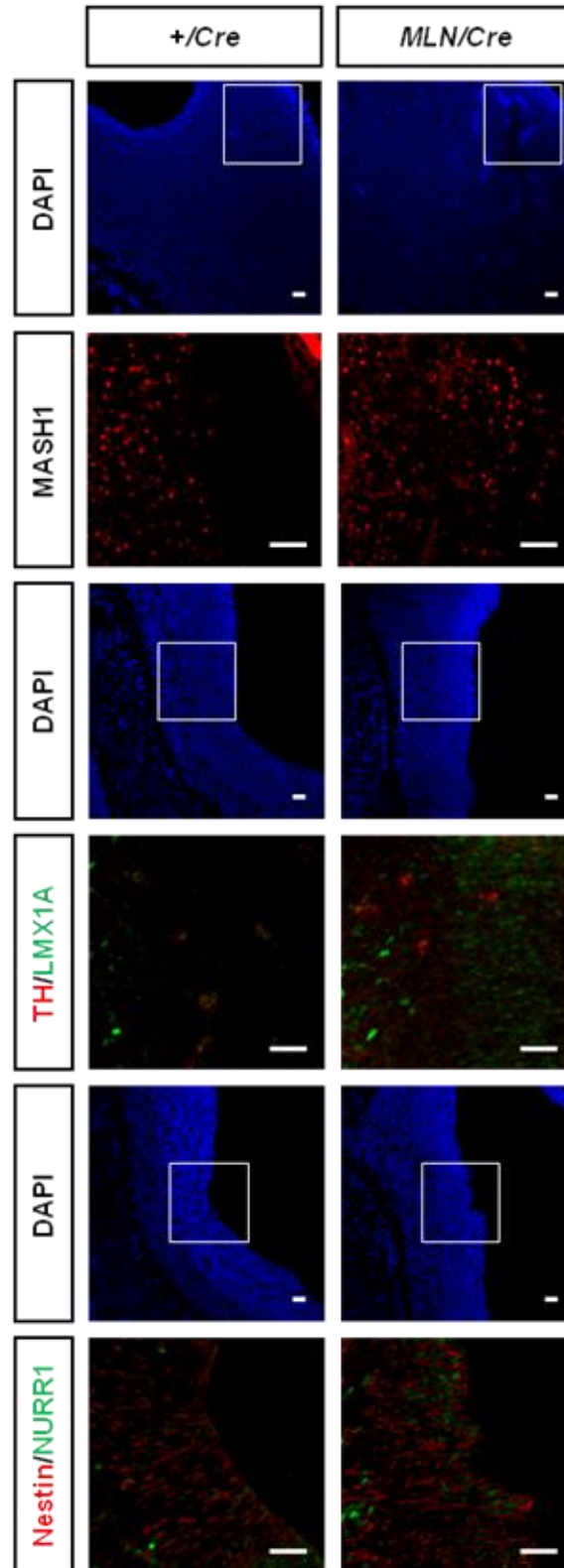


Figure 34: MLN expression is partially induced in *Rosa26^{CAG:MLN/+};Nestin-Cre E11.5* embryos. Immunohistochemical staining with antibodies against MASH1, LMX1A, NURR1, Nestin and TH in sagittal whole embryo sections of *+/Cre* and *MLN/Cre* at E11.5. Hindbrain regions are depicted. Scale bars: 50 μ m

4.2.4.5 Expression of MLN in all tissues

The results of crosses analyzed so far revealed no hints of in vivo reprogramming to DA neurons. Providing a proof-of-principle for in vivo reprogramming by MLN overexpression was necessary to prove the reprogramming potential of the generated mouse line. Hence the *Rosa26*^{Cre/+} mouse line was selected for the in vivo conversion of every mouse tissue/cell type by activation of Cre recombinase under the control of the *Rosa26* locus (Soriano, 1999).

Rosa26 is activated during the early stages of embryonic development and remains activated throughout adult life in all tissues. The ubiquitous Cre and consequently MLN expression led to lethality, as confirmed by the absence of double heterozygous animals at birth (data not shown). This provided another indication that extended MLN overexpression triggers death and precludes reprogramming.

4.2.5 In vitro activation and reprogramming potential of *Rosa26*^{CAG:MLN/+} mouse embryonic fibroblasts

Attempts to reprogram in vivo through the overexpression of MLN were so far unsuccessful. To assess whether the absence of reprogramming was due to inability of the polycistronic MLN to trigger reprogramming in vivo or due to general technical limitations of the system utilized, it was important to provide evidence that conversion to TH⁺ neurons was possible in vitro. Therefore, I isolated MEFs from the *Rosa26*^{CAG:MLN/+} mouse line and transfected them with *pCAG-Cre-bpA* to induce the MLN expression through Cre-mediated recombination. As a negative control, I transfected the MEFs with the *pmaxGFP* vector, which revealed 90% transfection efficiency (data not shown). Cre-mediated recombination was confirmed by a PCR reaction using primers as described above (Section 4.2.2) (Figure 35A), while expression of the TFs was also detected in the MEFs transfected with Cre (Figure 35B). However, there was no reprogramming observed in vitro either (Figure 35C). Yet there was increased cell death in the MLN expressing

Results

cultures, which could be related either to the previously observed death in vivo due to problems of the MLN transgene, or to the reprogramming medium, which lacks serum, or to a combination of both.

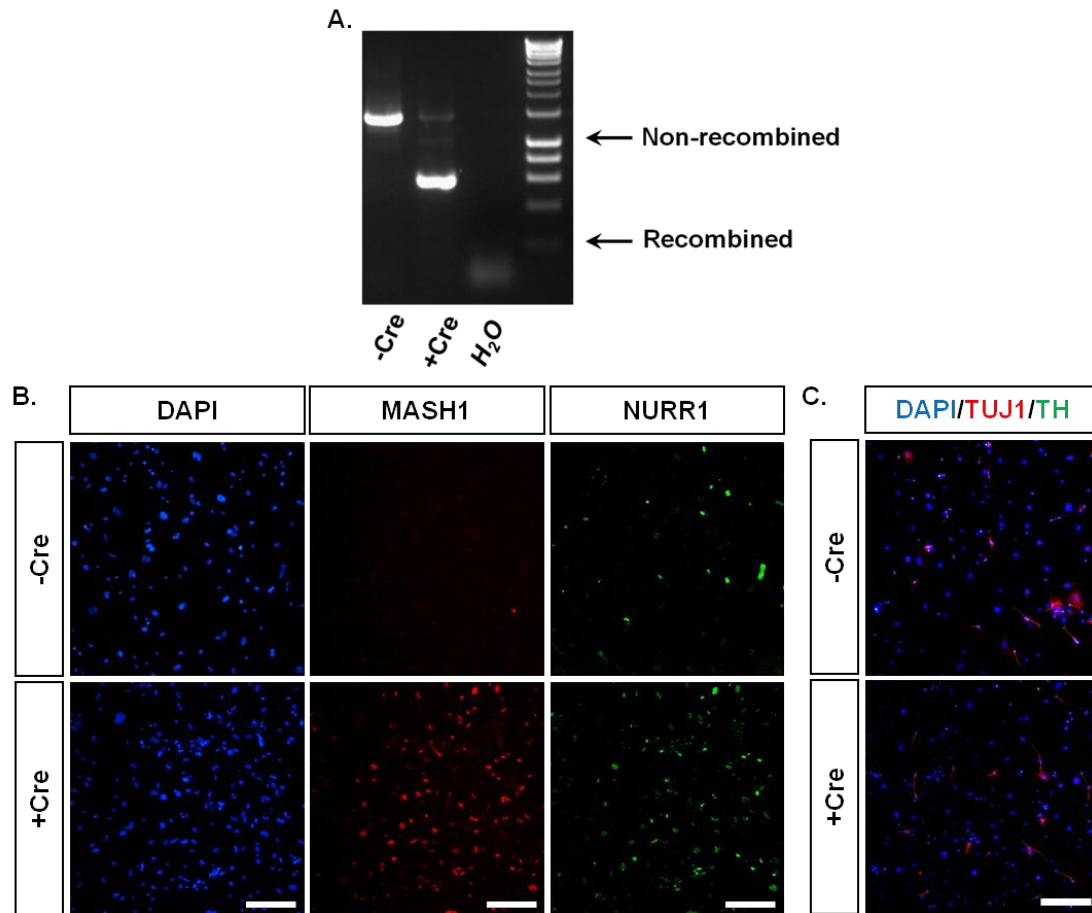


Figure 35: *Rosa26*^{CAG:MLN/+} MEFs are not reprogrammed in vitro

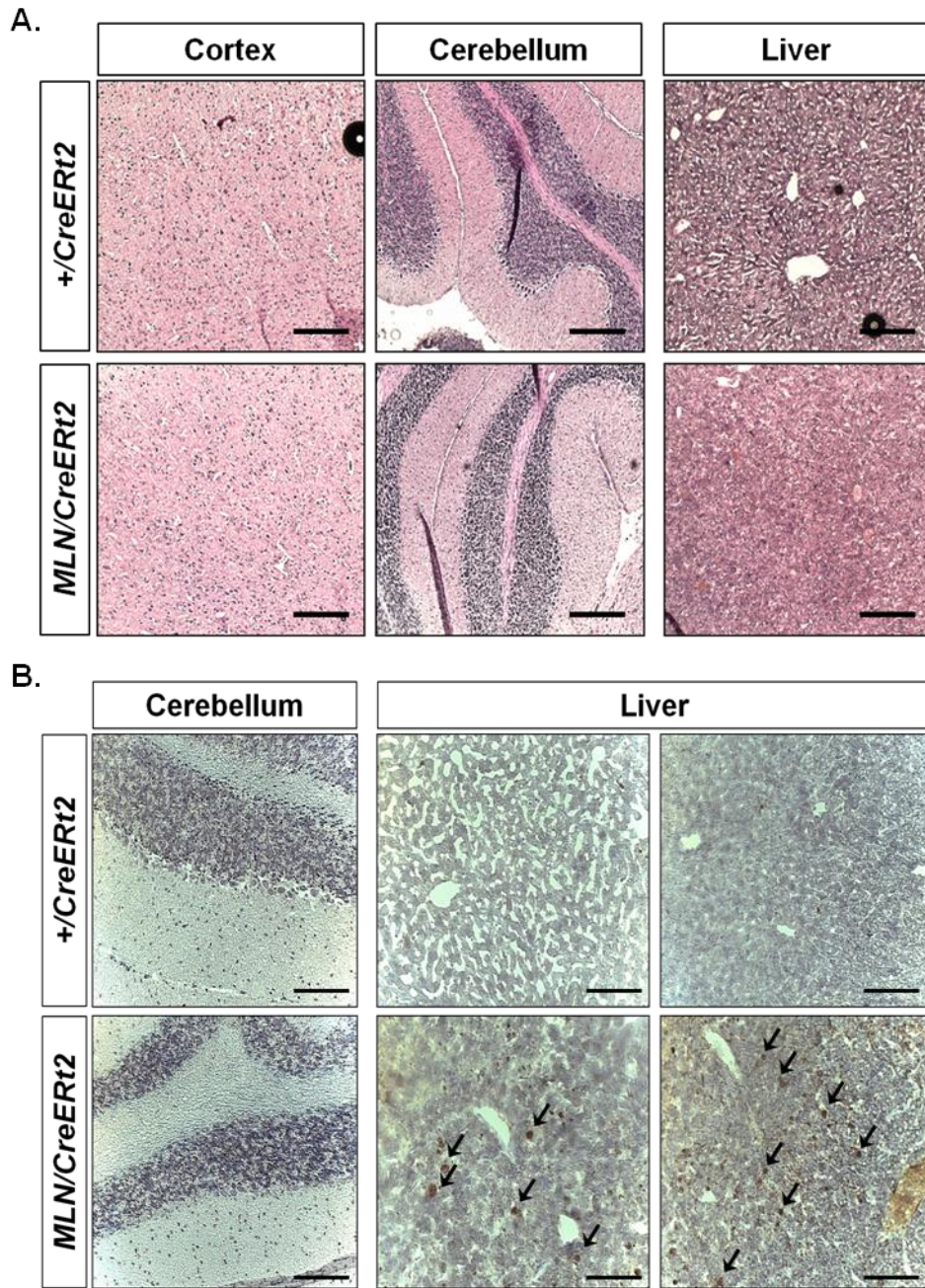
- PCR reaction for the detection of CRE-mediated recombination with (+Cre) or without (-Cre) transfection of the *pCAG-Cre-bpA* plasmid.
- Immunocytochemical staining with antibodies against MASH1 and NURR1 in *Rosa26*^{CAG:MLN/+} MEFs transfected with *pCAG-Cre-bpA*. The green signal in the control condition (-Cre) is background immunoreactivity.
- Reprogramming potential of *Rosa26*^{CAG:MLN/+} MEFs into dopaminergic neurons with (+Cre) or without (-Cre) transfection of the *pCAG-Cre-bpA* plasmid as assessed by immunofluorescent staining using antibodies against TUJ1 and TH. The TUJ1+ cells in both -Cre and +Cre conditions are likely contaminating neurons from the spinal cord.

Scale bars: 50 μ m (all pictures are the same size)

4.2.6 MLN expression induces endoplasmic-reticulum stress and the unfolded protein response

To observe the histology of mice where death was observed upon MLN induction, I performed hematoxylin-eosin staining on brain and liver sections of the *Rosa26*^{CAG:MLN/+}; *Tnap*^{TgCreERT2/+} P25 mice. There were no obvious abnormalities or disturbed structure in the brain; however, the liver sections revealed disorganized cellular morphology and loss of cellular integrity and structure (Figure 36A). The liver, as opposed to the brain, exhibited increased DNA fragmentation, as shown by a TUNEL assay (Figure 36B), indicative of apoptotic cell death, which was confirmed by immunohistochemical staining with an antibody against cleaved Caspase-3 (Figure 36C). In addition to apoptotic cell death, inflammation was also observed when MLN were expressed, as many cells were positive for C-Reactive Protein (CRP), an inflammation marker (Figure 36D); nevertheless there was no clear difference in the numbers of activated macrophages among the control and the double heterozygous animals, as shown by immunohistochemical staining with an antibody against F4/80, a marker for macrophages, a major player in inflammatory responses (Bianchi and Manfredi, 2014) (Figure 36E). Altogether, these results reveal liver failure accompanied by apoptotic cell death and inflammation.

Cell death was also observed when trying to differentiate the *Rosa26*^{CAG:MLN/+}; *CAG:MERC* ESC clones to DA neurons. When treated with tamoxifen and incubated under neuronal differentiation conditions, the cells died rapidly. To confirm cell death, the cells were followed-up every day using an antibody against cleaved Caspase-3, which revealed significantly more apoptotic cells when MLN expression was induced (with tamoxifen) compared to the control (without tamoxifen). Four days after the induction all the ESCs were dead, rendering me unable to estimate their differentiation potential (Figure 37).



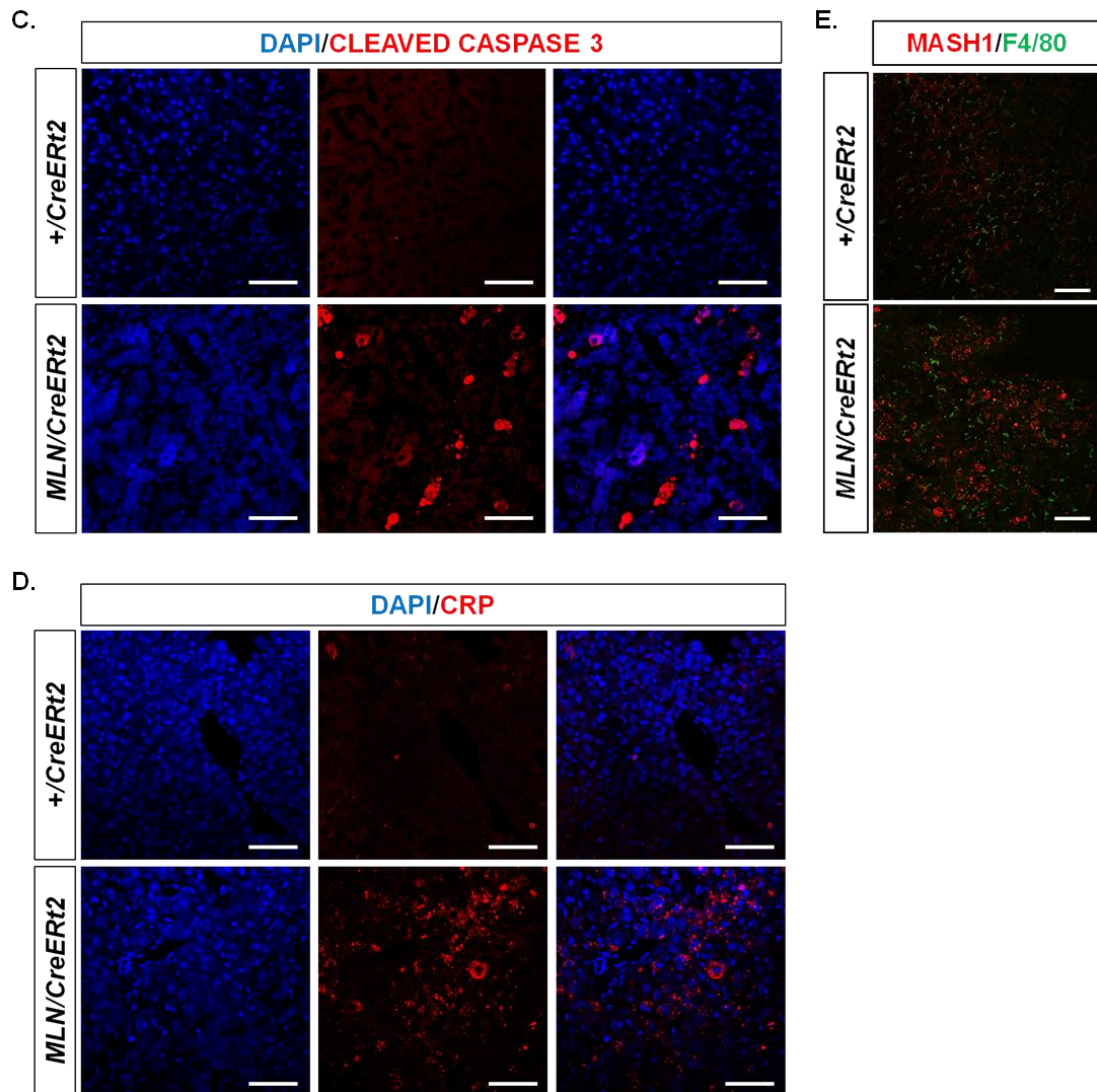
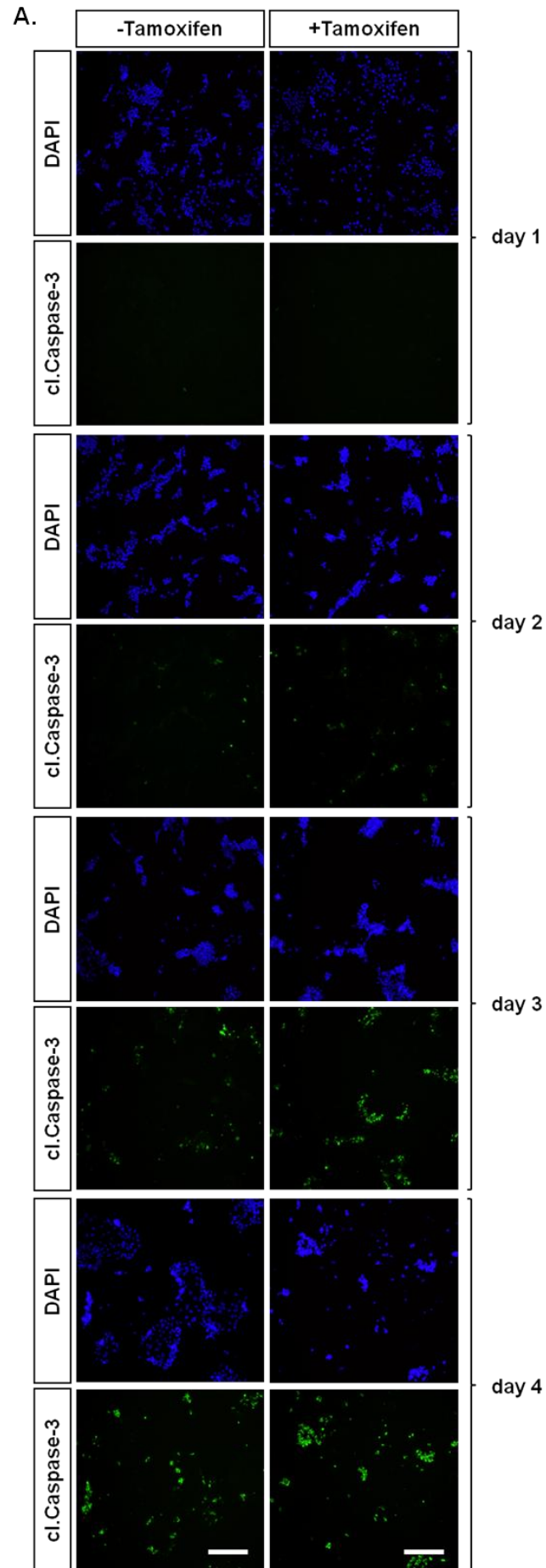


Figure 36: *MLN* induction causes liver defects and cell death in *Rosa26^{CAG:MLN/+};Tnfr1^{TgCreERT2/+}* animals

- A. Hematoxylin-Eosin staining in liver and sagittal brain sections of +/CreERT2 and *MLN/CreERT2* P25 mice.
- B. TUNEL assay in liver and sagittal brain sections of +/CreERT2 and *MLN/CreERT2* P25 mice, indicating DNA fragmentation (arrows).
- C. Immunohistochemical staining with an antibody against cleaved Caspase-3 in liver sections of +/CreERT2 and *MLN/CreERT2* P25 mice.
- D. Immunohistochemical staining with an antibody against CRP in liver sections of +/CreERT2 and *MLN/CreERT2* P25 mice.
- E. Immunohistochemical staining with antibodies against MASH1 and F4/80 in liver sections of +/CreERT2 and *MLN/CreERT2* P25 mice.

Scale bars: 50 μm



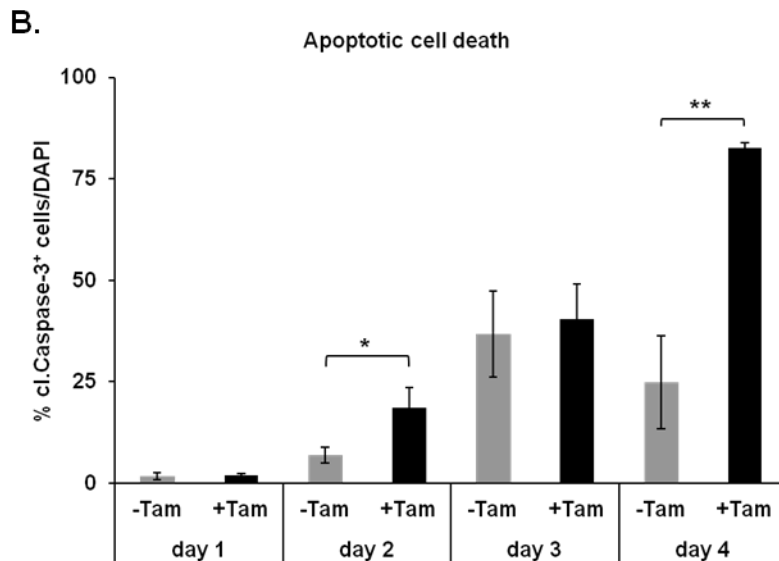


Figure 37: Cell death is induced by MLN expression in *Rosa26^{CAG:MLN/+};CAG:MERCreMER* ESCs under neuronal differentiation conditions

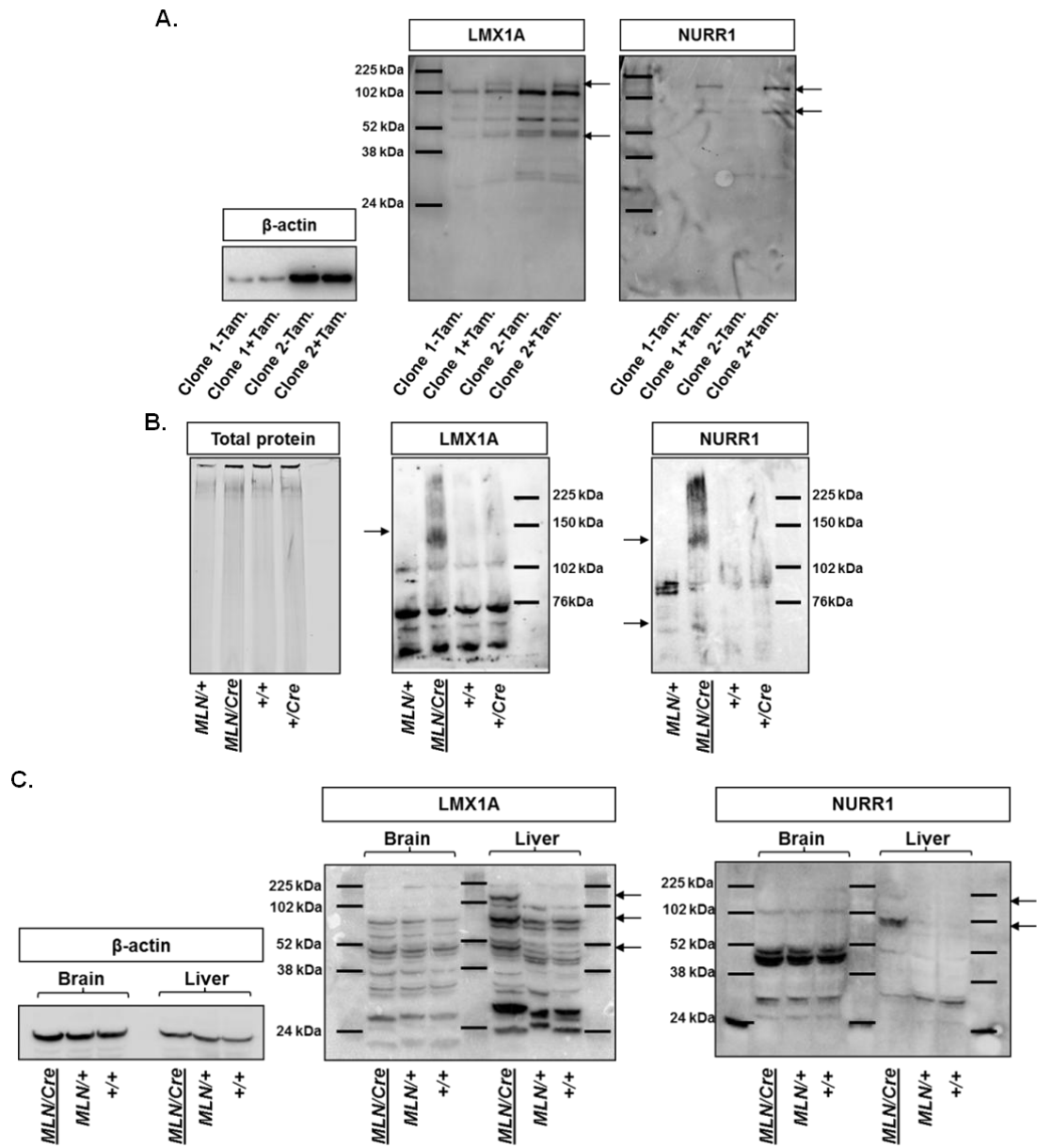
- A. Immunocytochemical staining with an antibody against cleaved Caspase-3 in *Rosa26^{CAG:MLN/+};CAG:MerCreMer* ESCs with and without tamoxifen administration over the course of 4 days.
- B. Quantification of the cleaved Caspase-3⁺ cells over the total cell population (DAPI⁺) shown in A. * $p \leq 0.05$, ** $p \leq 0.01$, $n=3$. Error bars represent mean \pm SD.

Tam: tamoxifen, Scale bars: 50 μ m (all pictures are the same size)

The observed cell death indicated problems due to MLN expression. To test whether MLN are properly expressed via this polycistronic construct, I performed Western analysis. Protein extracts from *Rosa26^{CAG:MLN/+};CAG:MERCreMER* ESCs (Figure 38A), *Rosa26^{CAG:MLN/+};Nestin-Cre* E19.5 embryos (Figure 38B) and *Rosa26^{CAG:MLN/+};Tnap^{TgCreERT2/+}* P25 brains and livers (Figure 38C) were utilized for the detection of LMX1A and NURR1 in Western blots. Interestingly, apart from the single TFs, bigger bands were also detected in the MLN expressing cells and tissues (except for the brain, arrows). The presence of bigger bands implied the presence of uncleaved forms of the MLN protein, which revealed insufficient “cleavage” of the 2A peptides, a fact that has previously been reported (Donnelly et al., 2001; Kim et al., 2011b).

Protein folding and post-translational modifications are mediated by cytosolic and endoplasmic reticulum (ER) chaperones. Misfolded or unfolded proteins may trigger unfolded protein response (UPR), (Hampton, 2000; Schröder and Kaufman, 2005; Xu et al., 2005), which can trigger apoptotic cell death. To test whether the insufficient “cleavage” was related to the observed cell death, I performed immunohistochemical staining with an antibody against Calnexin, an ER chaperone involved in apoptotic cell death triggered by ER stress (Schröder and Kaufman, 2005; Wu and Kaufman, 2006; Xu et al., 2005). Staining of brains sections of *Rosa26^{CAG:MLN/+};En1^{Cre/+}* (*MLN/Cre*) (Figure 38D) and liver sections of *Rosa26^{CAG:MLN/+};Tnap^{TgCreERT2/+}* (*MLN/CreERT2*) (Figure 38E) double heterozygous animals, exhibited considerably more Calnexin⁺ cells compared to the control animals, indicating that apoptotic cell death may be a consequence of the ER stress-related unfolded protein response, which may be triggered by the accumulation of uncleaved MLN protein.

Results



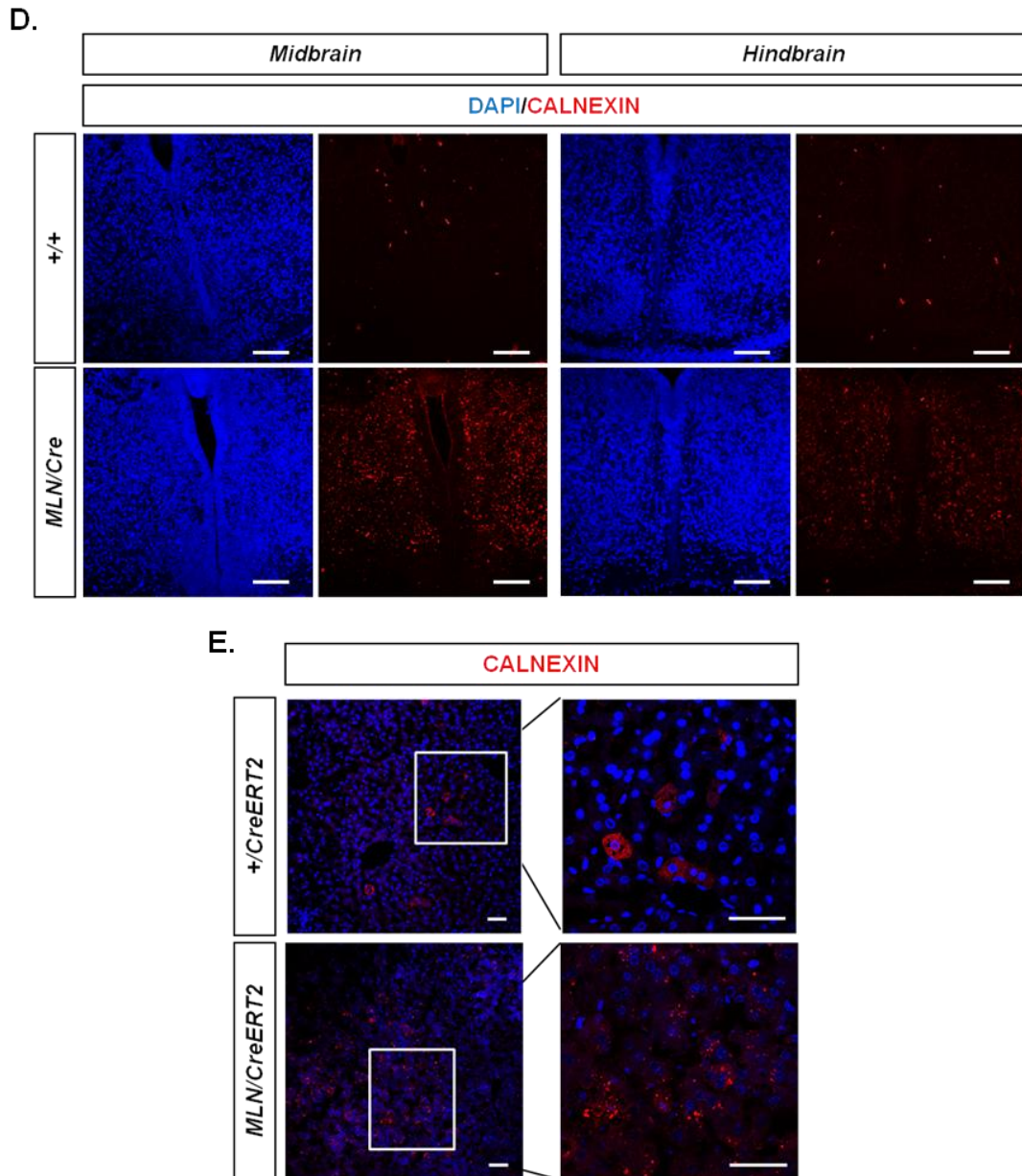


Figure 38: Cell death might be related to unfolded protein response

A, B, C. Western blot depicting the expression of LMX1A and NURR1 in *Rosa26^{CAG:MLN/+};CAG:MERCReMER* ESCs with and without tamoxifen administration (A), *Rosa26^{CAG:MLN/+};Nestin-Cre* E19.5 embryos (B) and *Rosa26^{CAG:MLN/+};Tnap^{TgCreERT2/+}* P25 brains and livers. The single proteins as well as uncleaved forms of the MLN protein are detected (arrows). The expected sizes in our system were calculated by in silico translation as followed: T2A 3' overhang+LMX1A+P2A 5' overhang 44.8 kDa, P2A 3' overhang+NURR1 66.7 kDa, MASH1+T2A+LMX1A+P2A 5' overhang 71.3 kDa, T2A 3' overhang+LMX1A+P2A+NURR1 111.5 kDa and MASH1+T2A+LMX1A+P2A+NURR1 138 kDa.

D, E. Immunohistochemical staining with an antibody against Calnexin of *Rosa26^{CAG:MLN/+};En1^{Cre/+}* E13.5 coronal brain sections and *Rosa26^{CAG:MLN/+};Tnap^{TgCreERT2/+}* P25 liver sections.

Scale bars: 50 μ m

4.2.7 Brain injury does not influence the activation and reprogramming potential of the *CAG MLN* transgene in vivo

Although reprogramming to DA neurons has not yet been achieved, there have been several demonstrations for neuronal reprogramming in vivo (Guo et al., 2014; Niu et al., 2013; Su et al., 2014; Torper et al., 2013). However, the conversion in each case was accomplished by injection of viruses coding for reprogramming factors directly in the tissue. Injection is known to cause an artificial environment of injury with reactive gliosis and neurogenesis accompanying the series of events. These events result in increased plasticity of the cells around the injury, which perhaps become more susceptible to obtaining the desired identity (Robel et al., 2011).

To test whether injury would promote activation of the *MLN* transgene and subsequent reprogramming in the brain, I crossed the *Rosa26*^{CAG:MLN/+} mouse line to the *Glast*^{CreERT2/+} and performed tamoxifen induction as depicted in the experimental scheme (Figure 39A). 35 days after the last tamoxifen injection, a stab wound was created in the cortex of all the *Rosa26*^{CAG:MLN/+}; *Glast*^{CreERT2/+} progeny (in collaboration with Prof. Dr. Magdalena Goetz, Physiological Institute/Physiological Genomics, Ludwig-Maximilians Universitaet). After either 7 or 25 days of healing process, the mice were sacrificed and dissected for the assessment of the ectopic presence of TH⁺ neurons. However, MLN expression was still not activated (data not shown). The immunohistochemical analysis with antibodies against GFAP (a marker of reactive astrocytes) and NEUN showed increased numbers of GFAP⁺ and NEUN⁺ cells around the injured area. This was expected since increased reactive gliosis and neurogenesis respectively occur at the injury site during the healing process (Figure 39B). DCX immunoreactivity was not detected. This could perhaps be correlated with the absence of DCX signal that was also previously observed in the progeny of the same breeding scheme but without brain injury (Section 4.2.4.2). Nonetheless, the absence of TH signal in the injured area confirmed that even the injury that creates a potentially permissive environment cannot assist towards in vivo reprogramming to DA neurons (Figure 39C), pointing to the

Results

limitations of the applied overexpressing strategy, among which most prominent here was the lack of MLN expression in the brain.

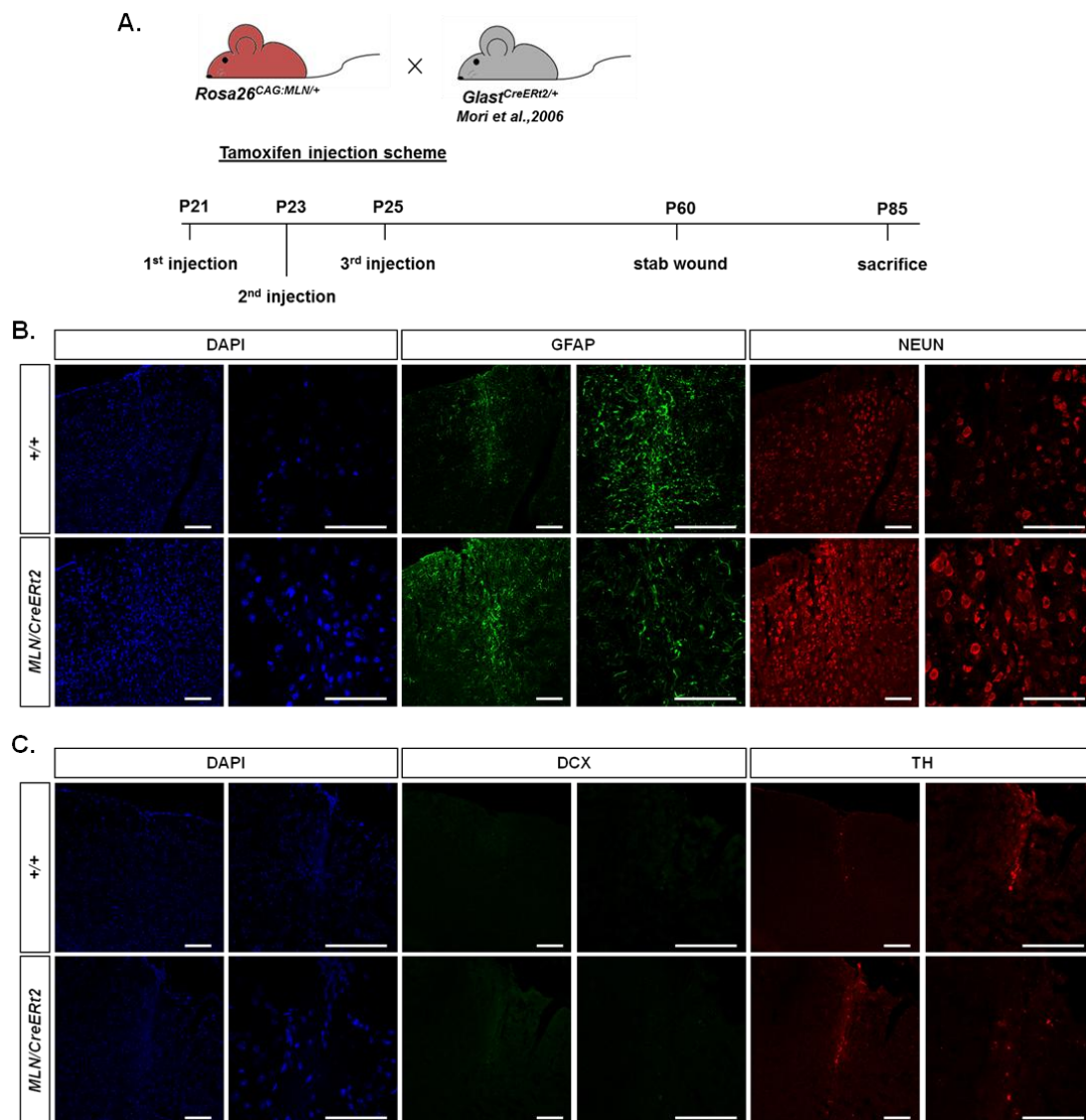


Figure 39: In vivo reprogramming is not induced even after stab wound injury in the cortex of $Rosa26^{CAG:MLN/+};Glast^{CreERT2/+}$ animals

- A. Schematic representation of the breeding and experimental design.
- B. Immunohistochemical staining with antibodies against GFAP and NEUN in cortices of $Rosa26^{CAG:MLN/+};Glast^{CreERT2/+}$ P85 animals after stab wound injury.
- C. Immunohistochemical staining with antibodies against DCX and TH in cortices of $Rosa26^{CAG:MLN/+};Glast^{CreERT2/+}$ P85 animals after stab wound injury.

Scale bars: 50 μ m

5. Discussion

Parkinson's disease (PD) is characterized by the death of dopaminergic (DA) neurons of the substantia nigra pars compacta in the midbrain. This results in reduced dopamine levels and subsequently to tremor, bradykinesia, rigidity, postural instability. Although symptoms may vary from patient to patient, PD may lead to total disability, depression and decreased quality of life. Current therapy relies mainly on increasing the levels of dopamine by administration of dopamine precursors (L-Dopa) or dopamine agonists. Such approaches can at best alleviate some of the symptoms, without delaying the progression of neurodegeneration, while they are responsible for side effects (e.g. cognition problems, hallucinations) (Friedman, 2010).

Alternative methods focusing on restoring the lost DA neurons or supporting their survival, instead of just increasing the dopamine levels have been tested in clinical trials. These include a) fetal nigral transplantations (Hauser et al., 1999; Kordower and Brundin, 2009; Olanow et al., 2003), b) infusion of neurotrophic factors (GDNF) (Gill et al., 2003) and c) viral delivery of genes important for the dopamine synthesis (*AADC*, *TH*) and/or the survival of the DA neurons (*GDNF*, *neurturin*) (Mittermeyer et al., 2012; Muramatsu et al., 2010; Palfi et al., 2014; Richardson et al., 2011). However, these methods offer only minor symptomatic relief and still need further development.

The generation of DA neurons has been the focus of current research and has been demonstrated through ESC differentiation (Kriks et al., 2011; Lee et al., 2000), pluripotent reprogramming (iPSC differentiation) (Hartfield et al., 2014; Stanslowsky et al., 2014) and lineage reprogramming (Caiazzo et al., 2011; Liu et al., 2012; Pfisterer et al., 2011a). Such methodologies are required in order to develop optimal regenerative tools with minor side effects, as well as improve our understanding for the progression of the disease.

In this study, I performed in vitro differentiation of ESCs, unlike which has previously been applied (Kriks et al., 2011; Lee et al., 2000). In contrast to published protocols, the differentiation towards DA neurons was instructed by

the overexpression of selected polycistronic combinations of transcription factors (TFs) under the control of an endogenous promoter. In addition, I applied an in vitro lineage reprogramming protocol (Caiazzo et al., 2011) in an in vivo context via the polycistronic overexpression of MASH1, LMX1A and NURR1 in a genetic mouse model.

5.1 Targeting vectors versus viral infection for the overexpression of multiple genes

The use of TFs for directing cell fate decisions is rapidly evolving in research related to regeneration. Numerous studies employing the overexpression of specific TFs provide the proof-of-principle for the feasibility of TFs to promote the generation of DA neurons (Cho et al., 2011; Chung et al., 2002, 2005b; Kim et al., 2006; Sánchez-Danés et al., 2012). One commonly accepted way to achieve overexpression of specific genes is through viral infection. Viral particles which carry plasmids containing the selected gene are administered to the cells. This results in expression of the viral DNA as instructed by the host cell. This method has already been applied for the generation of DA neurons from ESCs and iPSCs (Sánchez-Danés et al., 2012), as well as for lineage reprogramming (Caiazzo et al., 2011; Liu et al., 2012; Pfisterer et al., 2011b).

However, when the simultaneous overexpression of multiple genes is required, viral infection can generate discrepancies. The production of multiple viruses each expressing a single gene is feasible, albeit the percentage of cells co-infected by all viruses is limited (De Felipe, 2002). Alternatively, a polycistronic vector expressing all genes would be advantageous. Polycistronic constructs are consisting of sequences (2A peptides, internal ribosomal entry sites (IRES)) which allow simultaneous transcription of all genes (De Felipe, 2002) and thus ensures that all genes are expressed by the infected cells. However, such constructs are usually large and viral vectors pose limitations on the length of the inserted DNA. For example, the packaging capacity of lentiviruses does not exceed 10 kb and

for adenoviruses this size is even further reduced to less than 5 kb (Zhang et al., 2010). When viral plasmids exceed the DNA length limit, the virus titer is substantially hampered.

In regards to genome integrating viruses, viral infection leads to random integration of the gene(s) of interest into the host genome, often in multiple copies. This results in unpredictable overexpression and risk of oncogenic transformation (Woods et al., 2003). Concerning the non-integrating viruses, it is possible that the duration of the transient expression of the transgene is not adequate for instructing cell fates (Colosimo et al., 2000; Kim and Eberwine, 2010) in cases where a stable overexpression system would be advantageous.

Accordingly, viral delivery may limit reprogramming efficiency. In this regard, targeting vectors may be beneficial. Large, polycistronic targeting vectors can easily be inserted into the locus of interest, providing stable cell lines without random integrations. This tool also bypasses the viral production and transduction, whose efficiency is dependent on variable parameters (co-transfection of viral plasmids for the generation of the viral particles, virus titer) (Okada et al., 2009).

5.2 Differentiation of embryonic stem cells by targeted overexpression of transcription factors

One of the first and still widely used approaches for the generation of DA neurons is the differentiation of ESCs in vitro. However, bioethical concerns hamper the clinical application of these methods for transplantations in patients (Gibson et al., 2012). Nevertheless, they can be utilized as tools for deciphering the underlying molecular mechanisms by which PD occurs.

Existing protocols for ESC differentiation to DA neurons implement the overexpression of TFs by viral delivery (Sánchez-Danés et al., 2012). In the current study however, a set of different polycistronic combinations of TFs was targeted into the *Sox1* locus. Consequently, the expression of each TF

combination was controlled by the endogenous *Sox1* promoter, which is activated during the neural progenitor cell stage. These TFs are involved in the development and specification of DA neurons. Hence, the aim was to drive ESCs towards the neuronal and subsequently the DA cell fate, by simulating the in vivo developmental program.

5.2.1 Recombinase-mediated cassette exchange in the *Sox1* locus for targeted overexpression creates an artificially inducible system

Recombinase-mediated cassette exchange (RMCE) has previously been utilized for targeting genetic loci (Prosser et al., 2011; Tchorz et al., 2012; Toledo et al., 2006) and includes two steps. First, a stable cell line with a *loxP*-flanked positive/negative selection cassette in the locus of interest is generated. Subsequently, a donor plasmid carrying gene(s) also flanked by *loxP* sites is co-transfected with a Cre-expressing plasmid. Cre recombinase then mediates the exchange between the positive/negative selection cassette and the cassette of the donor plasmid. Screening for clones which are missing the negative selection cassette determines the clones which have successfully integrated the gene(s) of interest in the selected locus. This two-step procedure resulted in stable cell lines expressing selected TFs under the control of the *Sox1* promoter. Therefore, the TFs were expressed only during the early stages of neural tube formation, when *Sox1* promoter is active, in order to stimulate DA neuronal development at this early neural stage.

5.2.2 *Ngn2* and *Lmx1b* simultaneous overexpression generates dopaminergic neurons from embryonic stem cells

Growth/survival factors (e.g. FGF2, FGF20) (Correia et al., 2007; Lee et al., 2000; Rolletschek et al., 2001) and/or signaling molecules (e.g. activators of Shh and canonical Wnt signaling) (Kriks et al., 2011) are generally ectopically administered in the culture medium of all existing protocols for ESC differentiation towards DA neurons. This study was

designed in order to eliminate such expensive molecules from the differentiation protocol. In addition to being expensive, it is possible that not all cells are equally exposed to their action when these factors are supplemented in the differentiation medium. This creates a heterogeneous cell population, rather than a clean homogeneous population of the desired cell type.

The use of TFs implicated in DA neuronal development was considered as an alternative to the heterogeneity and high cost of these molecules. Hence, modifying the genetic program of the ESCs in order to overexpress selected genes in a controlled manner could closely resemble the in vivo situation and provide substantial quantities of DA neurons.

Following this strategy, DA neurons were generated; however the differentiation efficiencies were lower than expected. Differences in the yield of DA (TH⁺) or even neuronal (TUJ1⁺) numbers were observed among the different combinations utilized. *Ngn2* and *Lmx1b* overexpression (*NL* combination) yielded the highest achieved efficiency followed by the *NEOL* combination (*Ngn2, En1, Otx2, Lmx1b*). *NL* in some instances rendered increased neuronal differentiation (TUJ1⁺) as well, compared to other combinations. These results indicate that *Ngn2* and *Lmx1b* comprise a potent combination for the generation of neurons and most importantly DA neurons. This is not surprising since *Ngn2* is a proneural gene known to be implicated in the normal development of midbrain DA neurons (Andersson et al., 2007), while *Lmx1b* contributes to the ventral midbrain identity of the newly formed neurons during the early stages of DA neuronal differentiation (Smidt et al., 2000).

Administration of retinoic acid (RA) inhibited the activation of Tyrosine Hydroxylase (TH), whereas forskolin promoted DA neuronal differentiation. This can be explained by the fact that forskolin is an activator of cAMP synthesis (Li et al., 2000). The cAMP responsive element binding protein (CREB) is subsequently activated (Michel and Agid, 2002) and upon its phosphorylation it regulates the expression of *Bcl-2* (Wilson et al., 1996). *Bcl-2* has been shown to be implicated in promoting the survival of neuronal populations, by preventing apoptosis (Dubois-Dauphin, 1994; Farlie and

Dringen, 1995). Moreover, CREB is known to activate CREB-binding protein (CBP) and p300 which results in transcriptional activation through the recruitment of RNA polymerase II and histone acetyltransferases (HATs) (Yuan and Gamber, 2001). Therefore, supplementing the differentiation medium with forskolin, which has previously been shown to protect and promote the differentiation of DA neurons (Paldino et al., 2014), resulted in accessible to the TFs chromatin and increased numbers of surviving TH⁺ neurons. This indicates that the DA phenotype could not be triggered without the addition of forskolin and/or that TH⁺ neurons could not survive the differentiation conditions and died via apoptosis during the procedure.

5.2.3 How can the differentiation efficiency be improved?

Various differentiation schemes were tested; however the efficiency could not be improved. The *Sox1* promoter utilized here is activated only in the neural progenitor cell and is later inactivated. It is possible that a promoter activated at an earlier stage during development might be more beneficial (e.g. *Sox2*, *Oct4*) (Abranches et al., 2009; Pevny et al., 1998). This would ensure that the cells are committed to the neural fate at an earlier time point. However, it would generate other technical difficulties. Guiding the overexpression of fate-determining TFs at this early stage would perhaps pose difficulties in maintaining ESCs at their undifferentiated state under routine culture conditions, since such promoters are activated already at the ESC stage.

It is possible that *Sox1* promoter's activity is not adequate to drive high overexpression of the downstream genes. Transgenes with the implementation of an exogenous promoter (e.g. *CAG*, *CMV*) could perhaps increase the levels of expression. Alternatively, inducible vectors could be employed. It has been demonstrated for example that the tetracycline-controlled transactivator protein (tTA) can efficiently be utilized for controlled overexpression of transgenes in vitro, providing in addition the possibility of turning the expression off when required (Caiazza et al., 2011). Yet, additional

vector and media components are required (tet-responsive element and doxycycline), in order to control the timing and duration of overexpression. Nevertheless, such inducible strategies could be beneficial, offering high and controlled levels of expression.

An additional drawback of the current system may have been introduced by the T2A sequences. Incomplete cleavage of these peptides results in misfolded proteins, as discussed later in more detail. This could hamper expression and function of the TFs, which may eventually fail to efficiently program cells towards the DA neuronal lineage. Therefore, the construction of improved polycistronic vectors or the development of alternative strategies for overexpressing multiple selected endogenous genes would be beneficial.

The deprivation of neurotrophic or growth factors has previously been correlated with increased neuronal death, which can be prevented by the synthesis of cAMP (Michel and Agid, 2002). No such factors were utilized in the current study and as a consequence, only with the addition of forskolin could the DA neurons be rescued. However, the DA neurons generated were very few and their numbers could not compete with the numbers obtained by other differentiation protocols, where exogenous growth/neurotrophic factors and/or signaling molecules were utilized (Kriks et al., 2011; Lee et al., 2000).

The beneficial effect of forskolin in the differentiation to DA neurons was also indicative of the role of the chromatin state in determining cell fate, as forskolin indirectly activates transcription. The approach presented here could thus be enhanced by the addition of genes controlling nucleosome modifications (histone acetyltransferases, deacetylases, methyltransferases, demethylases) and chromatin remodeling (e.g. CREB/p300, SWI/SNF). The chromatin would thus be more accessible to the action of TFs. miRNAs could also be beneficial. They have been implicated in neurogenesis and were demonstrated to generate neurons when overexpressed in combination with selected TFs (Ambasudhan et al., 2011; Victor et al., 2014). The additional effect of such molecules could thus facilitate the action of the selected TFs to more effectively generate DA neurons.

5.2.4 Differentiation of embryonic stem cells by targeted overexpression of transcription factors: concluding remarks

Overall, the approach used in the current study provided information on several aspects of DA neuronal differentiation. It was shown that genetic engineering of ESCs can easily be achieved by RMCE. I was thus able to generate a number of stable ESC lines overexpressing selected TFs in a polycistronic construct, circumventing the weaknesses of other commonly used methods (viral infection). This allowed parallel screening of different TF combinations that can trigger DA neuronal development. Among these, one combination, the *Ngn2* and *Lmx1b* (*NL*), was proven to be more potent than all the rest tested. The observed divergence in the differentiation efficiency among the different combinations implies that perhaps even more potent combinations exist and remain unexplored. New combinations could easily be tested using the genetic tool described here by a simple cassette exchange step.

Therefore, the existing ESC differentiation protocols could be enhanced by a) controlled overexpression of selected TFs, like the *Ngn2* and *Lmx1b* combination which gave rise to DA neurons in vitro, b) addition of factors promoting the DA neuronal survival and c) chromatin remodelers/epigenetic modifiers. In that regard, it would be worth exploring alternative promoters that could drive spatiotemporally controlled high overexpression. Providing thus the required positional and developmental cues, a higher yield of mature and functional midbrain DA neurons can potentially be acquired for in vitro modeling of PD and drug screening approaches.

5.3 In vivo reprogramming to dopaminergic neurons

ESC or iPSC differentiation to DA neurons is extensively applied in cell replacement approaches. However, considering the high risk of tumor formation, as well as bioethical limitations or chromosomal abnormalities often accompanying the iPSC conversion procedure (Jacobs, 2014; Roessler et al.,

2013), the need for alternatives is imperative. The advent of lineage reprogramming provides new possibilities.

The term lineage reprogramming (or reprogramming) describes the conversion of abundant somatic cells to the cell type of interest, bypassing the intermediate pluripotent stage (i.e. iPSCs). Reprogramming to DA neurons has mainly been achieved by the overexpression of selected TFs through viral infection of the cell of interest (usually fibroblasts and astrocytes) (Addis et al., 2011c; Caiazzo et al., 2011; Kim et al., 2014; Liu et al., 2012; Pfisterer et al., 2011a; Sheng et al., 2012a; Torper et al., 2013).

Direct reprogramming has been applied both in vitro and in vivo to instruct the generation of neurons (Guo et al., 2014; Niu et al., 2013; Rouaux and Arlotta, 2013; Su et al., 2014; Torper et al., 2013). However, in vivo reprogramming is advantageous over in vitro for several reasons. Delivering in vitro reprogrammed cells in the brain might be particularly difficult, requiring high-risk surgical operations. In addition, their integration into the neuronal circuitry may be questionable. The in vitro manipulation of cells and their cultivation for long periods until they are reprogrammed may cause chromosomal changes, compromising thus the quality of delivered cells. These problems may be ameliorated by in vivo reprogramming. The laborious and time-consuming in vitro conversion and transplantation are skipped and reprogramming takes place in situ, where it may be promoted by the local niche.

5.3.1 Utilization of a genetic mouse model for conditional overexpression of three reprogramming TFs

Several neuronal populations have been generated by in vivo reprogramming e.g. GABAergic, glutamatergic neurons (Guo et al., 2014; Niu et al., 2013; Rouaux and Arlotta, 2013; Su et al., 2014; Torper et al., 2013). In the current study in vivo reprogramming to DA neurons was attempted through the generation of a mouse line conditionally overexpressing three TFs, namely MASH1, LMX1A and NURR1 (MLN). These TFs could

successfully convert fibroblasts to DA neurons in vitro (Caiazzo et al., 2011). However, in this study, none of the neurons obtained in vitro expressed PITX3, a TF characteristic of the ventral midbrain DA neuronal identity. To achieve that, I included PITX3 in the MLN combination in a second step, with the aim to self-activate its expression in the formed neurons.

The two combinations of TFs were targeted into the *Rosa26* locus under the control of a CAG promoter. Expression could be conditionally activated by the removal of a *loxP* flanked SV40 poly(A) located upstream of the TFs by Cre-mediated recombination. Unfortunately, only the MLN combination eventually gave stable progeny in mice. In order to induce MLN expression in specific cell types/tissues, mouse lines using tissue specific promoters expressing Cre or CreERt2 were utilized.

For the simultaneous overexpression of all the TFs, polycistronic constructs consisting of the “self-cleaving” 2A peptides were synthesized. These viral peptides offer advantages over other polycistronic strategies. IRES sequences have been widely used for such strategies; however, in addition to being large (around 500bp), they often result in lower expression levels of downstream genes (Paquin et al., 2001). The use of multiple promoters is another option. Yet, vectors carrying many different promoters may result in variable expression levels of the downstream genes. In addition, depending on the cell type, promoter silencing may occur, inhibiting thus expression (Metz et al., 1996). The generation of three or four transgenic mice each one overexpressing one of the TFs would be an alternative. However, this encompasses the need of multiple breeding steps in order to have all the TFs expressed in the same mouse at the cell type/tissue of interest.

The self-processing 2A viral peptides have been shown to overcome such difficulties. They allow simultaneous expression of multiple genes mediated by their high “self-cleavage” efficiency in vitro and in vivo, which is based on a ribosome skipping translational mechanism (Donnelly et al., 2001; Kim et al., 2011b; Lin et al., 2013). This feature in combination with their small size (54-66 nucleotides) made them optimal for the polycistronic strategy applied in the current study.

The genetic mouse model was generated in order to provide: a) overexpression of MASH1, LMX1A and NURR1 driven by the strong CAG promoter, b) controlled timing, duration and position of expression, c) simultaneous overexpression of the three reprogramming TFs at the cell type/tissue of interest and d) proof-of-principle of in vivo reprogramming to DA neurons. Successful demonstration with this strategy would provide information regarding the optimal conditions for in vivo reprogramming to DA neurons, i.e. the cell type/tissue, the appropriate starting point and length of expression, as well as prove whether the MLN combination is as potent for generating DA neurons in vivo as in vitro. In addition, considering that PD occurs mainly in elderly people, it is important to know whether in vivo reprogramming to DA neurons can be achieved in adult tissue.

5.3.2 Technical limitations of the reprogramming in the *Rosa26*^{CAG:MLN/+} mouse line

The conditional induction of MLN expression mediated by Cre/CreERT2 in different cells/tissues led to unexpected results, summarized in Table 7.

Cre/CreERT2 mouse line	Stage	Cre recombination	MLN expression	Reprogramming	Death (cells/mouse)
<i>En1</i>	E13.5	✓	X	X	?
	P0	?	?	?	✓
<i>Glast</i>	P30	✓	X	X	X
	P60	✓	X	X	X
	P67 (sw)	✓	X	X	X
	P85 (sw)	✓	X	X	X
<i>Nestin</i>	E11.5	✓	✓ CNS (not MASH1)	X	?
	E19.5	✓	✓ CNS (not MASH1)	X	?
	P0	?	?	?	✓
<i>Rosa26</i>	P0	?	?	?	✓
<i>Tnap</i>	P26	?	?	?	✓
	P25	✓	✓ liver X brain	X	✓

Table 7: Summary of the results from breeding the *Rosa26*^{CAG:MLN/+} mouse line with Cre/CreERT2 mouse lines at several stages

sw: stab wound, ?: could not be assessed

As depicted in the table, Cre-mediated recombination was successful in all cases, except for the cases that the embryos/pups were not viable and recombination could not be assessed. However, transgene expression was found only in the livers of the *Rosa26*^{CAG:MLN/+};*Tnap*^{TgCreERT2/+} progeny and partially in the CNS of the *Rosa26*^{CAG:MLN/+};*Nestin-Cre* progeny, where ectopic MASH1 could not be detected. Reprogrammed cells were never seen, even in the cases where all TFs were expressed. Instead tissue abnormalities (*En1*^{Cre/+}), increased cell death (*Tnap*^{TgCreERT2/+}) and embryonic (*En1*^{Cre/+}, *Nestin-Cre*, *Rosa26*^{Cre/+}) or postnatal lethality (*Tnap*^{TgCreERT2/+}) were observed. It is noteworthy that transgene expression was linked to lethality and/or cell death in both embryonic and postnatal animals.

Interestingly, the only exception to that observation was the progeny of the *Rosa26*^{CAG:MLN/+};*Glast*^{CreERT2/+} intercross. The double heterozygous offspring of this breeding pair (MLN/CreERT2) exhibited no obvious phenotype or cell death upon tamoxifen induction; however I observed diminished DCX⁺ cell population in the highly neurogenic regions of the brain, i.e. dentate gyrus, subventricular zone. This could be a side-effect of the MLN induction upon CreERT2-mediated recombination, which could not be further addressed. It is likely that overexpression of the MLN transgene was detrimental to this early neural stem cell population (*Glast*⁺ cells). Alternatively, the molecular identity of these cells was altered by the overexpression of MLN and were no longer expressing DCX. However, the complete absence of DCX⁺ cells from these regions indicates lack of Dcx-driven neurogenesis rather than a gradual change in the expression profile of these cells.

Considering in addition a) the lack of reprogramming of the *Rosa26*^{CAG:MLN/+} MEFs in vitro and b) the increased cell death observed with time during reprogramming of MEFs or differentiation of *Rosa26*^{CAG:MLN/+};*CAG:MERCReMER* ESCs in vitro, it was obvious that the MLN induction both in vitro and in vivo triggered cell death instead of reprogramming. However, as revealed by luciferase assays in the *Rosa26*^{CAG:MLN/+};*CAG:MERCReMER* ESCs, the TFs exhibited binding on

known targets and subsequent activation, indicating that the construct was functional.

The cell death was linked to apoptosis, as demonstrated by the TUNEL assay performed in the livers of the *Rosa26*^{CAG:MLN/+}; *Tnap*^{TgCreERT2/+} animals and by the increased numbers of cleaved Caspase-3⁺ cells compared to the controls. This has probably caused the subsequent death of the mice. The apoptotic effect was related to ER stress via the UPR, as shown by Calnexin immunoreactivity, which is an ER chaperone related to ER stress. It is therefore suspected that ER stress was elicited by the uncleaved forms of the MLN protein, which potentially could not be properly folded, leading thus to UPR.

The “cleavage” efficiency of the viral 2A self-processing peptides has previously been evaluated (Donnelly et al., 2001; Kim et al., 2011b). By assessing the levels of single proteins compared to the uncleaved forms, the authors identified T2A and P2A as the most efficient viral peptides for simultaneous expression of individual genes (Kim et al., 2011b). In the current study, the T2A and P2A were selected as the optimal candidates for the tricistronic approach. Not surprisingly, in addition to the single proteins, I also detected bigger bands in the Western analysis, corresponding to the uncleaved forms. Unexpectedly though, it is possible that these uncleaved proteins coincided with UPR-mediated cell death due to misfolding (Hampton, 2000; Schröder and Kaufman, 2005; Xu et al., 2005). Consequently, although Cre/CreERT2-mediated recombination was successful and in some instances MLN expression was activated, direct analysis of reprogramming was precluded. The apoptotic cell death occurred quite rapidly upon Cre-mediated recombination (2-4 days). Complete in vitro reprogramming driven by the MLN combination has been demonstrated to require at least 16 days (Caiazza et al., 2011). However, the early occurring cell death observed here rendered reprogramming rather impossible during the short period while MLN expressing cells were alive.

The strong CAG promoter driving MLN expression could have had an additional effect on cell death, by accumulating high amounts of

misfolded/unfolded MLN protein. Constitutive expression of the uncleaved proteins may have enhanced this negative outcome. Previous reprogramming studies report the utilization of inducible systems and mainly the tetracycline-controlled transcriptional activation for controlled overexpression of the selected TFs during a limited period (Caiazzo et al., 2011; Pfisterer et al., 2011b; Torper et al., 2013). However, when it comes to reprogramming brain cells in vivo, the penetration of doxycycline, which is required for the activation, can be restricted by the blood-brain barrier (Smith et al., 2003), limiting thus the control of expression. Furthermore, this potentially negative effect of constitutive activation could not have been predicted, since prolonged administration of doxycycline and therefore prolonged overexpression of reprogramming factors seemed to have no negative effect in the reprogramming efficiencies observed in vitro (Caiazzo et al., 2011).

Nevertheless, cell death is often observed during any reprogramming process, which could be the result of the reprogramming conditions (i.e. medium deprived of serum, accumulation of toxic byproducts), or a consequence in the course of switching cell fate (Cheung et al., 2012). Hence, the cell death noted herein could be a combination of all the above or some of these factors, possibilities whose verification could not be assessed.

Another limitation of the in vivo system was the lack of MLN expression in the brain. The only exception were early *Rosa26*^{CAG:MLN/+}; *Nestin-Cre* double heterozygous embryos (*MLN/Cre*) (E11.5), which displayed LMX1A and NURR1, but no MASH1 ectopic expression in the CNS. The lack of expression of all or some of the reprogramming TFs in the brain, while being expressed in liver may indicate variable epigenetic modifications, which eventually may affect expression. I verified a differential methylation pattern of *Mash1* depending on the tissue where *MLN* were induced. This observation may indicate that the lack of MLN expression in the brain could be due to transcriptional repression of the whole transcript (Jaenisch and Bird, 2003; Rhee et al., 2013; Shilatifard, 2006; Tate and Bird, 1993). Moreover, it has also been shown that large transcripts are more susceptible to decay in the

brain (Zetoune et al., 2008). Those possibilities, alone or in combination may have hampered MLN expression in the brain.

5.3.3 Biological limitations of reprogramming in the *Rosa26*^{CAG:MLN/+} mouse line

In vivo neuronal reprogramming has been achieved by viral injections of the reprogramming factors directly in the area of interest (Guo et al., 2014; Niu et al., 2013; Rouaux and Arlotta, 2013; Su et al., 2014; Torper et al., 2013). Consequently scar formation is initiated and several cell populations are recruited in response. These events include reactive gliosis (accumulation of dividing astrocytes and glia cells for the healing process) and neurogenesis (for the replenishment of the lost neuronal populations), which contribute to the generation of a more plastic microenvironment (Robel et al., 2011). Exogenously delivered reprogramming factors (TFs, signaling molecules etc.) may thus be more effective on a permissive environment, where neurogenesis is anyway taking place and more efficiently determine the cell fate of interest on these plastic cells.

Reprogramming occurred only around the injured area (Niu et al., 2013). Therefore it would be insightful to test whether MLN overexpression in the context of a deliberate cortical injury can also trigger reprogramming in vivo. However, even under injury conditions, MLN expression could not be induced in the brain and subsequently no reprogramming was observed. It is thus obvious that the technical limitations (misfolded/unfolded protein, high and constitutive expression, cell death etc.) were suppressive even in such a permissive and plastic environment as the damaged cortical area.

In vitro reprogramming to DA neurons has been demonstrated in several studies (Addis et al., 2011c; Caiazzo et al., 2011; Kim et al., 2014; Liu et al., 2012; Pfisterer et al., 2011a; Sheng et al., 2012a; Torper et al., 2013). However, in vivo reprogramming to DA neurons has never been reported. This observation underscores the difficulty of directly translating the in vitro results to an in vivo system. The optimal conditions can be strictly selected

during in vitro reprogramming. These may vary from cell density, medium composition, oxygen levels, to supporting stromal cell types if any etc. The in vivo microenvironment is more complex, therefore the reprogramming to DA neurons may be influenced in an unpredictable way. Exploring and knowing in more detail the role of the local niche in DA neurogenesis would thus be beneficial.

The DA neurons of the SNc are susceptible to regional genetic and epigenetic signals, such as DNA methylation and histone modifications. For example, it has been shown that the acetylation and methylation status of histone 3 correlates with the potential of NURR1 to bind on the promoter of the *Th* gene and regulate thus its expression and indirectly the demethylation of other DA-specific genes, like *Dat* (He et al., 2011). DA neurons are characterized by a defined expression profile of TFs (i.e. defined expression profile of TFs, e.g. LMX1A and signaling molecules, e.g. Wnt), which guide their differentiation and survival. They interact with other neurons and several other brain cells. All these features grant them with their unique identity, which, as confirmed by the current literature status, cannot be completely acquired. The obtained DA neurons usually express most of the DA neuronal markers (e.g. TH, DAT, VMAT2, ALDH etc.); however, they do not always acquire the pure identity and functionality of SNc DA neurons. For example, they do not express PITX3 and are often morphologically or functionally immature (Caiazzo et al., 2011; Liu et al., 2012; Pfisterer et al., 2011b). Subsequently, simulating their developmental pathway in order to acquire fully functional, mature and pure DA neurons in vivo remains, not surprisingly, a big challenge. The difficulties faced should not be discouraging. Instead innovative and improved tools must be developed in order to create these neurons in situ.

5.3.4 In vivo reprogramming to dopaminergic neurons: how can future strategies be improved?

Future in vivo strategies may be improved with the implementation of novel or optimized tools/approaches. The most obvious way would be the overexpression of a single protein or reprogramming factor. This entails screening of individual factors. According to recent publications however, probably more than one TF are required for efficient reprogramming. Comparison of combinations successfully instructing in vitro reprogramming to DA neurons revealed that proneural genes are indispensable (*Mash1* or *Ngn2*) (Addis et al., 2011c; Caiazzo et al., 2011; Liu et al., 2012; Pfisterer et al., 2011b; Sheng et al., 2012b; Torper et al., 2013). In addition, either *Lmx1a* or *Lmx1b* are important components of the reprogramming cocktail (Addis et al., 2011c; Caiazzo et al., 2011; Pfisterer et al., 2011b; Sheng et al., 2012b; Torper et al., 2013). These two genes are closely linked to the generation of DA neurons and have partly overlapping functions (Chung et al., 2009; Yan et al., 2011). The rest of the utilized reprogramming factors vary among different studies. Some observed commonalities (e.g. *Nurr1*, *Brn2*, *Myt1l*) could be attributed to their popularity and reprogramming efficiency in previously published combinations. Therefore, it is hard to theoretically predict which genes could constitute a more optimal reprogramming mix. It is evident that genes triggering neurogenesis and being related to the generation of DA neurons should comprise basic elements of novel reprogramming combinations. However, they should be enriched with additional factors.

From the results presented here, it is possible that chromatin modifiers play a crucial role in controlling expression. Therefore, reprogramming strategies could be supplemented with epigenetic remodelers for the guided regulation of the chromatin state (Gifford and Meissner, 2012). DNA demethylases/methyltransferases or histone deacetylases/acetyltransferases for example could act in favor of generating DA neurons by silencing non-DA genes and activating genes related to the DA identity. Components of ATP-dependent nucleosome remodeling complexes (e.g. SWI/SNF complex) could also constitute a valuable tool for changing the accessibility of chromatin to

fate-determining TFs. Furthermore, the beneficial action of forskolin in generating DA neurons from ESCs is indicative of the role of chromatin modifiers in the differentiation of DA neurons.

Avoiding complicated targeting or knock-in strategies could also be beneficial in that regard. Episomal vectors (Zhang, 2013) or mRNA transfection (Schlaeger et al., 2014) could offer an alternative solution for transient ectopic expression and may also reduce insertional mutagenesis. Lastly, the Clustered regularly interspaced short palindromic repeats loci and their associated CRISPR-associated genes (CRISPR/Cas) technology provides an additional option. Using this revolutionary tool, one can selectively activate or inactivate *in vivo* the expression of specific gene(s) (Bikard and Marraffini, 2013; Doench et al., 2014; Perez-Pinera et al., 2013), without the need for several different mouse lines or polycistronic vectors.

In vivo reprogramming in the brain poses additional challenges. The aim of *in vivo* reprogramming is to replace DA neurons *in situ*. This implies that the optimal cells to be converted should reside in close proximity to the target cell type (i.e. midbrain). Astrocytes, a brain cell type, have been successfully reprogrammed *in vitro* (Addis et al., 2011c). However, successful reprogramming of astrocytes would result in neurons being deprived of their essential supportive and protective role, which could entail problems. Midbrain astrocytes support DA neurogenesis by the secretion of neurotrophic factors and cytokines, which also instruct neuronal function (Harada et al., 2013; Yang et al., 2014). The elimination or reduction of their numbers may thus compromise DA neuronal development, while additionally hamper their functional properties.

Concerning the application of *in vivo* reprogramming in humans, there are also some ethical issues to be considered. The genetic approach presented here can only provide information about *in vivo* reprogramming to DA neurons and cannot be applied in humans. The information that could be obtained concern all the different aspects of reprogramming (i.e. gene combination, timing and duration, expression level, optimal tissue/cell type) and may be translated in an optimized strategy to be applied in humans. This

could be feasible by viral injections in the brain of individuals. Several trials have already employed viral delivery for gene therapy in PD (Mittermeyer et al., 2012; Muramatsu et al., 2010; Palfi et al., 2014; Richardson et al., 2011); however the questions of how receptive the human society is for such strategies and what dangers it may entail arise. The success of such approaches for in vivo reprogramming will depend on the responsiveness of the individual to the gene therapy, the side-effects (e.g. tumor formation, rejection of the viral vector, etc.), the effectiveness of in vivo conversion, the symptomatic relief, the potential of cure and quite importantly the financial burden.

5.3.5 In vivo reprogramming to dopaminergic neurons: concluding remarks

The genetic mouse model generated in this study did not show reprogramming in any of the tissues examined; however it provided valuable technical knowledge. I confirmed that not only 2A viral peptides do not perform efficiently in the context analyzed here, but also that the uncleaved proteins potentially mediate apoptotic cell death via UPR. In addition, I showed differential transgene expression among different tissues, due to the differential DNA methylation pattern. If such discrepancies can be overcome, future models could establish the most critical parameters, including gene combination, timing, expression level, optimal tissue/cell type for successful in vivo reprogramming to DA neurons. It is evident that there are still technical, biological and perhaps ethical obstacles to be circumvented; however, with further improvement and optimization in vivo reprogramming to DA neurons may be achieved, opening thus new routes towards novel regenerative approaches for PD and personalized medicine.

6. Materials and Methods

This section describes the methods applied in the study. All detailed information about materials, instruments, media compositions, antibodies and primers are given in tables at the end of the section.

6.1 Molecular biology

6.1.1 Genomic DNA isolation

For the isolation of genomic DNA from cell pellets or mouse tissues three different protocols were applied, depending on the subsequent intended use.

6.1.1.1 NaOH extraction

Cell pellets or mouse tissues were incubated in 25 mM NaOH/0.2 mM EDTA solution for 30 minutes at 99°C. Subsequently, reaction was terminated by the addition of 40 mM Tris HCl (pH 5.5) and the samples were centrifuged for 3 minutes at 4000 rpm. The supernatant or dilutions of it were subsequently utilized for further analysis.

6.1.1.2 Extraction using the Promega Wizard genomic DNA purification kit

The genomic DNA isolation was done according to the manufacturer's instructions for eukaryotic cells and mouse tissues.

6.1.1.3 Phenol-Chloroform extraction

Cell pellets and mouse tissues were incubated in lysis buffer at 55°C for 4 hours to overnight with the addition of 160 ug/ml proteinase K. On the

next day, they were homogenized for almost 1 minute. Equal volume of phenol was added and they were centrifuged at 15000 rpm for 5 minutes at 4°C. The supernatant was transferred to a fresh tube and was mixed with an equal volume of chloroform. The samples were centrifuged as above and the supernatant was transferred again to a fresh tube. 2.5 volumes of 100% ethanol supplemented with 5 M NaCl were added and after gentle mixing, the samples were centrifuged at 15000 rpm for 10 minutes at 4°C. The pellet was washed with 70% ethanol by short, full speed (15000 rpm) centrifugation and resuspended in the appropriate volume of H₂O depending on the size of the pellet.

6.1.2 Plasmid DNA isolation

6.1.2.1 Small scale plasmid DNA isolation (Mini Prep)

Small scale extraction of plasmid DNA was performed using the Qiagen Mini Prep Kit according to the manufacturer's instructions.

6.1.2.2 Large scale plasmid DNA isolation (Maxi Prep)

Large scale extraction of plasmid DNA was performed using the Qiagen Maxi Prep Kit according to the manufacturer's instructions.

6.1.2.3 Plasmid DNA isolation from yeast cells

Single or pooled yeast colonies were centrifuged at 3000 rpm for 3 minutes. The pellets (around 20 ul) were resuspended in 200 ul of 10 mM Tris-EDTA buffer, supplemented with 3 ul of Zymolyase (stock: 5 U/ul), for the lysis of the yeast cell wall for one hour. The lysis was followed by a standard plasmid DNA isolation procedure (Section 6.1.2.1).

6.1.3 DNA extraction from agarose gel

The DNA extraction from agarose gel was done with the Promega Wizard SV Gel and PCR Clean-Up System according to the manufacturer's instructions.

6.1.4 Polymerase Chain Reaction

Different Polymerase Chain Reaction (PCR) protocols were utilized depending on the application.

6.1.4.1 Short PCR for genotyping of cells or mice

DNA extracted from cells or mouse tissue was used as a template for PCR amplification. The PCR was done with the following reagents:

Template	0.5 ug
Forward primer (stock: 100 pmol/ul)	0.5 ul
Reverse primer (stock: 100 pmol/ul)	0.5 ul
dNTPs (stock: 10 mM)	0.6 ul
5x Buffer	3 ul
DMSO	0.75 ul
LongAmp (2.5 U/ul)	0.4 ul
H ₂ O	(15-x)ul
TOTAL VOLUME	15 ul

The amplification protocol was as follows:

STEP	TEMPERATURE (°C)	DURATION	NUMBER OF CYCLES
Initial denaturation	94	30 sec	1
Denaturation	94	30 sec	30
Annealing	65	1 min	
Elongation	65	1-2 min	
Final extension	65	10 min	1
Hold	12	∞	

6.1.4.2 Long Range PCR for genotyping of cells or mice

DNA extracted from cells or mouse tissue was used as a template for PCR amplification. The PCR was done with reagents as described for the short PCR (Section 6.1.4.1). The amplification protocol differed as follows:

STEP	TEMPERATURE (°C)	DURATION	NUMBER OF CYCLES
Initial denaturation	93	10 min	1
Denaturation	94	15 sec	8
Annealing	65 (-1 per cycle)	30 sec	
Elongation	65	9 min	
Denaturation	94	15 sec	30
Annealing	55	30 sec	
Elongation	65	9 min	
Final extension	65	10 min	1
Hold	12	∞	

6.1.4.3 Bacterial/Yeast colony PCR

Bacterial or yeast single colonies were utilized as templates. The reaction was performed using the same reagents as described above; however, the amplification protocol was modified as follows:

STEP	TEMPERATURE (°C)	DURATION	NUMBER OF CYCLES
Initial denaturation	93	10 min	1
Denaturation	92	15 sec	8
Annealing	65 (-1 per cycle)	30 sec	
Elongation	65	2 min	
Denaturation	92	15 sec	30
Annealing	55	30 sec	
Elongation	65	2 min	
Final extension	65	9 min	1
Hold	12	∞	

6.1.5 Southern blotting

Genomic DNA isolated from ESCs (10 ug) was digested with 10 U *PvuII*. The digestion mix was supplemented with 4 mM spermidine (stock: 0.1 M) and 100 ug/ml RNase (stock: 10 mg/ml) and was incubated at 37°C overnight. Subsequently, the digested DNA was run on a 0.8% agarose gel in 1x TBE buffer at 15 V overnight. On the next day, the gel was washed with distilled water and incubated in denaturation buffer on a shaker for 30 minutes at room temperature for the denaturation of the DNA strands. After another washing step, the gel was incubated twice in neutralization buffer, each time for 15 minutes for restoring neutral pH. A nitrocellulose membrane was used for the transfer. Membrane and gel were set up in 20x SSC buffer overnight with application of weight for the transfer overnight (or longer). Subsequently, the membrane was briefly washed with 20x SSC and UV cross-linked. A

prehybridization step for blocking in Church buffer at 65°C for 90 minutes followed. The DNA probe was 450 bp and was labeled with P³² radioactivity using the RediprimeTMII Random Prime Labelling System. To purify the radioactive labeled probe from DNA fragments less than 100bp, it was centrifuged through a Microspin S-300 column. Next, it was denatured at 95°C, incubated on ice and added to the hybridization buffer. The membrane was then hybridized at 65°C overnight. On the next day, the blot was washed with washing buffer I (50 ml 20x SSC, 5 ml 10% SDS and water to 500 ml) for 30 minutes at room temperature, with washing buffer II (25 ml 20x SSC, 5 ml 10% SDS and water to 500 ml) for 15-30 minutes at 42°C and if the radioactivity levels were very high, with washing buffer III (2.5 ml 20x SSC and water to 500 ml) for 15 minutes at 65°C. Finally, the membrane was placed in an X-Ray film cassette and exposed on an autoradiography film for 3-6 days. The development was done with an Agfa developing machine.

6.1.6 Restriction digests

Plasmid DNA was digested with either one or more restriction enzymes in 1x of the buffer (stock: 10x) recommended by the company. The reaction was incubated at 37°C for one hour or at room temperature overnight. When necessary, heat inactivation of the enzymes was performed according to the manufacturer's instructions.

6.1.7 Agarose gel electrophoresis

1% or 2% agarose gels were made by the addition of the required amount of agarose in 1x TAE buffer. Agarose was dissolved by microwave heating and after short cooling down, 1x Sybr Safe (stock: 10000x) was added. The liquid gel was subsequently applied on a plastic tray with combs and was incubated at room temperature until solid. For loading, DNA, RNA or cDNA samples were mixed with 1x DNA loading dye (stock: 5x). The gel was run in a plastic chamber with 1x TAE buffer and at voltage and duration

relevant to each experiment. The imaging of the bands on the gel was performed with the BioRad Chemidoc MP Imaging System, using the Image Lab software from BioRad.

6.1.8 Molecular cloning

6.1.8.1 Cloning with DNA ligase

Digested plasmid DNAs and PCR products with specified 5' and 3' ends were utilized for the reaction. Molar ratios of backbone (3x) and insert (1x) were joined by NEB T4 DNA ligase according to the manufacturer's instructions.

6.1.8.2 In-Fusion cloning

Molecular cloning was also performed with the In-Fusion HD Cloning Kit from Clontech Laboratories according to the protocol suggested by the manufacturer for Spin-Column Purified PCR Fragments.

6.1.8.3 Yeast cloning and transformation

The yAF7 yeast strain (Falcon et al., 2005) was grown overnight in 2x YPD medium at 30°C. On the next day, a 1:50 dilution of the yeast culture per cloning reaction was prepared in fresh 2x YPD and grown at 30°C for about 4 hours, until they reached an OD₆₀₀ of 1.0-1.2. 3 ml of the yeast culture were centrifuged at 3000 rpm for 3 minutes and the pellet was resuspended in an equal volume of sterile water. After a second spinning step, the pellet was resuspended in half a volume of 100 mM LiAc (TE pH8.0). This was repeated once more; however the pellet was now resuspended in 50 ul of 100 mM LiAc per cloning reaction. For the cloning reaction, the DNA fragments intended to be joined, 10 ul of heat-denatured carrier DNA (2 mg/ml salmon sperm DNA) and 300 ul 40% PEG4000 100mM LiAc (TE pH8.0) were mixed thoroughly (vortex for 1 minute) in the yeast solution. Subsequently, the mix was

incubated at 42°C for 40 minutes. After the heat shock, the yeast cells carrying the exogenous DNA were centrifuged at 3000 rpm for 3 minutes. The pellet was resuspended in 200 ul 1x TE and plated on CSD agar plates. The plates were incubated at 30°C for 2 days, upon which yeast colonies were visible (Gietz and Woods, 2002).

6.1.9 Bacterial transformation

6.1.9.1 Transformation of chemical competent bacteria

Chemical competent XL1-Blue bacteria (*E. coli* strain) were thawed on ice and 75 ul of the cells were mixed with plasmid DNA, carrying an ampicillin-resistance cassette. The mix of bacteria and DNA was incubated on ice for 1 minute and heat shock followed at 42°C for 1 minute. An incubation step of 2 minutes on ice followed (no longer required in the case of ampicillin) and the transformed bacteria were plated on LB agar plates, which was supplemented with 500 ul of ampicillin (stock: 10 mg/ml). The plates were incubated at 37°C overnight. Bacteria carrying the plasmid DNA were resistant to ampicillin and formed colonies.

6.1.9.2 Transformation of electrocompetent bacteria

Electrocompetent XL1-Blue bacteria (*E. coli* strain) were thawed on ice and 50 ul of the cells were mixed with plasmid DNA, carrying an ampicillin-resistance cassette. If required, the DNA was dialyzed with nitrocellulose membranes in distilled water for 10-15 minutes. The mix of bacteria and DNA was placed at the bottom of a 2mm cuvette. The cuvette was placed in an electroporator and current of 2500 V was pulsed through the sample. Immediately after the shock, LB medium was added to the cuvette. The bacteria cells were then plated on LB agar plates, supplemented with 500 ul of ampicillin (stock: 10 mg/ml). The plates were incubated at 37°C overnight. Bacteria carrying the plasmid DNA were resistant to ampicillin and formed colonies.

6.1.10 DNA sequencing

6.1.10.1 Big Dye DNA sequencing

Plasmid or PCR amplified DNA was used as a template in the following reaction:

Template	1 ug
Primer (Stock: 100 pmol/ul)	0.5 ul
SRD	1 ul
BigDye 3.1	0.6 ul
BigDye 3.0	0.2 ul
H₂O	(5-x) ul
TOTAL VOLUME	5 ul

STEP	TEMPERATURE (°C)	DURATION	NUMBER OF CYCLES
Initial denaturation	95	5 min	1
Denaturation	95	30 sec	25
Annealing	57	15 sec	
Elongation	60	4 min	
Hold	12	∞	

Next, the DNA was precipitated with a solution consisting of 0.5 ul of 125 mM EDTA, 2 ul of 3 M Na-Acetate and 50 ul 100% ethanol. The plate containing the DNA samples was then incubated at room temperature for 15 minutes in the dark. Centrifugation at 2000 g for 30 minutes at 4°C followed and after a second short centrifugation step, 70 ul of 70% ethanol per well were added. The plate was centrifuged again as previously and also inverted for the removal of residual ethanol (at 180 g). It was put in the dark for 15-30 minutes for evaporation and subsequently 20 ul of sterile water were added in

each well. Half of that volume was used for sequencing with an ABI 3730 DNA analyzer.

6.1.10.2 DNA sequencing by GATC Biotech

Alternatively, sequencing was performed by GATC Biotech. Plasmid or PCR amplified DNA, as well as primers were prepared according to the company's instructions and were sent to GATC Biotech, where sequencing was performed according to standard procedures.

6.1.11 In vitro Cre-mediated recombination

Plasmid DNA carrying *loxP* sites was utilized as a template for the deletion of the *loxP*-flanked cassette, catalyzed by Cre-recombinase from NEB with a protocol recommended by the manufacturer.

6.1.12 RNA extraction

Total RNA from cells was isolated with the Qiagen RNeasy Mini Kit according to the manufacturer's instructions.

6.1.13 Reverse transcription

Reverse transcription was performed with the iScript cDNA synthesis kit from BioRad according to the manufacturer's instructions.

6.1.14 Primer design for quantitative PCR analysis

Intron spanning-if applicable-gene specific primers for quantitative PCR analysis were designed using the online ProbeFinder tool from Roche (<http://qpcr.probefinder.com/organism.jsp>).

6.1.15 Quantitative Real Time PCR

Relative expression levels were assessed with Real Time PCR in triplicates in an ABI Prism 7500HT machine, using SYBR Green PCR master mix. *Gapdh* or *Hprt* were utilized as housekeeping genes for the normalization of the values and the relative expression levels were calculated according to the $\Delta\Delta^{ct}$ method. The reaction was performed as follows:

cDNA	0.5 ul
Forward primer (Stock: 1 ug/ul)	1 ul
Reverse primer (Stock: 1 ug/ul)	1 ul
SYBR Green Master mix (stock: 2x)	10 ul
H ₂ O	(20ul-x) ul
TOTAL VOLUME	20 ul

STAGES	TEMPERATURE (°C)	DURATION	NUMBER OF CYCLES
1	50	2 min	1
2	95	10 min	1
3	95	15 sec	40
	60	1 min	
Dissociation stage	95	15 sec	1
	60	15 sec	1
	95	15 sec	1

6.1.16 Western blotting

Cells and unperfused mouse tissues were treated with 1x NuPAGE LDS Sample Buffer, homogenized, centrifuged and aliquoted. The running was performed with the BioRad Mini Protean Tetra Cell, using 12% Mini

Protean TGX Stain-Free precast gels and 1x NuPAGE MES SDS Running Buffer. The transfer was performed in the Trans-Blot Turbo Transfer System from BioRad, using the Trans-Blot Turbo Transfer Pack. The membranes were blocked in 5% milk or 5% BSA and incubated with the primary antibodies overnight at 4°C. On the next day, the membranes were washed and incubated with HRP-conjugated secondary antibodies for 1 hour at room temperature. Clarity Western ECL Substrate was added on the membranes and development was performed with the BioRad Chemidoc MP Imaging System. The stripping of the membranes was performed with 0.5 M NaOH solution.

6.1.17 Luciferase assays

Rosa26^{CAG:MLN/+} ESCs were electroporated for the integration of a MERCreMER expressing plasmid (electroporation is described in section 6.2.2.1). Hence, upon tamoxifen administration, expression of MLN was induced. Untreated ESCs were lipofected in triplicates with luciferase reporter plasmids for MASH1, LMX1A and NURR1 (Castro et al., 2006; Jehn et al., 2014; Peng et al., 2011). Subsequently, the transfected cells were treated with 1 μ M of tamoxifen. Some transfected cells were kept untreated to serve as a negative control. One day later, all cells were processed as recommended by the manufacturer of the Dual-Luciferase Reporter Assay system (Promega). The measurement of Firefly and Renilla Luciferase luminescence was conducted with a Centro LB 960 luminometer (Berthold Technologies).

6.2 Cellular biology

6.2.1 Cell culture

6.2.1.1 Embryonic stem cell culture

129/Ola mouse ESCs can grow in feeder-free cultures, but gelatin-coating of the plastic dishes is required, prior to plating. 0.1% gelatin was

applied on the plastic surface of the dish of interest, which was then incubated at 37°C until use. The cells were cultivated in E14 medium in the presence of LIF at 37°C and 4% CO₂. When they reached around 80% of confluence, they were ready to be passaged. The medium was aspirated off and the cells were gently washed with PBS. Subsequently, trypsin, enough to cover the plastic surface, was added on the dish and the reaction was terminated with the addition of medium (serum-containing) after successful dissociation of the cells. The gelatin of the fresh dish was aspirated off and an aliquot of the dissociated cells was plated in fresh medium on the gelatin-coated dish. The confluence was about 20% after plating. The cells were passaged every two days; however medium was replaced daily.

6.2.1.2 Isolation and cell culture of primary mouse embryonic fibroblasts

E14.5 mouse embryos were dissected and viscera, heads and spinal cords were removed. The remaining tissue was cut in small pieces and incubated with 0.05% Gibco Trypsin-EDTA solution at 37°C for 10 minutes. Trypsin was inactivated with the addition of MEF medium (serum-containing). The cell suspension was passed through a 100 µm cell strainer (VWR, Cat. No. 21008-950) and the MEFs acquired (P0) were centrifuged at 1200 rpm for 3 minutes. The cell pellets were resuspended in fresh MEF medium and were cultivated for 1-2 passages (P1-P2), before they were frozen down. When the MEFs reached 80% confluence, they were washed with PBS after aspiration of the old medium. Trypsin (the same as for the dissociation of the tissue) was subsequently added to cover the plastic surface and upon dissociation, fresh medium was added to terminate the reaction. An aliquot of the dissociated cells was plated in fresh medium on a new dish. The confluence was around 20% after plating. Passage numbers of primary MEFs were kept to a minimum.

6.2.1.3 Freezing and thawing of cells

After trypsinization and cell counting-if required, the cells were centrifuged and the pellets were resuspended in medium containing 10% DMSO for cryopreservation. They were subsequently placed into cryopreservation vials, which were stored in cryo-containers containing isopropanol. This allowed slow freezing of the cells when put at -80°C . One or two days later, the vials were transferred in the liquid nitrogen tank for long-term storage.

Vials containing the frozen cells were thawed in water bath (37°C) and were then centrifuged at 1200 rpm for 3 minutes for DMSO removal. The cell pellets were resuspended in fresh medium and plated on a culture dish (gelatin-coated when required). Finally, the dish was put in the incubator for cell growth.

6.2.1.4 Metaphase chromosome counting

Colcemid was added to the medium of highly proliferating cells at a concentration of 0.2 $\mu\text{g/ml}$ (stock: 10 $\mu\text{g/ml}$) and the dish was incubated at 37°C for an hour. The cells were trypsinized under standard conditions and they were centrifuged at 1200 rpm for 10 minutes. The supernatant was discarded, except for 500 μl . The pellet was resuspended in the remaining medium by gently flicking the tube. 10 ml of hypotonic solution were added dropwise while gently flicking the tube. The cells were left at room temperature for 10 minutes and were then centrifuged and resuspended as previously. 2-3 ml of fixative were added dropwise, while gently flicking the tube. More fixative was added to fill up the tube. If not immediately used, the tube was stored at -20°C . To proceed, the fixative was added only to a volume of 1.5-3.0 ml. A glass cover slip was dipped into tap water and 10-15 μl of cell suspension were applied on its surface. The cover slip was then dried for at least 2 hours. 300 μl of DAPI solution (stock: 10 mg/ml) were added on the dried cover slip, which was subsequently mounted on a glass slide. The slide was kept in dark for 1 hour. The metaphase chromosomes

were counted for at least 30 cells in each case under an inverted fluorescent microscope with a 100x objective.

6.2.2 Transfection

6.2.2.1 Electroporation

2.5 ug of plasmid DNA containing a selection cassette (for neomycin or puromycin selection), was linearized by restriction digestion overnight. On the next day, it was precipitated and resuspended in 50 ul of sterile PBS. 10^7 ESCs for each electroporation was trypsinized and washed with PBS. The pellet was resuspended in 70 ul of sterile PBS. DNA and cells were mixed and pipetted at the bottom of a EP cuvette's wells, avoiding bubbles. The cuvette was placed into a BTX electroporator and current was pulsed through the samples. The settings of the machine were 700 V, 400 Ω and 25 uF and the time constant 100-150 usec. The electroporated cells were incubated at room temperature for 20 minutes for recovery and then plated on 10 cm dishes in fresh E14 medium. 24 hours later, selection of the positive clones was initiated by administration of 125 ug/ml of G418, 1 ug/ml of puromycin, or 0.4 uM of FIAU and medium was changed daily. 10 days later, colonies of the positive clones were formed and picked for PCR analysis and further growth.

6.2.2.2 Lipofection

Lipofectamine 2000 was utilized for the transfection of cells according to the manufacturer's instructions.

6.2.2.3 Nucleofection

Nucleofection of MEFs was performed with the Mouse/Rat Hepatocyte Nucleofector kit (Lonza) and the Nucleofector 2b device (Lonza) according to the manufacturer's instructions.

6.2.3 Neuronal differentiation and reprogramming

6.2.3.1 Monolayer neuronal differentiation

Cell culture plates were coated overnight with 100 ug/ml poly-L-ornithine diluted in distilled water. On the next day, they were washed with PBS and 1ug/well laminin diluted in PBS was added for at least 2 hours. ESCs were seeded at a density of $1,75 \times 10^4$ cells/cm² in E14 medium deprived of LIF. When required, 1 uM of tamoxifen was also added. 4-5 hours later, the media was replaced by neuronal differentiation media (either NDM1 or NDM2), in some cases supplemented with either 5 uM RA (only during the first 3 days), or 2 uM dorsomorphin or 10 uM forskolin, while maintaining tamoxifen treatment when required. The cells were subsequently incubated at 37°C for at least 10 days, a period during which neurons were formed.

6.2.3.2 EB-based neuronal differentiation

For EB-based neuronal differentiation, a modified version of the protocol by Bibel et al. was applied (Bibel et al., 2007). More specifically, the period for EB formation was reduced from 8 (4 days without and 4 days with RA) to 4 days (2 days without and 2 days with RA). Neuronal differentiation was performed in either NDM1 or NDM2 medium and was terminated 10 days after the plating of the dissociated EBs. When required, the cells were treated with tamoxifen, dorsomorphin or forskolin, as described in section 6.2.3.1.

6.2.3.3 In vitro reprogramming of mouse embryonic fibroblasts

Rosa26^{CAG:MLN/+} MEFs (passage 1 or 2) were nucleofected as described in section 6.2.2.3 either with the *pCAG-Cre-bpA* for Cre-mediated recombination of the stop cassette, or the *pmaxGFP* vector (negative control) and were seeded on polyornithin and laminin coated 24 well plates in MEF medium. The cells from each nucleofection reaction were seeded on 4 wells and were incubated at 37°C for 14 days, after which reprogramming potential was assessed.

6.2.4 Immunocytochemistry

Cells were washed with PBS, fixed in 4% PFA at room temperature for 10 minutes and then blocked in staining solution at room temperature for 1 hour. Primary antibodies were added to the solution and the cells were incubated at 4°C overnight. On the next day, the cells were washed twice with PBS and incubated with fluorophore-conjugated secondary antibodies at room temperature for 1 hour. 0.5ug/ml DAPI was added and the images were obtained with a Leica DMIL LED microscope, using the Leica Application Suite V4 software. The numbers of cleaved Caspase-3 positive ESCs over DAPI were quantified using the CellInsight NXT High Content Screening Platform (Thermo Scientific) and the Thermo Scientific HCS Studio Cellomics software.

6.2.5 Flow cytometry

Cells were washed with PBS, trypsinized as described previously (Section 6.2.1.1) and centrifuged at 1200 rpm for 3 minutes. Subsequently, ice-cold isopropanol was added dropwise in the pellets while gently vortexing. The cells could then be stored at -20°C until further use. For staining, the cells were centrifuged at 3000 rpm for 3 minutes and the isopropanol was carefully removed. Two washing steps with PBS followed and subsequently cell pellets were resuspended in FACS staining solution. After incubation at room temperature for 20 minutes, primary antibodies were added. The cells were incubated at room temperature for 30 minutes, centrifuged and washed again twice with PBS. Secondary antibodies were added and incubation at room temperature for 20 minutes followed. Alternatively, the staining was performed as described in section 6.2.3, upon trypsinization. The cells were subsequently washed with PBS and the pellets were resuspended in fresh PBS. Before the analysis, the cells were filtered through a strainer snap cap for the removal of big clumps.

Flow cytometry analysis was conducted with a Cantoll machine (BD Biosciences) and the DIVA software. For analyzing double-stained cells,

single-stained samples were initially utilized in order to calculate the bleeding-through of each fluorochrome to all other channels. This value, calculated by the BD software, was then subtracted for each channel. Gates were set as indicated by negative controls.

6.3 Histology

6.3.1 Whole body perfusion fixation of mice

Mice were euthanized with CO₂ and the thoracic cavity was opened. A needle connected to a pump was inserted through the left ventricle into the ascending aorta of the heart and the right atrium was cut. Blood vessels were subsequently washed with PBS until the liver turned pale and PBS was then replaced with freshly prepared 4% PFA for perfusion for around 5 min (10 ml/min). After perfusion, the mouse was ready for dissection.

6.3.2 Cryosectioning

Brain and liver tissues or embryos were dissected and were (post)fixed in 4% PFA for 2 hours at 4°C. Subsequently, they were washed twice with PBS and were put in 20% sucrose for at least 2 days at 4°C. The equilibrated tissues and embryos were then embedded in NEG50 cryopreservative reagent on dry ice and the object holders containing the frozen tissues were stored at -80°C until sectioning. The cryosectioning was conducted with a cryostat at 12 μm. The sections were placed on slides and were stored at -20°C.

6.3.3 Hematoxylin-Eosin staining

Slides with tissue sections were washed in PBS and then incubated in Hematoxylin solution for 20 minutes. Subsequently, they were washed with tap water for 5 minutes. Eosin staining was done for 5 minutes and another 5 minute washing step followed. The slides were then mounted with the

Aquatex mounting agent and the images were obtained with a light microscope (Zeiss), using the AxioVision 3.1 software.

6.3.4 TUNEL assay

For the TUNEL assay the ApopTag Peroxidase In Situ Apoptosis Detection Kit was utilized according to the manufacturer's instructions for cryosections. The slides were mounted with the Aquatex mounting agent and the images were obtained with a light microscope (Zeiss), using the AxioVision 3.1 software.

6.3.5 Immunohistochemistry

Cryosections were washed with PBS and blocked in blocking solution at room temperature for 1 hour. Primary antibodies were added to the solution and were incubated at 4°C overnight. On the next day, the slides were washed with PBS and incubated with fluorophore-conjugated secondary antibodies at room temperature for 1 hour. 0.5 ug/ml DAPI was added and the slides were subsequently mounted with Vectashield Mounting medium. The images were obtained with a Confocal Olympus BX61 microscope, using the Fluoview FV1200 software.

6.4 Mouse genetics and colony maintenance

6.4.1 Blastocyst injections and embryo transfer

C57BL/6J female mice were superovulated by PMSG (pregnant mare's serum gonadotropin), an analog of the follicle-stimulating hormone (FSH) and hCG (human chorionic gonadotropin) intraperitoneal injection. More specifically, 7.5 units (U) of PMSG were injected at 12:00 to induce maturation of the follicles. 48 hours later 7.5 U of hCG were injected to initiate the ovulation of the oocytes and the mice were mated with one male for 24 hours. 3 days post coitum, the uteri of pregnant females were dissected and

blastocysts were obtained. 10-20 genetically modified ESCs were injected into each blastocyst. BALB/c females were mated with vasectomized males and they were subsequently utilized as foster mothers for these early embryos.

6.4.2 Generation of the *Rosa26*^{CAG:MLN/+} mouse line

Two successfully recombined *Rosa26*^{CAG:MLN/+} ESC clones were independently injected into BALB/c blastocysts and the blastocysts were injected into pseudopregnant females. The pregnant mice gave birth to 90% chimeric male mice, which were bred to C57BL/J6 female wild type mice to generate the *Rosa26*^{CAG:MLN/+} knock-in mouse line. The germline transmission was confirmed by PCR.

6.4.3 Mouse facility

The animals were kept in Helmholtz Zentrum Muenchen and all experiments were performed in accordance with national and institutional guidelines. They were housed in groups of five mice per cage. The cages were maintained on a 12 hour-light/dark cycle with food and water supply. Temperature was at 22±2°C and relative humidity at 55±5%. For breeding, matings of one male per one female or per 2 females were set up and pups were weaned three weeks after birth (around P21). For identification purposes, the mice were earmarked at weaning age and for genotyping, a few mm of the tail (3 to 5 mm) were removed. When required, mice were intraperitoneally injected with 2 mg of tamoxifen dissolved in Miglyol, usually 3 times every other day, unless otherwise mentioned. The mice were euthanized with CO₂ application or by cervical dislocation.

6.4.4 Stab wound lesion

The stab wound lesion experiment was performed in collaboration with Prof. Dr. Magdalena Goetz, Physiological Institute/Physiological Genomics,

Ludwig-Maximilians Universitaet, according to the policies of the state of Bavaria under license number 55.2-1-54-2532-171-11. For anesthesia, the mice were intraperitoneally injected with 400 ul sleep solution. Once anesthetized, the hairs around the area of interest were removed. The mouse was subsequently put in the stereotactic frame and the mouth frame was placed in the mouth, hooking the teeth. Protective paste was applied on the eyes. The hair-free area was cleaned with a paper impregnated with NaCl solution. The skin of the skull was cut with a scalpel and the thin layer of muscles and connective tissue were gently removed. The area was cleaned with a paper impregnated with NaCl solution. With a drill, a small window in the skull was opened, avoiding disrupting meninges. The area was wet with a drop of NaCl solution and the skull window was removed carefully and stored in NaCl solution. The wound was achieved with a V-lance blade, which was adjusted in the frame at the level of the bregma (coordinates 0). The frame was moved according to the following coordinates: anterior-posterior axis -2.0 mm, dorsoventral -0.6 mm and medio-lateral within the range 1.2 mm-2.2 mm. The bone window was restored in its position and the skin was sewed. 350 ul of awake solution was intraperitoneally injected and the mouse was placed in a 37°C incubator until recovery from anesthesia.

6.5 Statistical analysis

The values represent mean and standard deviation (STDEV). For comparison of two groups the Unpaired t-test was applied. P-values ≤ 0.05 were considered significant.

6.6 Materials

Material	Company	Cat. No.
Agarose	Biozym	840004
Ampicilin	Sigma	A9393

Materials and Methods

Aquatex mounting agent	Merck	1.08562.0050
ApopTag Peroxidase In Situ Apoptosis Detection Kit	Merck Millipore	S7100
Big Dye 3.0 dGTP terminator	Applied Biosystems	4390229
Big Dye 3.1	Life Technologies	4337455
Carrier DNA	Sigma	D1626
Cell strainer	VWR	21008-950
Chloroform	Merck Millipore	102442
Clarity Western ECL Substrate	BioRad	170-5061
Colcemid	Gibco	15212-012
Cre recombinase	NEB	M0298
DAPI	Roche Diagnostics	10236276001
DMSO	Sigma-Aldrich	D2650
dNTPs	Roche Diagnostics	11969064001
Dorsomorphin	Sigma-Aldrich	P5499
Dual-Luciferase Reporter Assay System	Promega	E1910
Eosin	Roth	3137.2
Ethanol	Merck Millipore	100983
Forskolin	Sigma-Aldrich	F6886
G418	Gibco	11811-023
Gelatin	PAN	P06-20410
Hematoxylin	Roth	T865.2
In-Fusion HD Cloning kit	Clontech Laboratories, Inc.	638909
iScript cDNA synthesis kit	BioRad	170-8891

KAPA HiFi PCR Kit	Peqlab	07-KK2100-02
Laminin	Roche	11243217001
LIF	Merck Millipore	LIF2010
Lipofectamine 2000	Life Technologies	11668027
Loading dye	Bioline	BIO-37045
LongAmp	NEB	M0323
MaxiPrep	Qiagen	12163
Microspin S-300 column	GE Healthcare Life Sciences	27-5130-01
MiniPrep	Qiagen	27104
Mini Protean TGX Stain-Free precast gels	BioRad	456-8043
Mouse/Rat Hepatocyte Nucleofector kit	Lonza	VAPL-1004
NEG50	Thermo Scientific	6502
Nitrocellulose membrane	GE Healthcare Life Sciences	RPN2020D
NuPAGE LDS Sample buffer	Life Technologies	NP0007
NuPAGE MES SDS Running buffer	Life Technologies	NP0002
PBS	Life Technologies	14190235
PEG4000	Sigma-Aldrich	81240
Phenol/Chloroform/Isoamyl alcohol	Roth	A156.2
Poly-L-ornithin	Sigma-Aldrich	P4957
Proteinase K	Sigma-Aldrich	P2308
Puromycin	Sigma-Aldrich	P8833
Rediprime II Random Prime Labeling System	GE Healthcare Life Sciences	RPN1633
Restriction enzymes	NEB	-

Retinoic acid	Sigma-Aldrich	R2625
RNase	Roche	10109169001
RNeasy Mini Kit	Qiagen	74104
Spermidine	Sigma-Aldrich	S2626
Sybr Green	Life Technologies	4309155
Sybr Safe	Life Technologies	S33102
T4 DNA ligase	NEB	M0202
Tamoxifen	Sigma-Aldrich	T5648
Trans-Blot Turbo Transfer Pack	BioRad	170-4156
Trypsin	Life Technologies	25300-054
Trypsin	PAN	P10-100100
Vectashield Mounting medium	Vector	VECH1000
Wizard Genomic DNA Purification Kit	Promega	A1120
Wizard SV Gel & PCR Clean-up system	Promega	A9282
Zymolyase	Zymo Research	E1004

6.7 Equipment

Instrument	Company
Centrifuges	Eppendorf, Thermo Scientific
Cryostat	Mikrom, HM560
Cyclers	MJ Research, BioRad
DNA analyzer	ABI 3730
Developing machine	Agfa, Curix 60

Electroporators	BTX
	BioRad, Gene Pulser Xcell
Flow cytometer	Cantoll
Heater	Eppendorf
High Content	Cell Insight NTX High Content Screening Platform
Homogenizer	Ultra-Turrax
Imaging system	BioRad Chemidoc MP Imaging System
Luminometer	Berthold Technologies, Centro LB960
Microscopes	Zeiss Axioplan 2
	Olympus BX61
	Leica
Nucleofector	Nucleofector 2b device
Power supply (electrophoresis)	Consort EV265
Real Time PCR cycler	ABI 100252
Running system (Western)	Mini Protean Tetra Cell, BioRad, 165-8004
Transfer system (Western)	Trans-Blot Turbo Transfer System

6.8 Buffers, media, solutions

Buffer/Medium/Solution	Composition
Awake solution	Buprenorphine
	Flumazenil
	Atipamezol
	NaCl

Materials and Methods

	0,5% milk
	1% BSA
Blocking solution	1% FCS
	0,05% Triton-X (BioRad, 161-0407)
	H ₂ O
Church buffer	0.5 M NaP pH 7.2
	7% SDS
	1 mM EDTA pH 8
CSD (2x)	10 g/l Ammonium sulfate (Scharlau, AM04001000)
	3 g/l Yeast Nitrogen Base (Becton Dickinson, 233520)
	3,84 g/l Drop-out CS-ura (Sigma-Aldrich, Y1501)
	30 ml of 40% Glucose (Sigma-Aldrich, G8270)
Denaturation buffer	1.5 M NaCl
	0.5 M NaOH
E14 medium	Glasgow MEM (P04-97500)
	L-Glutamin (P04-80100)
	β-Mercaptoethanol (P07-05100)
	Sodium Pyruvate (P04-43100)
	MEM NEAA (P08-32100)
	Hyclone, FBS (3302-P121707)
	LIF (Merck Millipore, LIF2010)
FACS staining solution	5% goat serum in PBS
Fixative	Methanol : Acetic acid (3:1)
Hypotonic solution	75 mM KCl in H ₂ O
	10 mM EDTA
Lysis buffer	10mM Tris-HCl pH 7.6
	0.5% SDS

	10 mM NaCl
MEF medium	Gibco Dulbecco's Modified Eagle Medium (DMEM, Life Technologies, 21969-035) 10% FBS (PAN Biotech, P40-37500) 2 mM L-glutamine (Life Technologies, 25030-081) 1% Penicillin-Streptomycin (Life Technologies, 15070-063)
NDM1	48.3 ml DMEM/F12 (Life Technologies, 31331-028) 1 ml N2 (Life Technologies, 17502-048) 0.5 ml insulin (Life Technologies, 12585-014) 0.2 ml Fraction V BSA (stock: 25 mg/ml) (Carl-Roth, 0163.4) 48 ml Neurobasal (Life Technologies, 12348-017) 2 ml B27 (Life Technologies, 17504-044)
NDM2	Neurobasal (Life Technologies, 12348-017) 1x B27 minus vitamin A (Life Technologies, 12587-010) 1x L-glutamine (Life Technologies, 25030-081) 500 uM L-Ascorbic acid (Sigma-Aldrich, A4403)
Neutralization buffer	0.2 M Tris-HCl pH 7.7 0.5 M NaCl
40% PEG4000 100 mM LiAc	400 g PEG4000 (Sigma-Aldrich, 81240) 10,2 g LiAc (Sigma-Aldrich, L60883) 100 ml 10xTE MilliQ H ₂ O to 1l
PFA	4% in PBS
Sleeping solution	Fentanylcitrat Midazolam Medetomidin

	NaCl
SSC buffer (20x)	3 M NaCl 0.3 M Na ₃ Citrate (to pH 7.3)
Staining solution	PBS 5% BSA 0.3% Triton-X 10% normal goat serum
YPD (2x)	20 g Peptone (Formedium, PEP03) 10 g Yeast extract (Formedium, YEA02) 50 ml 40% Glucose (VWR, 101176K) 450 ml MilliQ H ₂ O

6.9 Antibodies

Antigen	Company	Cat. No.	Dilution
Calnexin	Thermo Scientific	MA3-027	1:40
Cleaved Caspase-3	Cell Signaling	9661	1:600
C-Reactive protein (CRP)	Thermo Scientific	MA5-17061	1:200
Dopamine transporter (DAT)	Merck Millipore	MAB369	1:500
Doublecortin (DCX)	Abcam	Ab18723	1:2000
F4/80 (macrophage)	Acris Antibodies	BM4007S	1:500
GFAP	Dako Cytomation	20334	1:400
LMX1A	Merck Millipore	AB10533	1:1000
MASH1	BD Pharmingen	556604	1:200
MYC	Sigma-Aldrich	M4439	1:500
NEUN	Merck Millipore	MAB377	1:500

Nestin	BD Biosciences	556309	1:100
NURR1	Santa Cruz Biotechnology	sc-990	1:2000 (IHC) 1:100 (Western)
PITX3	Life Technologies	38-2850	1:300
TH	Merck Millipore	MAB318	1:600
TUJ1	Abcam	ab18207	1:500

6.10 Primers & other sequences

Application	Forward (5'→3')	Reverse (5'→3')
Yeast cloning <i>PuroΔtk</i>	ttgcggtaccggtgaacccgcta gccgccagattataacttcgta taaagtctctatacgaagtata attctaccgggtaggggaggcg ct	tcagtctaagaggccagtctgg tgcagcattataacttcgtata atgtatgctatacgaagttattca gtagcctccccatctcccg gca
Yeast cloning <i>LF/LMF</i>	ggctaaataacttcgtataaagt ctctatacgaagttatgccacc atgttgacggcctgaagatgg aggaga	aagtattcacagatcctctcg ctaatcagttctgttcggatgag ttcataataggcctggagtaca
Yeast cloning <i>LMN</i>	ggctaaataacttcgtataaagt ctctatacgaagttatgccacc atgttgacggcctgaagatgg aggaga	aagtattcacagatcctctcg ctaatcagttctgttcgatacag tcctggcgaggggagcaggatga
Yeast cloning <i>Lmx1a</i> <i>VP16</i>	gagggccgaggctcgctgctaa cctgtggcgatgtggaagagaa tccaggcccgatgctgggagcc gtgaagatggaaggca	cgtccccaggctgacatcggt gctgccgctgccgctgccaga ggtgaaataggaattctgcatg gagtaca
Yeast cloning <i>Mash1</i> <i>VP16</i>	gaagttatagcggccgcccac catggagagttcaggcaagat	ccgctgcctgaggccgcaaac cagtttgtaagtcgagcagttc ct

Yeast cloning <i>ML</i>	ggctaaataacttcgtataaagt ctcctatacgaagttatgccacc atggagagttcaggcaagatg	aagttattcacagatcctcttcg ctaatacagtttctgttcgctggg aagatgaattctgcatactgta ca
Yeast cloning <i>MLN</i>	ggctaaataacttcgtataaagt ctcctatacgaagttatgccacc atggagagttcaggcaagatg	ttcacagatcctcttcgctaataca gtttctgttctctagagaatggca gtgtatccaggaacagttgt
Yeast cloning <i>NEOL/NL</i>	ggctaaataacttcgtataaagt ctcctatacgaagttatgccacc atgttcgtaaatctgagactctg gagttga	aagttattcacagatcctcttcg ctaatacagtttctgttcggaggc aaagtaggagctctgcatgga
<i>Sox1</i> genotyping	cctctcgggtctcatgagcaca gggtg	ctaaagcgcgatgctccagact gcctt
<i>Sox1</i> sequencing	caaccccccttctctccgcta	
<i>Sox1</i> expression	cgctgcacatgaaggaacacc cggattaca	cggccagcagactactgtccttc ttga
<i>Gapdh</i> expression	cccactgaagggcatcttgggct ac	gggtgggtgggtccagggtttctt ac
<i>Mash1</i> sequencing/genotyping	gcggtgcaaaaggagactgaa tttca	tgactccatcttgctgaactctc cat
	cagtgagttcatacagctccgac ga	accgctgaaattcagtctcctttt g
<i>Mash1</i> expression	ctgtcccctgtggcagac	ctgcttagcggcagacttg
<i>Mash1</i> methylation	ggagagttcaggcaagatgga gtca	gatggcgctctggaagtttctc cca
<i>Lmx1a</i> genotyping	gattgcttctcgccacttctgagg ct	tagactgacttctgagccctcat cac
<i>Lmx1a</i> sequencing	cgagtttgatgagggctcaga agt	
	cagcgagccaagatgaagaa actggca	
<i>Lmx1a</i> expression	aacccctctccacgacctggat tc	atggtcgatagggtttcccacc cgact

<i>Lmx1b</i> genotyping		cagaaccaagagcaaagat gaagaagct
<i>Foxa2</i> genotyping	ccttctctatcaacaacctcatgt cgt	
<i>NEOL</i> sequencing	gccccaaatgccagggaacga	
<i>Ngn2</i> genotyping	ctgcgcttcgccacaattacat ct	cagattgacgaacatggtggc ataact
<i>Ngn2</i> sequencing	aggatgccaagctcacgaaga tcgaga	
<i>Nurr1</i> genotyping	cagaacatgaatatcgacatttc tgattcagt	
<i>Nurr1</i> expression	agcagaggaagactcccgta gtaga	accatcgaatctcatctgacaa gagct
<i>Nurr1</i> methylation	cagtcttacagttatcacagttca ggcga	catttgatggactccgcgaga aggt
	cttctcgcggaagtccatcaa gaagga	ttgaactaaactcgacaatgga atcgatcc
<i>Ai9 MLN</i> sequencing	ggcgtcctgtcacctacaattag ccca	
	ttcacgacctggattccgacga taca	
	tacctgagcaaactgctcggga agct	
	cggcgaatgagagggaaag aaaccgggt	
	gccgtgtctccaaaagtgtctgt ga	
	ggatcataaaagacctaagcg cccacga	
	cacttctgaggctggaccactgc a	
gtactataagccatcaagccca		

	ccca	
	gcgcacagtgacagaaaaatgc	
	aaagtacgt	
	ggggaagctgatcttctgcaac	
	ggt	
	ggacggctctctgaagaagaa	
	gca	
	gcctttctcggatacccgcaggt	
	gt	
	ggagggctcgtggtagccttttaa	
	ct	
	ctccccctaagtcaccatcagct	
	agt	
	gcagaaattgtgtataagtcacc	
	cgtggt	
	caccctggtgaaccgcatcgag	
	ct	
In-Fusion cloning <i>Ai9</i> <i>MLN</i>	atcgaattcggccgggccacca tggagagctctggcaagatgga	cgaattcctgcagggttagaaa ggtaagggtgccaggaaaagt ttgtca
Cloning <i>Ai9 MLNPTe</i> (<i>Pitx3</i> primers)	cgcaatcatcgacaaactgttc tggatacactgccattcgagggc aggggcagcct	tcttggcgagggtcagccata ggaccagggtttctccacatc gccgca
Cloning <i>Ai9 MLNPTe</i> (<i>TaueGFP</i> primers)	tggaagaaaaccctggtcctat ggctgaccctcgccaggagtttg aca	ctggcttaactatgcggcatca gagcagattgtactgagaacta gtctactgtacagctcgtccat gccgagagtgat
<i>Rosa26</i> ^{CAG:MLN/+} 5' genotyping	tctcagagagcctcggctaggt a	tccatataatgggctatgaactaa tgaccccg
<i>Rosa26</i> ^{CAG:MLN/+} 3' genotyping	tcccgattcgcagcgcacgcct	tccatccttgatcaaaggaacc actttacc
Cre	gttattgtgctgtctcatcattttg	gtttctttccctctcatttcgccgtg

recombination/ <i>Rosa26^C</i> <i>AG:MLN/+</i> genotyping	caaaga	
	gaagttcctattctctagaaagta taggaact	cttgctcattttctgtttgcagct cca
Neo primer (genotyping, sequencing)	ccttctatcgccttcttgacgagtt ct	
<i>En1^{Cre/+}</i> genotyping	gtgccttcgctgaggctt	accctgatcctggcaatt
<i>Tnap^{CreERT2/+}</i> genotyping	cgctagatgagcctagggctg gctggagcacag	cagccaccagcttgcata
	ggtgcaagttgaataaccggaa atggt	ccatcgctcgaccagtttagtta cccca
Cre genotyping	cagaacctgaagatgttcgcga ttatcttct	catcagctacaccagagacg gaaatcca
	ctgctaaccatgttcagcc	ggtacattgagcaactgactg
GFP genotyping	aagttcatctgcaccaccg	tgctcaggtagtgggtgctg

Mash1-T2A-Lmx1a-P2A-Nurr1
(synthesized by Genscript)

ATGGAGAGTTCAGGCAAGATGGAGTCAGGCGCAGG
CCAGCAGCCACAGCCCCACAGCCCTTCTCCCC
CAGCCGCATGCTTTTTCGCAACCGCAGCTGCAGCC
GCCGCAGCAGCTGCAGCAGCTGCACAGTCCGCTCA
GCAGCAGCAGCCACAGGCTCCACCTCAGCAGGCAC
CACAGCTGTCCCCTGTGGCAGACAGCCATCC
GGAGGAGGACACAAGTCTGCCGCTAAGCAGGTCAA
ACGCCAGCGAAGCTCCTCTCCAGAGCTCATGCCGT
GCAAAAGGAGACTGAATTTAGCGGTTTTGGCTACT
CCCTGCCACAGCAGCAGCCAGCAGCAGTGGCAGC
GCGAAATGAGAGGGAAAGAAACCGGGTGAAGCTGG
TCAACCTCGGCTTCGCTACACTGCGCGAACACGTG
CCCAATGGAGCTGCAACAAGAAAATGAGCAAAGT
GGAAACTCTCCGGTCCGCTGTGAGTACATCCGCG
CACTGCAGCAGCTGCTCGACGAGCATGATGCTGTG
AGCGCCGCTTTTCAGGCAGGCGTCTGTACCTAC
AATTAGCCCAAATATTCCAATGATCTGAACTCTATG
GCCGGGAGTCCAGTGAGTTCATACAGCTCCGACGA
GGGTTCTTATGATCCACTGAGTCCCGAGGAACAGG
AACTGCTCGACTTCACAACTGTTTTGAGGGACGG
GGGTCTCTGCTCACTTGTGGAGATGTGGAGGAAAA
TCCCGGGCCTATGCTGGACGGTCTCAAGATGGAGG
AAAACCTCCAGAGCGCCATCGAGACCAGCGCCAGC
TTCAGCAGTCTGCTCGGCCGAGCCGTGTCTCCCAA
AAGTGTCTGTGAGGGATGCCAGAGAGTGATTTCCG
ACAGGTTCTGCTCCGCCTGAACGATTCTTTCTGGC
ACGAACAGTGCAGTGCAGTGCCTTCTGTAAGGAA
CCCCTGGAGACCACATGCTTCTACCGGATAAGAA
GCTCTACTGTAAGTACCATTACGAGAAGCTGTTCCG
CGTGAATGCGGTGGCTGTTTCGAAGCTATCGCAC
CTAACGAGTTTGTGATGAGGGCTCAGAAGTCAGTCT

ACCACCTGAGCTGCTTCTGCTGTTGCGTGTGCGAG
AGACAGCTCCAGAAGGGCGATGAATTTGCTCTGAAA
GAGGGGCAGCTGCTCTGCAAGGGTGACTATGAGAA
GGAAAGGGAGCTGCTCTCACTGGTTAGCCCTGCAG
CCTCTGACAGTGGCAAGTCCGACGATGAGGAATCA
CTGTGCAAGAGCGCCCACGGTGTGGCAAAGGAGC
CTCTGAAGACGGAAAGGATCATAAAAAGACCTAAGCG
CCCACGAACCATCCTGACTACCCAGCAGCGAAGGG
CATTCAAGGCCAGCTTTGAGGTGTCAAGCAAACCAT
GCAGGAAGGTCAGAGAAACCCTCGCTGCAGAGACA
GGCCTGTCCGTGCGCGTGGTCCAGGTCTGGTTCCA
GAATCAGCGAGCCAAGATGAAGAACTGGCAAGAC
GGCAGCAGCAGCAGCAGCAGGACCAGCAGAACAC
CCAGAGGCTGACATCCGCCAGACTAATGGGTCTG
GTAACGCTGGGATGGAAGGTATCATGAATCCTTACA
CAACTCTGCCAACCCCCAGCAGCTGCTCGCCATT
GAGCAGTCCGTGTATAACTCTGATCCCTTTAGACAG
GGACTGACACCACCCAGATGCCTGGTGACCACAT
GCATCCATACGGCGCTGAACCCCTCTTCCACGACC
TGGATTCCGACGATACATCACTGAGCAATCTCGGG
GATTGCTTTCTCGCCACTTCTGAGGCTGGACCACTG
CAGAGTCGGGTGGGAAACCCTATCGACCATCTGTA
CAGTATGCAGAATTCATACTTACCAGCGCCACAAA
CTTCTCTCTGCTCAAGCAGGCAGGCGACGTGGAGG
AAAACCCTGGACCAATGCCATGCGTGCAGGCACAG
TACGGATCCTCTCCTCAGGGAGCTTCCCCAGCATC
CCAGTCTTACAGTTATCACAGTTCAGGCGAATATAG
CTCCGATTTCTGACCCCTGAGTTCGTGAAGTTTTT
TATGGACCTGACAAATACTGAGATTACAGCTACCAC
AAGTCTGCCATCATTACAGCACTTTTATGGACAATA
CTCAACCGGATATGATGTGAAGCCTCCATGCCTCTA
CCAGATGCCCTGAGCGGGCAGCAGAGCAGTATCA
AAGTGGAGGACATTCAGATGCACAACATCAGCAGC
ACAGTCATCTGCCCCCTCAGTCTGAGGAAATGATGC
CTCATTCCGGGAGCGTGTACTATAAGCCATCAAGCC
CACCCACTCCCTCCACCCCTTCTTTCCAAGTGCAGC
ACTCACCCATGTGGGACGATCCTGGCAGCCTGCAC
AATTTTCATCAGAATACTGAGTGGCCACTACCCATATG
ATCGAGCAGAGGAAGACTCCCGTCAGTAGACTGTC
ACTCTTACAGCTTTAAACAGAGCCCTCCAGGGACCCC
CGTGAGCTCTTGTGATGAGATTCGATGGTCCCCT
GCACGTCCCTATGAATCCTGAGCCAGCCGGATCCC
ACCATGTGGTTCGACGGGCAGACATTCGCCGTGCC
AACCTATCCGGAAGCCAGCAAGTATGGGCTTTCC
CGGACTGCAGATTGGCCACGCCAGCCAGCTGCTCG
ATACTCAGGTGCCATCCCCACCTTCTCGCGGAAGTC
CATCAAATGAAGGACTGTGCGCCGTGTGCGGGGAC
AACGCAGCTTGCCAGCATTACGGAGTCCGGACCTG
CGAGGGGTGTAAAGGTTTCTTTAAGCGCACAGTGC
AGAAAAATGCAAAGTACGTCTGCCTGGCCAACAAGA
ATTGTCCTGTGGACAAACGCCGAAGGAACAGATGC
CAGTATTGTCGGTTCCAGAAGTGTCTGGCCGTGGG
CATGGTCAAAGAGGTGGTCAGGACAGATTCTCTCAA
GGGCAGACGGGGAAGACTGCCATCCAAGCCCAAAT
CTCCTCAGGACCCAAGTCCACCCTCACCTCCAGTG
AGCCTCATCTCCGCACTGGTGCGGGCACACGTGCA
CAGCAATCCTGCTATGACCAGTCTGGATTACTCACG
CTTCCAGGCAAACCCAGACTATCAGATGTCTGGAGA
CGATACTCAGCATATCCAGCAGTTTTACGACCTGCT

Rosa26 5' probe

```
GACCGGCAGCATGGAAATCATTAGGGGCTGGGCCG
AGAAGATTCCTGGATTTCGCAGACCTGCCAAAAGCC
GACCAGGATCTGCTCTTCGAAAGCGCATTCTGGAG
CTCTTCGTGCTGCGACTCGCCTATAGGTCCAATCCC
GTCGAGGGGAAGCTGATCTTCTGCAACGGTGTGGT
CCTGCACCGCCTCCAGTGCGTGAGGGGATTCGGAG
AATGGATCGATTCCATTGTGCGAGTTTGTTCAAACCT
GCAGAACATGAATATCGACATTTCTGCATTGAGTTG
CATCGCAGCCCTCGCCATGGTGACTGAACGACACG
GCCTGAAAGAGCCTAAGAGGGTTCGAGGAACCTCAG
AATAAGATTGTGAACTGTCTGAAAGACCATGTCACC
TTCAACAATGGAGGGGCTCAATAGACCAAACCTACCTG
AGCAAACCTGCTCGGGAAGCTGCCCCGAGCTCAGGAC
CCTGTGCACTCAGGGCCTGCAGCGGATCTTTTATCT
GAAGCTCGAAGACCTCGTGCCACCTCCCGCAATCA
TCGACAAACTGTTCCCTGGATACTGCCATTCTAG
AAGGATACTGGGGCATAACGCCACAGGGAGTCCAAG
AATGTGAGGTGGGGGTGGCGAAGGTAATGTCTTTG
GTGTGGGAAAAGCAGCAGCCATCTGAGATAGGAAC
TGAAAACCAGAGGAGAGGCGTTCAGGAAGATTAT
GGAGGGGAGGACTGGGCCCCACGAGCGACCAGA
GTTGTACAAGGCCGCAAGAACAGGGGAGGTGGG
GGGCTCAGGGACAGAAAAAAAGTATGTGTATTTTG
AGAGCAGGGTTGGGAGGCCTCTCCTGAAAAGGGTA
TAAACGTGGAGTAGGCAATACCCAGGCAAAAAGGG
GAGACCAGAGTAGGGGGAGGGGAAGAGTCCTGAC
CCAGGGAAGACATTA AAAAGGTAGTGGGGTCGACT
AGATGAAGGAGAGCCTTTCTCTCTGGGCAAGAGCG
GTGCAATGGTGTGTAAGGTAGCTGAGAAG
```

7. Literature

Abranches, E., Silva, M., Pradier, L., Schulz, H., Hummel, O., Henrique, D., and Bekman, E. (2009). Neural differentiation of embryonic stem cells in vitro: a road map to neurogenesis in the embryo. *PLoS One* 4, e6286.

Addis, R.C., Hsu, F.-C., Wright, R.L., Dichter, M. a., Coulter, D. a., and Gearhart, J.D. (2011). Efficient Conversion of Astrocytes to Functional Midbrain Dopaminergic Neurons Using a Single Polycistronic Vector. *PLoS One* 6, e28719.

Albéri, L., Sgadò, P., and Simon, H.H. (2004). Engrailed genes are cell-autonomously required to prevent apoptosis in mesencephalic dopaminergic neurons. *Development* 131, 3229–3236.

Allodi, I., and Hedlund, E. (2014). Directed midbrain and spinal cord neurogenesis from pluripotent stem cells to model development and disease in a dish. *Front. Neurosci.* 8, 109.

Alves dos Santos, M.T.M., and Smidt, M.P. (2011). En1 and Wnt signaling in midbrain dopaminergic neuronal development. *Neural Dev.* 6, 23.

Ambasudhan, R., Talantova, M., Coleman, R., Yuan, X., Zhu, S., Lipton, S. a, and Ding, S. (2011). Direct reprogramming of adult human fibroblasts to functional neurons under defined conditions. *Cell Stem Cell* 9, 113–118.

Andersson, E., Tryggvason, U., Deng, Q., Friling, S., Alekseenko, Z., Robert, B., Perlmann, T., and Ericson, J. (2006a). Identification of intrinsic determinants of midbrain dopamine neurons. *Cell* 124, 393–405.

Andersson, E., Jensen, J.B., Parmar, M., Guillemot, F., and Björklund, a (2006b). Development of the mesencephalic dopaminergic neuron system is compromised in the absence of neurogenin 2. *Development* 133, 507–516.

Andersson, E., Thompson, L.H., Marie, E., Hebsgaard, J.B., Nanou, E., Marklund, U., Kjellander, S., Hovatta, O., Manira, A. El, Björ-, A., et al. (2010).

Correction for Friling et al., Efficient production of mesencephalic dopamine neurons by Lmx1a expression in embryonic stem cells. *Proc. Natl. Acad. Sci.* *107*, 21229–21229.

Andersson, E.K.I., Irvin, D.K., Ahlsjö, J., and Parmar, M. (2007). Ngn2 and Nurr1 act in synergy to induce midbrain dopaminergic neurons from expanded neural stem and progenitor cells. *Exp. Cell Res.* *313*, 1172–1180.

Andres-Mateos, E., Perier, C., Zhang, L., Blanchard-Fillion, B., Greco, T.M., Thomas, B., Ko, H.S., Sasaki, M., Ischiropoulos, H., Przedborski, S., et al. (2007). DJ-1 gene deletion reveals that DJ-1 is an atypical peroxiredoxin-like peroxidase. *Proc. Natl. Acad. Sci. U. S. A.* *104*, 14807–14812.

Aubert, J., Dunstan, H., Chambers, I., and Smith, A. (2002). Functional gene screening in embryonic stem cells implicates Wnt antagonism in neural differentiation. *Nat. Biotechnol.* *20*, 1240–1245.

Bachoo, R., Kim, R., Ligon, K.L., Maher, E.A., Brennan, C., Billings, N., Chan, S., Li, C., Rowitch, D.H., Wong, W.H., et al. (2004). Molecular diversity of astrocytes with implications for neurological disorders. *Proc. ...* *101*.

Badger, J.L., Cordero-Llana, O., Hartfield, E.M., and Wade-Martins, R. (2014). Parkinson's disease in a dish - Using stem cells as a molecular tool. *Neuropharmacology 76 Pt A*, 88–96.

Barzilay, R., Melamed, E., and Offen, D. (2009). Introducing transcription factors to multipotent mesenchymal stem cells: making transdifferentiation possible. *Stem Cells* *27*, 2509–2515.

Berninger, B., Costa, M.R., Koch, U., Schroeder, T., Sutor, B., Grothe, B., and Götz, M. (2007). Functional properties of neurons derived from in vitro reprogrammed postnatal astroglia. *J. Neurosci.* *27*, 8654–8664.

Bertram, L., and Tanzi, R. (2005). The genetic epidemiology of neurodegenerative disease. *J. Clin. Invest.* *115*, 1449–1457.

Bianchi, M.E., and Manfredi, A. a (2014). How macrophages ring the inflammation alarm. *Proc. Natl. Acad. Sci. U. S. A.* *111*, 2866–2867.

Bibel, M., Richter, J., Lacroix, E., and Barde, Y.-A. (2007). Generation of a defined and uniform population of CNS progenitors and neurons from mouse embryonic stem cells. *Nat. Protoc.* *2*, 1034–1043.

Bikard, D., and Marraffini, L. a (2013). Control of gene expression by CRISPR-Cas systems. *F1000Prime Rep.* *5*, 47.

Buganim, Y., Itskovich, E., Hu, Y.-C., Cheng, A.W., Ganz, K., Sarkar, S., Fu, D., Welstead, G.G., Page, D.C., and Jaenisch, R. (2012). Direct reprogramming of fibroblasts into embryonic Sertoli-like cells by defined factors. *Cell Stem Cell* *11*, 373–386.

Cai, J., Donaldson, A., Yang, M., German, M.S., Enikolopov, G., and Iacovitti, L. (2009). The role of *Lmx1a* in the differentiation of human embryonic stem cells into midbrain dopamine neurons in culture and after transplantation into a Parkinson's disease model. *Stem Cells* *27*, 220–229.

Caiazzo, M., Dell'anno, M.T., Dvoretzkova, E., Lazarevic, D., Taverna, S., Leo, D., Sotnikova, T.D., Menegon, A., Roncaglia, P., Colciago, G., et al. (2011). Direct generation of functional dopaminergic neurons from mouse and human fibroblasts. *Nature* *476*, 224–227.

Carey, B.W., Markoulaki, S., Hanna, J., Saha, K., Gao, Q., Mitalipova, M., and Jaenisch Rudolf (2009). Reprogramming of murine and human somatic cells using a single polycistronic vector. *Proc. Natl. Acad. Sci.* *106*, 11818–11818.

Castro, D.S., Skowronska-Krawczyk, D., Armant, O., Donaldson, I.J., Parras, C., Hunt, C., Critchley, J. a, Nguyen, L., Gossler, A., Göttgens, B., et al. (2006). Proneural bHLH and Brn proteins coregulate a neurogenic program through cooperative binding to a conserved DNA motif. *Dev. Cell* *11*, 831–844.

Literature

Chen, X.L., Xiong, Y.Y., Xu, G.L., and Liu, X.F. (2013). Deep brain stimulation. *Interv. Neurol.* 1, 200–212.

Cheung, H.-H., Liu, X., and Rennert, O.M. (2012). Apoptosis: Reprogramming and the Fate of Mature Cells. *ISRN Cell Biol.* 2012, 1–8.

Cho, E.-G., Zaremba, J.D., McKercher, S.R., Talantova, M., Tu, S., Masliah, E., Chan, S.F., Nakanishi, N., Terskikh, A., and Lipton, S. a. (2011). MEF2C Enhances Dopaminergic Neuron Differentiation of Human Embryonic Stem Cells in a Parkinsonian Rat Model. *PLoS One* 6, e24027.

Cho, M.-S., Hwang, D.-Y., and Kim, D.-W. (2008). Efficient derivation of functional dopaminergic neurons from human embryonic stem cells on a large scale. *Nat. Protoc.* 3, 1888–1894.

Chung, S.J. (2010). Genetics in Parkinson's disease. *J. Korean Med. Assoc.* 54, 70.

Chung, C.Y., Seo, H., Sonntag, K.C., Brooks, A., Lin, L., and Isacson, O. (2005a). Cell type-specific gene expression of midbrain dopaminergic neurons reveals molecules involved in their vulnerability and protection. *Hum. Mol. Genet.* 14, 1709–1725.

Chung, S., Sonntag, K.-C., Andersson, T., Bjorklund, L.M., Park, J.-J., Kim, D.-W., Kang, U.J., Isacson, O., and Kim, K.-S. (2002). Genetic engineering of mouse embryonic stem cells by Nurr1 enhances differentiation and maturation into dopaminergic neurons. *Eur. J. ...* 16, 1829–1838.

Chung, S., Hedlund, E., Hwang, M., Kim, D.W., Shin, B.-S., Hwang, D.-Y., Kang, U.J., Isacson, O., and Kim, K.-S. (2005b). The homeodomain transcription factor Pitx3 facilitates differentiation of mouse embryonic stem cells into AHD2-expressing dopaminergic neurons. *Mol. Cell. Neurosci.* 28, 241–252.

Literature

Chung, S., Leung, A., Han, B., and Chang, M. (2009). Wnt1-lmx1a forms a novel autoregulatory loop and controls midbrain dopaminergic differentiation synergistically with the SHH-FoxA2 pathway. *Cell Stem Cell* 5, 646–658.

Colosimo, a., Goncz, K.K., Holmes, a. R., Kunzelmann, K., Bennet, M.J., and Gruenert, D.C. (2000). Review Transfer and Expression of Foreign Genes in Mammalian Cells. *Biotechniques* 29, 314–331.

Connolly, B.S., and Lang, A.E. (2014). Pharmacological treatment of Parkinson disease: a review. *JAMA* 311, 1670–1683.

Cooper, O., Hargus, G., Deleidi, M., Blak, A., Osborn, T., Marlow, E., Lee, K., Levy, A., Perez-Torres, E., Yow, A., et al. (2010). Differentiation of human ES and Parkinson's disease iPS cells into ventral midbrain dopaminergic neurons requires a high activity form of SHH, FGF8a and specific regionalization by retinoic acid. *Mol. Cell. Neurosci.* 45, 258–266.

Correia, A.S., Anisimov, S. V, Roybon, L., Li, J.-Y., and Brundin, P. (2007). Fibroblast growth factor-20 increases the yield of midbrain dopaminergic neurons derived from human embryonic stem cells. *Front. Neuroanat.* 1, 4.

Correia, A.S., Anisimov, S. V, Li, J.-Y., and Brundin, P. (2008). Growth factors and feeder cells promote differentiation of human embryonic stem cells into dopaminergic neurons: a novel role for fibroblast growth factor-20. *Front. Neurosci.* 2, 26–34.

Corti, S., Nizzardo, M., Simone, C., Falcone, M., Donadoni, C., Salani, S., Rizzo, F., Nardini, M., Riboldi, G., Magri, F., et al. (2012). Direct reprogramming of human astrocytes into neural stem cells and neurons. *Exp. Cell Res.* 318, 1528–1541.

Daadi, M.M., and Weiss, S. (1999). Generation of tyrosine hydroxylase-producing neurons from precursors of the embryonic and adult forebrain. *J. Neurosci.* 19, 4484–4497.

Dahlstrand, J., Lardelli, M., and Lendahl, U. (1995). Nestin mRNA expression correlates with the central nervous system progenitor cell state in many, but not all, regions of developing central nervous system. *Dev. Brain Res.* *84*, 109–129.

Daniels, R.W., Rossano, A.J., Macleod, G.T., and Ganetzky, B. (2014). Expression of multiple transgenes from a single construct using viral 2A peptides in *Drosophila*. *PLoS One* *9*, e100637.

Deleidi, M., Cooper, O., Hargus, G., Levy, A., and Isacson, O. (2011). Oct4-induced reprogramming is required for adult brain neural stem cell differentiation into midbrain dopaminergic neurons. *PLoS One* *6*, e19926.

Dellavalle, A., Maroli, G., Covarello, D., Azzoni, E., Innocenzi, A., Perani, L., Antonini, S., Sambasivan, R., Brunelli, S., Tajbakhsh, S., et al. (2011). Pericytes resident in postnatal skeletal muscle differentiate into muscle fibres and generate satellite cells. *Nat. Commun.* *2*, 411–499.

Deng, Q., Andersson, E., Hedlund, E., Alekseenko, Z., Coppola, E., Panman, L., Millonig, J.H., Brunet, J.-F., Ericson, J., and Perlmann, T. (2011). Specific and integrated roles of *Lmx1a*, *Lmx1b* and *Phox2a* in ventral midbrain development. *Development* *138*, 3399–3408.

Desbaillets, I., Ziegler, U., Groscurth, P., and Gassmann, M. (2000). Embryoid bodies : an in vitro model of mouse embryogenesis. *Exp. Physiol.*

Desbordes, S.C., Placantonakis, D.G., Ciro, A., Socci, N.D., Lee, G., Djaballah, H., and Studer, L. (2008). High-throughput screening assay for the identification of compounds regulating self-renewal and differentiation in human embryonic stem cells. *Cell Stem Cell* *2*, 602–612.

Dias, V., Junn, E., and Mouradian, M.M. (2014). The Role of Oxidative Stress in Parkinson's Disease. *J. Parkinsons. Dis.* *3*, 461–491.

Díaz, N., and Díaz-Martínez, N. (2009). Estradiol promotes proliferation of dopaminergic precursors resulting in a higher proportion of dopamine neurons derived from mouse embryonic stem cells. *Int. J. ...* 27, 493–500.

Doench, J.G., Hartenian, E., Graham, D.B., Tothova, Z., Hegde, M., Smith, I., Sullender, M., Ebert, B.L., Xavier, R.J., and Root, D.E. (2014). Rational design of highly active sgRNAs for CRISPR-Cas9-mediated gene inactivation. *Nat. Biotechnol.*

Donnelly, M.L., Hughes, L.E., Luke, G., Mendoza, H., ten Dam, E., Gani, D., and Ryan, M.D. (2001). The “cleavage” activities of foot-and-mouth disease virus 2A site-directed mutants and naturally occurring “2A-like” sequences. *J. Gen. Virol.* 82, 1027–1041.

Dubois-Dauphin, M. (1994). Neonatal motoneurons overexpressing the bcl-2 protooncogene in transgenic mice are protected from axotomy-induced cell death. *Proc. ...* 91, 3309–3313.

Elkouris, M., Balaskas, N., and Poulou, M. (2011). Sox1 Maintains the Undifferentiated State of Cortical Neural Progenitor Cells via the Suppression of Prox1-Mediated Cell Cycle Exit and Neurogenesis. *Stem ...* 89–98.

Falcon, A. a, Rios, N., and Aris, J.P. (2005). 2-Micron Circle Plasmids Do Not Reduce Yeast Life Span. *FEMS Microbiol. Lett.* 250, 245–251.

Farlie, P., and Dringen, R. (1995). bcl-2 transgene expression can protect neurons against developmental and induced cell death. *Proc. ...* 92, 4397–4401.

Fearnley, J.M., and Lees, A.J. (1991). Ageing and Parkinson’S Disease: Substantia Nigra Regional Selectivity. *Brain* 114, 2283–2301.

De Felipe, P. (2002). Polycistronic viral vectors. *Curr. Gene Ther.* 355–378.

Ferri, A.L.M., Lin, W., Mavromatakis, Y.E., Wang, J.C., Sasaki, H., Whitsett, J. J. a, and Ang, S.-L. (2007). Foxa1 and Foxa2 regulate multiple phases of

midbrain dopaminergic neuron development in a dosage-dependent manner. *Development* 134, 2761–2769.

Fong, C.-Y., Gauthaman, K., and Bongso, A. (2010). Teratomas from pluripotent stem cells: A clinical hurdle. *J. Cell. Biochem.* 111, 769–781.

Friedman, J.H. (2010). Parkinson's disease psychosis 2010: A review article. *Park. Relat. Disord.* 16, 553–560.

Gale, E., and Li, M. (2008). Midbrain dopaminergic neuron fate specification: Of mice and embryonic stem cells. *Mol. Brain* 1, 8.

García-parra, P., Maroto, M., Cavaliere, F., Naldaiz-gastesi, N., and Álava, J.I. (2013). A neural extracellular matrix-based method for in vitro hippocampal neuron culture and dopaminergic differentiation of neural stem cells. *BMC*

Geeta, R., Ramnath, R.L., Rao, H.S., and Chandra, V. (2008). One year survival and significant reversal of motor deficits in parkinsonian rats transplanted with hESC derived dopaminergic neurons. *Biochem. Biophys. Res. Commun.* 373, 258–264.

Gibson, S. a J., Gao, G.-D., McDonagh, K., and Shen, S. (2012). Progress on stem cell research towards the treatment of Parkinson's disease. *Stem Cell Res. Ther.* 3, 11.

Gietz, R.D., and Woods, R. (2002). Transformation of yeast by lithium acetate/single-stranded carrier DNA/polyethylene glycol method. *Methods Enzymol.* 350, 87–96.

Gifford, C. a, and Meissner, A. (2012). Epigenetic obstacles encountered by transcription factors: reprogramming against all odds. *Curr. Opin. Genet. Dev.* 22, 409–415.

Gill, S.S., Patel, N.K., Hotton, G.R., O'Sullivan, K., McCarter, R., Bunnage, M., Brooks, D.J., Svendsen, C.N., and Heywood, P. (2003). Direct brain

infusion of glial cell line-derived neurotrophic factor in Parkinson disease. *Nat. Med.* 9, 589–595.

Goetz, C.G. (2011). The history of Parkinson's disease: early clinical descriptions and neurological therapies. *Cold Spring Harb. Perspect. Med.* 1, a008862.

Goldman, S.M. (2014). Environmental toxins and Parkinson's disease. *Annu. Rev. Pharmacol. Toxicol.* 54, 141–164.

Goridis, C., and Brunet, J.-F. (1999). Transcriptional control of neurotransmitter phenotype. *Curr. Opin. Neurobiol.* 9, 47–53.

Greene, J.C., Whitworth, A.J., Andrews, L. a, Parker, T.J., and Pallanck, L.J. (2005). Genetic and genomic studies of *Drosophila parkin* mutants implicate oxidative stress and innate immune responses in pathogenesis. *Hum. Mol. Genet.* 14, 799–811.

Greenfield, J.G., and Bosanquet, F.D. (1953). The Brain-Stem Lesions in Parkinsonism. *J. Neurol. Neurosurg. Psychiatry* 16, 213–226.

Gröger, A., Kolb, R., Schäfer, R., and Klose, U. (2014). Dopamine reduction in the substantia nigra of Parkinson's disease patients confirmed by in vivo magnetic resonance spectroscopic imaging. *PLoS One* 9, e84081.

Guo, Z., Zhang, L., Wu, Z., Chen, Y., Wang, F., and Chen, G. (2014). In Vivo direct reprogramming of reactive glial cells into functional neurons after brain injury and in an Alzheimer's disease model. *Cell Stem Cell* 14, 188–202.

Gutierrez-Aranda, I., Ramos-Mejia, V., Bueno, C., Munoz-Lopez, M., Real, P.J., Mácia, A., Sanchez, L., Ligeró, G., Garcia-Parez, J.L., and Menendez, P. (2010). Human induced pluripotent stem cells develop teratoma more efficiently and faster than human embryonic stem cells regardless the site of injection. *Stem Cells* 28, 1568–1570.

Hampton, R.Y. (2000). ER stress response: getting the UPR hand on misfolded proteins. *Curr. Biol.* 10, R518–R521.

Han, D.W., Tapia, N., Hermann, A., Hemmer, K., Höing, S., Araúzo-Bravo, M.J., Zaehres, H., Wu, G., Frank, S., Moritz, S., et al. (2012). Direct reprogramming of fibroblasts into neural stem cells by defined factors. *Cell Stem Cell* 10, 465–472.

Harada, S., Nakamoto, K., and Tokuyama, S. (2013). The involvement of midbrain astrocyte in the development of morphine tolerance. *Life Sci.* 93, 573–578.

Hartfield, E.M., Yamasaki-Mann, M., Ribeiro Fernandes, H.J., Vowles, J., James, W.S., Cowley, S. a, and Wade-Martins, R. (2014). Physiological characterisation of human iPS-derived dopaminergic neurons. *PLoS One* 9, e87388.

Hauser, R. a, Freeman, T.B., Snow, B.J., Nauert, M., Gauger, L., Kordower, J.H., and Olanow, C.W. (1999). Long-term evaluation of bilateral fetal nigral transplantation in Parkinson disease. *Arch. Neurol.* 56, 179–187.

Hayashi, H., Morizane, A., Koyanagi, M., Ono, Y., Sasai, Y., Hashimoto, N., and Takahashi, J. (2008). Meningeal cells induce dopaminergic neurons from embryonic stem cells. *Eur. J. Neurosci.* 27, 261–268.

He, X.B., Yi, S.H., Rhee, Y.H., Kim, H., Han, Y.M., Lee, S.H., Lee, H., Park, C.H., Lee, Y.S., Richardson, E., et al. (2011). Prolonged membrane depolarization enhances midbrain dopamine neuron differentiation via epigenetic histone modifications. *Stem Cells* 29, 1861–1873.

Hegarty, S. V, Sullivan, A.M., and O’Keeffe, G.W. (2013). Midbrain dopaminergic neurons: a review of the molecular circuitry that regulates their development. *Dev. Biol.* 379, 123–138.

Heinrich, C., Blum, R., Gascón, S., Masserdotti, G., Tripathi, P., Sánchez, R., Tiedt, S., Schroeder, T., Götz, M., and Berninger, B. (2010). Directing

astroglia from the cerebral cortex into subtype specific functional neurons. *PLoS Biol.* 8, e1000373.

Hendry, C.E., Vanslambrouck, J.M., Ineson, J., Suhaimi, N., Takasato, M., Rae, F., and Little, M.H. (2013). Direct transcriptional reprogramming of adult cells to embryonic nephron progenitors. *J. Am. Soc. Nephrol.* 24, 1424–1434.

Hindle, J. V. (2010). Ageing, neurodegeneration and Parkinson's disease. *Age Ageing* 39, 156–161.

Hirai, H., Tani, T., and Kikyo, N. (2010). Structure and functions of powerful transactivators: VP16, MyoD and FoxA. *Int. J. Dev. Biol.* 54, 1589–1596.

Hong, S., Chung, S., Leung, K., Hwang, I., Moon, J., and Kim, K.-S. (2014). Functional roles of Nurr1, Pitx3, and Lmx1a in neurogenesis and phenotype specification of dopamine neurons during in vitro differentiation of embryonic stem cells. *Stem Cells Dev.* 23, 477–487.

Hotton, D., Mauro, N., Lezot, F., Forest, N., and Berdal, a. (1999). Differential Expression and Activity of Tissue-nonspecific Alkaline Phosphatase (TNAP) in Rat Odontogenic Cells In Vivo. *J. Histochem. Cytochem.* 47, 1541–1552.

Hsieh, W., and Chiang, B. (2014). A Well-Refined In Vitro Model Derived from Human Embryonic Stem Cell for Screening Phytochemicals with Midbrain Dopaminergic Differentiation-Boosting Potential for Improving Parkinson's Disease. *J. Agric. Food Chem.*

Huang, P., Zhang, L., Gao, Y., He, Z., Yao, D., Wu, Z., Cen, J., Chen, X., Liu, C., Hu, Y., et al. (2014). Direct reprogramming of human fibroblasts to functional and expandable hepatocytes. *Cell Stem Cell* 14, 370–384.

Hurwitz, B. (2014). Urban Observation and Sentiment in James Parkinson's Essay on the Shaking Palsy (1817). *Lit. Med.* 32, 74–104.

Iacovitti, L., Donaldson, A.E., Marshall, C.E., Suon, S., and Yang, M. (2007). A protocol for the differentiation of human embryonic stem cells into

dopaminergic neurons using only chemically defined human additives: Studies in vitro and in vivo. *Brain Res.* 1127, 19–25.

Ieda, M., Fu, J.-D., Delgado-Olguin, P., Vedantham, V., Hayashi, Y., Bruneau, B.G., and Srivastava, D. (2010). Direct reprogramming of fibroblasts into functional cardiomyocytes by defined factors. *Cell* 142, 375–386.

Jacobs, B.M. (2014). Stemming the hype: what can we learn from iPSC models of Parkinson's disease and how can we learn it? *J. Parkinsons. Dis.* 4, 15–27.

Jacobs, F.M.J., van Erp, S., van der Linden, A.J. a, von Oerthel, L., Burbach, J.P.H., and Smidt, M.P. (2009). Pitx3 potentiates Nurr1 in dopamine neuron terminal differentiation through release of SMRT-mediated repression. *Development* 136, 531–540.

Jaenisch, R., and Bird, A. (2003). Epigenetic regulation of gene expression: how the genome integrates intrinsic and environmental signals. *Nat. Genet.* 33 *Suppl*, 245–254.

Jankovic, J. (2008). Parkinson's disease: clinical features and diagnosis. *J. Neurol. Neurosurg. Psychiatry* 79, 368–376.

Jehn, B.M., Bielke, W., Pear, W.S., and Osborne, B.A. (2014). Cutting Edge: Protective Effects of Notch-1 on TCR-Induced Apoptosis.

Jellinger, K. a (2001). Cell death mechanisms in neurodegeneration. *J. Cell. Mol. Med.* 5, 1–17.

Jetti, R., and Raghuvver, C. (2014). Neuroprotective effect of Ascorbic acid and Ginkgo biloba against Fluoride caused Neurotoxicity. *IOSR J. ...* 8, 30–36.

Kadkhodaei, B., Ito, T., Joodmardi, E., Mattsson, B., Rouillard, C., Carta, M., Muramatsu, S., Sumi-Ichinose, C., Nomura, T., Metzger, D., et al. (2009).

Nurr1 is required for maintenance of maturing and adult midbrain dopamine neurons. *J. Neurosci.* 29, 15923–15932.

Karow, M., Sánchez, R., Schichor, C., Masserdotti, G., Ortega, F., Heinrich, C., Gascón, S., Khan, M. a, Lie, D.C., Dellavalle, A., et al. (2012). Reprogramming of pericyte-derived cells of the adult human brain into induced neuronal cells. *Cell Stem Cell* 11, 471–476.

Kawamoto, S., Niwa, H., Tashiro, F., Sano, S., Kondohc, G., Takedac, J., Tabayashi, K., and Miyazaki, J. (2000). A novel reporter mouse strain that expresses enhanced green fluorescent protein upon Cre-mediated recombination. *FEBS Lett.* 470, 263–268.

Kawasaki, H., Suemori, H., Mizuseki, K., Watanabe, K., Urano, F., Ichinose, H., Haruta, M., Takahashi, M., Yoshikawa, K., Nishikawa, S.-I., et al. (2002). Generation of dopaminergic neurons and pigmented epithelia from primate ES cells by stromal cell-derived inducing activity. *Proc. Natl. Acad. Sci. U. S. A.* 99, 1580–1585.

Kehat, I., Kenyagin-Karsenti, D., Snir, M., Segev, H., Amit, M., Gepstein, a, Livne, E., Binah, O., Itskovitz-Eldor, J., and Gepstein, L. (2001). Human embryonic stem cells can differentiate into myocytes with structural and functional properties of cardiomyocytes. *J. Clin. Invest.* 108, 407–414.

Kele, J., Simplicio, N., Ferri, A.L.M., Mira, H., Guillemot, F., Arenas, E., and Ang, S.-L. (2006). Neurogenin 2 is required for the development of ventral midbrain dopaminergic neurons. *Development* 133, 495–505.

Kim, T.K., and Eberwine, J.H. (2010). Mammalian cell transfection: The present and the future. *Anal. Bioanal. Chem.* 397, 3173–3178.

Kim, D., Chung, S., Hwang, M., and Ferree, A. (2006). Stromal cell-derived inducing activity, Nurr1, and signaling molecules synergistically induce dopaminergic neurons from mouse embryonic stem cells. *Stem ...* 24, 557–567.

Literature

Kim, H.-S., Kim, J., Jo, Y., Jeon, D., and Cho, Y.S. (2014). Direct lineage reprogramming of mouse fibroblasts to functional midbrain dopaminergic neuronal progenitors. *Stem Cell Res.* 12, 60–68.

Kim, J., Efe, J.A., Zhu, S., Talantova, M., Yuan, X., Wang, S., and Lipton, S.A. (2011a). Direct reprogramming of mouse fibroblasts to neural progenitors. *Proc. Natl. Acad. Sci.*

Kim, J.H., Lee, S.-R., Li, L.-H., Park, H.-J., Park, J.-H., Lee, K.Y., Kim, M.-K., Shin, B.A., and Choi, S.-Y. (2011b). High cleavage efficiency of a 2A peptide derived from porcine teschovirus-1 in human cell lines, zebrafish and mice. *PLoS One* 6, e18556.

Kim, J.-Y., Koh, H.C., Lee, J.-Y., Chang, M.-Y., Kim, Y.-C., Chung, H.-Y., Son, H., Lee, Y.-S., Studer, L., McKay, R., et al. (2003a). Dopaminergic neuronal differentiation from rat embryonic neural precursors by Nurr1 overexpression. *J. Neurochem.* 85, 1443–1454.

Kim, K.-S., Kim, C.-H., Hwang, D.-Y., Seo, H., Chung, S., Hong, S.J., Lim, J.-K., Anderson, T., and Isacson, O. (2003b). Orphan nuclear receptor Nurr1 directly transactivates the promoter activity of the tyrosine hydroxylase gene in a cell-specific manner. *J. Neurochem.* 85, 622–634.

Kimmel, R.A., Turnbull, D.H., Blanquet, V., Wurst, W., Loomis, C.A., and Joyner, A.L. (2000). formation Two lineage boundaries coordinate vertebrate apical ectodermal ridge formation. 1377–1389.

Kinney, M. a, Sargent, C.Y., and McDevitt, T.C. (2011). The multiparametric effects of hydrodynamic environments on stem cell culture. *Tissue Eng. Part B. Rev.* 17, 249–262.

Knoepfler, P., Cheng, P.F., and Eisenman, R.N. (2002). N-myc is essential during neurogenesis for the rapid expansion of progenitor cell populations and the inhibition of neuronal differentiation. *Genes ...* 2699–2712.

Kordower, J.H., and Brundin, P. (2009). Lewy body pathology in long-term fetal nigral transplants: is Parkinson's disease transmitted from one neural system to another? *Neuropsychopharmacology* 34, 254.

Krabbe, C., Courtois, E., Jensen, P., Jørgensen, J.R., Zimmer, J., Martínez-Serrano, A., and Meyer, M. (2009). Enhanced dopaminergic differentiation of human neural stem cells by synergistic effect of Bcl-xL and reduced oxygen tension. *J. Neurochem.* 110, 1908–1920.

Kriks, S., Shim, J.-W., Piao, J., Ganat, Y.M., Wakeman, D.R., Xie, Z., Carrillo-Reid, L., Auyeung, G., Antonacci, C., Buch, A., et al. (2011). Dopamine neurons derived from human ES cells efficiently engraft in animal models of Parkinson's disease. *Nature* 480, 547–551.

Le, W., Conneely, O.M., He, Y., Jankovic, J., and Appel, S.H. (1999). Reduced Nurr1 Expression Increases the Vulnerability of Mesencephalic Dopamine Neurons to MPTP-Induced Injury. *J. Neurochem.* 2218–2221.

Le, W., Pan, T., Huang, M., Xu, P., and Xie, W. (2008). Decreased NURR1 gene expression in patients with Parkinson's disease. *J. ...* 273, 29–33.

Lebel, Â., Gauthier, Y., Moreau, A., and Drouin, J. (2001). Pitx3 activates mouse tyrosine hydroxylase promoter via a high-affinity binding site. *J. Neurochem.* 558–567.

Lee, H.-S., Bae, E.-J., Yi, S.-H., Shim, J.-W., Jo, A.-Y., Kang, J.-S., Yoon, E.-H., Rhee, Y.-H., Park, C.-H., Koh, H.-C., et al. (2010). Foxa2 and Nurr1 synergistically yield A9 nigral dopamine neurons exhibiting improved differentiation, function, and cell survival. *Stem Cells* 28, 501–512.

Lee, S.H., Lumelsky, N., Studer, L., Auerbach, J.M., and McKay, R.D. (2000). Efficient generation of midbrain and hindbrain neurons from mouse embryonic stem cells. *Nat. Biotechnol.* 18, 675–679.

Lesage, S., and Brice, A. (2009). Parkinson's disease: from monogenic forms to genetic susceptibility factors. *Hum. Mol. Genet.* 18, R48–R59.

Literature

Li, M., Wang, X., and Meintzer, M. (2000). Cyclic AMP promotes neuronal survival by phosphorylation of glycogen synthase kinase 3 β . *Mol. Cell. Biol.* 20, 9356–9363.

Li, Y., Liu, Z., Dong, C., He, P., Liu, X., Zhu, Z., Jia, B., Li, F., and Wang, F. (2013). Noninvasive detection of human-induced pluripotent stem cell (hiPSC)-derived teratoma with an integrin-targeting agent (99m)Tc-3PRGD2. *Mol. Imaging Biol.* 15, 58–67.

Lim, D., Tramontin, A., and Trevejo, J. (2000). Noggin antagonizes BMP signaling to create a niche for adult neurogenesis. *Neuron* 28, 713–726.

Lin, M.T., and Beal, M.F. (2006). Mitochondrial dysfunction and oxidative stress in neurodegenerative diseases. *Nature* 443, 787–795.

Lin, W., Metzakopian, E., Mavromatakis, Y.E., Gao, N., Balaskas, N., Sasaki, H., Briscoe, J., Whitsett, J. a, Goulding, M., Kaestner, K.H., et al. (2009). Foxa1 and Foxa2 function both upstream of and cooperatively with Lmx1a and Lmx1b in a feedforward loop promoting mesodiencephalic dopaminergic neuron development. *Dev. Biol.* 333, 386–396.

Lin, Y.-J., Huang, L.-H., and Huang, C.-T. (2013). Enhancement of heterologous gene expression in *Flammulina velutipes* using polycistronic vectors containing a viral 2A cleavage sequence. *PLoS One* 8, e59099.

Liu, S., Qu, Y., Stewart, T.J., Howard, M.J., Chakraborty, S., Holekamp, T.F., and McDonald, J.W. (2000). Embryonic stem cells differentiate into oligodendrocytes and myelinate in culture and after spinal cord transplantation. *Proc. Natl. Acad. Sci.* 97, 6126–6131.

Liu, X., Li, F., Stubblefield, E. a, Blanchard, B., Richards, T.L., Larson, G. a, He, Y., Huang, Q., Tan, A.-C., Zhang, D., et al. (2012). Direct reprogramming of human fibroblasts into dopaminergic neuron-like cells. *Cell Res.* 22, 321–332.

Literature

Longo, G.S., Pinhel, M.S., Sado, C.L., Gregório, M.L., Amorim, G.S., Florim, G.S., Mazeti, C.M., Martins, D.P., Oliveira, F.N., Tognola, W. a, et al. (2013). Exposure to pesticides and heterozygote genotype of GSTP1-Alw26I are associated to Parkinson's disease. *Arq. Neuropsiquiatr.* 71, 446–452.

Lopez, G., and Sidransky, E. (2010). Autosomal recessive mutations in the development of Parkinson's disease R eview. *Biomarkers Med.* 4, 713–721.

Lu, J., Tan, L., Li, P., Gao, H., Fang, B., Ye, S., Geng, Z., Zheng, P., and Song, H. (2009). All-trans retinoic acid promotes neural lineage entry by pluripotent embryonic stem cells via multiple pathways. *BMC Cell Biol.* 10, 57.

Lujan, E., Chanda, S., Ahlenius, H., Südhof, T.C., and Wernig, M. (2012). Direct conversion of mouse fibroblasts to self-renewing, tripotent neural precursor cells. *Proc. Natl. Acad. Sci. U. S. A.* 109, 2527–2532.

Luk, K.C., Rymar, V. V, van den Munckhof, P., Nicolau, S., Steriade, C., Bifsha, P., Drouin, J., and Sadikot, A.F. (2013). The transcription factor Pitx3 is expressed selectively in midbrain dopaminergic neurons susceptible to neurodegenerative stress. *J. Neurochem.* 125, 932–943.

Lumelsky, N., Blondel, O., Laeng, P., Velasco, I., Ravin, R., and McKay, R. (2001). Differentiation of embryonic stem cells to insulin-secreting structures similar to pancreatic islets. *Science* 292, 1389–1394.

Madisen, L., Zwingman, T. a, Sunkin, S.M., Oh, S.W., Zariwala, H. a, Gu, H., Ng, L.L., Palmiter, R.D., Hawrylycz, M.J., Jones, A.R., et al. (2010). A robust and high-throughput Cre reporting and characterization system for the whole mouse brain. *Nat. Neurosci.* 13, 133–140.

Malkus, K. a, Tsika, E., and Ischiropoulos, H. (2009). Oxidative modifications, mitochondrial dysfunction, and impaired protein degradation in Parkinson's disease: how neurons are lost in the Bermuda triangle. *Mol. Neurodegener.* 4, 24.

Masip, M., Veiga, A., Izpisua Belmonte, J.C., and Simón, C. (2010). Reprogramming with defined factors: from induced pluripotency to induced transdifferentiation. *Mol. Hum. Reprod.* *16*, 856–868.

McLenachan, S., Sarsero, J.P., and Ioannou, P. a (2007). Flow-cytometric analysis of mouse embryonic stem cell lipofection using small and large DNA constructs. *Genomics* *89*, 708–720.

McNaught, K., and Olanow, C. (2001). Failure of the ubiquitin–proteasome system in Parkinson’s disease. *Nat. Rev.* ... *2*.

Meiser, J., Weindl, D., and Hiller, K. (2013). Complexity of dopamine metabolism. *Cell Commun. Signal.* *11*, 34.

Mery, M., Matsumoto, L., Winters, K.A., Doroshov, J.H., and Kane, S.E. (1996). Bicistronic and Two-Gene Retroviral Vectors for Using MDR 1 as a Selectable Marker and a Therapeutic Gene. *Virology* *241*, 230–241.

Metzakopian, E., Lin, W., Salmon-Divon, M., Dvinge, H., Andersson, E., Ericson, J., Perlmann, T., Whitsett, J. a, Bertone, P., and Ang, S.-L. (2012). Genome-wide characterization of Foxa2 targets reveals upregulation of floor plate genes and repression of ventrolateral genes in midbrain dopaminergic progenitors. *Development* *139*, 2625–2634.

Mfopou, J.K., Geeraerts, M., Dejene, R., Van Langenhoven, S., Aberkane, A., Van Grunsven, L. a, and Bouwens, L. (2014). Efficient definitive endoderm induction from mouse embryonic stem cell adherent cultures: a rapid screening model for differentiation studies. *Stem Cell Res.* *12*, 166–177.

Michel, P.P., and Agid, Y. (2002). Chronic Activation of the Cyclic AMP Signaling Pathway Promotes Development and Long-Term Survival of Mesencephalic Dopaminergic Neurons. *J. Neurochem.* *67*, 1633–1642.

Mittermeyer, G., Christine, C.W., Rosenbluth, K.H., Baker, S.L., Starr, P., Larson, P., Kaplan, P.L., Forsayeth, J., Aminoff, M.J., and Bankiewicz, K.S.

(2012). Long-Term Evaluation of a Phase 1 Study of AADC Gene Therapy for Parkinson's Disease. *Hum. Gene Ther.* 23, 377–381.

Mori, T., Tanaka, K., Buffo, A., and Wurst, W. (2006). Inducible Gene Deletion in Astroglia and Radial Glia — A Valuable Tool for Functional and Lineage Analysis Generation of Mice. *Glia* 21–34.

Morizane, A., Takahashi, J., Takagi, Y., Sasai, Y., and Hashimoto, N. (2002). Optimal conditions for in vivo induction of dopaminergic neurons from embryonic stem cells through stromal cell-derived inducing activity. *J. Neurosci. Res.* 69, 934–939.

Mullen, R., Buck, C., and Smith, A. (1992). NeuN, a neuronal specific nuclear protein in vertebrates. *Development* 211, 201–211.

Van den Munckhof, P. (2003). Pitx3 is required for motor activity and for survival of a subset of midbrain dopaminergic neurons. *Development* 130, 2535–2542.

Muramatsu, S., Fujimoto, K., Kato, S., Mizukami, H., Asari, S., Ikeguchi, K., Kawakami, T., Urabe, M., Kume, A., Sato, T., et al. (2010). A phase I study of aromatic L-amino acid decarboxylase gene therapy for Parkinson's disease. *Mol. Ther.* 18, 1731–1735.

Muraoka, N., Yamakawa, H., Miyamoto, K., Sadahiro, T., Umei, T., Isomi, M., Nakashima, H., Akiyama, M., Wada, R., Inagawa, K., et al. (2014). MiR-133 promotes cardiac reprogramming by directly repressing Snai1 and silencing fibroblast signatures. *EMBO J.* 33, 1565–1581.

Najm, F.J., Lager, A.M., Zaremba, A., Wyatt, K., Caprariello, A. V, Factor, D.C., Karl, R.T., Maeda, T., Miller, R.H., and Tesar, P.J. (2013). Transcription factor-mediated reprogramming of fibroblasts to expandable, myelogenic oligodendrocyte progenitor cells. *Nat Biotechnol* 31, 426–433.

Nandy, S.B., Mohanty, S., Singh, M., Behari, M., and Airan, B. (2014). Fibroblast Growth Factor-2 alone as an efficient inducer for differentiation of

human bone marrow mesenchymal stem cells into dopaminergic neurons. *J. Biomed. Sci.* *21*, 83.

Nefzger, C., Su, C., Fabb, S., and Hartley, B. (2012). Lmx1a Allows Context-Specific Isolation of Progenitors of GABAergic or Dopaminergic Neurons During Neural Differentiation of Embryonic Stem Cells. *Stem ...* 1349–1361.

Niu, W., Zang, T., Zou, Y., Fang, S., Smith, D.K., Bachoo, R., and Zhang, C.-L. (2013). In vivo reprogramming of astrocytes to neuroblasts in the adult brain. *Nat. Cell Biol.* *15*, 1164–1175.

Nivet, E., Sancho-Martinez, I., and Izpisua Belmonte, J.C. (2013). Conversion of pericytes to neurons: a new guest at the reprogramming convention. *Stem Cell Res. Ther.* *4*, 2.

Nunes, I., Tovmasian, L.T., Silva, R.M., Burke, R.E., and Goff, S.P. (2003). Pitx3 is required for development of substantia nigra dopaminergic neurons. *Proc. Natl. Acad. Sci. U. S. A.* *100*, 4245–4250.

Oakeley, E. (1999). DNA methylation analysis a review of current methodologies. *Pharmacol. Ther.* *84*, 389–400.

Oh, S., Park, H., Hwang, I., Park, H., Choi, K.-A., Jeong, H., Kim, S.W., and Hong, S. (2014). Efficient reprogramming of mouse fibroblasts to neuronal cells including dopaminergic neurons. *ScientificWorldJournal.* *2014*, 957548.

Okada, T., Nonaka-Sarukawa, M., Uchibori, R., Kinoshita, K., Hayashita-Kinoh, H., Nitahara-Kasahara, Y., Takeda, S., and Ozawa, K. (2009). Scalable purification of adeno-associated virus serotype 1 (AAV1) and AAV8 vectors, using dual ion-exchange adsorptive membranes. *Hum. Gene ...* *1021*, 1013–1021.

Olanow, C.W., Goetz, C.G., Kordower, J.H., Stoessl, a J., Sossi, V., Brin, M.F., Shannon, K.M., Nauert, G.M., Perl, D.P., Godbold, J., et al. (2003). A

Double-blind Controlled Trial of Bilateral Fetal Nigral Transplantation in Parkinson ' s Disease. *Ann. Neurol.* 403–414.

Omodei, D., Acampora, D., Mancuso, P., Prakash, N., Di Giovannantonio, L.G., Wurst, W., and Simeone, A. (2008). Anterior-posterior graded response to *Otx2* controls proliferation and differentiation of dopaminergic progenitors in the ventral mesencephalon. *Development* 135, 3459–3470.

Paldino, E., Cenciarelli, C., Giampaolo, A., Milazzo, L., Pescatori, M., Hassan, H.J., and Casalbore, P. (2014). Induction of dopaminergic neurons from human Wharton's jelly mesenchymal stem cell by forskolin. *J. Cell. Physiol.* 229, 232–244.

Palfi, S., Gurruchaga, J.M., Ralph, G.S., Lepetit, H., Lavisse, S., Buttery, P.C., Watts, C., Miskin, J., Kelleher, M., Deeley, S., et al. (2014). Long-term safety and tolerability of ProSavin , a lentiviral vector-based gene therapy for Parkinson ' s disease: a dose escalation , open-label , phase 1 / 2 trial. *Lancet* 383, 1138–1146.

Pan-Montojo, F., and Reichmann, H. (2014). Considerations on the role of environmental toxins in idiopathic Parkinson's disease pathophysiology. *Transl. Neurodegener.* 3, 10.

Papanikolaou, T., Lenington, J.B., Betz, A., Figueiredo, C., Salamone, J.D., and Conover, J.C. (2008). In vitro generation of dopaminergic neurons from adult subventricular zone neural progenitor cells. *Stem Cells Dev.* 17, 157–172.

Paquin, A., Jaalouk, D., and Galipeau, J. (2001). Retrovector encoding a green fluorescent protein-herpes simplex virus thymidine kinase fusion protein serves as a versatile suicide/reporter for cell and gene therapy. *Hum. Gene Ther.* 23, 13–23.

Park, C.-H., Kang, J.S., Kim, J.-S., Chung, S., Koh, J.-Y., Yoon, E.-H., Jo, a Y., Chang, M.-Y., Koh, H.-C., Hwang, S., et al. (2006). Differential actions of

the proneural genes encoding Mash1 and neurogenins in Nurr1-induced dopamine neuron differentiation. *J. Cell Sci.* 119, 2310–2320.

Park, J., Ho, D., Yun, H.J., Kim, H., Lee, C.H., Park, S.W., Kim, Y.H., Son, I., and Seol, W. (2013). Dexamethasone induces the expression of LRRK2 and α -synuclein, two genes that when mutated cause Parkinson's disease in an autosomal dominant manner. *BMB Rep.* 46, 454–459.

Parras, C.M., Schuurmans, C., Scardigli, R., Kim, J., Anderson, D.J., and Guillemot, F. (2002). Divergent functions of the proneural genes Mash1 and Ngn2 in the specification of neuronal subtype identity. *Genes Dev.* 16, 324–338.

Peng, C., Aron, L., Klein, R., Li, M., Wurst, W., Prakash, N., and Le, W. (2011). Pitx3 is a critical mediator of GDNF-induced BDNF expression in nigrostriatal dopaminergic neurons. *J. Neurosci.* 31, 12802–12815.

Perez-Pinera, P., Kocak, D.D., Vockley, C.M., Adler, A.F., Kabadi, A.M., Polstein, L.R., Thakore, P.I., Glass, K. a, Ousterout, D.G., Leong, K.W., et al. (2013). RNA-guided gene activation by CRISPR-Cas9-based transcription factors. *Nat. Methods* 10, 973–976.

Pevny, L.H., Sockanathan, S., Placzek, M., and Lovell-badge, R. (1998). A role for SOX1 in neural determination. *Development* 1978, 1967–1978.

Pfisterer, U., Wood, J., Nihlberg, K., Hallgren, O., Bjermer, L., Westergren-Thorsson, G., Lindvall, O., and Parmar, M. (2011a). Efficient induction of functional neurons from adult human fibroblasts. *Cell Cycle* 10, 3311–3316.

Pfisterer, U., Kirkeby, A., Torper, O., Wood, J., Nelander, J., Dufour, A., Björklund, A., Lindvall, O., Jakobsson, J., and Parmar, M. (2011b). Direct conversion of human fibroblasts to dopaminergic neurons. *Proc. Natl. Acad. Sci. U. S. A.* 108, 10343–10348.

Pikaart, M.J., Recillas-Targa, F., and Felsenfeld, G. (1998). Loss of transcriptional activity of a transgene is accompanied by DNA methylation and

histone deacetylation and is prevented by insulators. *Genes Dev.* 12, 2852–2862.

Plun-Favreau, H., Klupsch, K., Moiso, N., Gandhi, S., Kjaer, S., Frith, D., Harvey, K., Deas, E., Harvey, R.J., McDonald, N., et al. (2007). The mitochondrial protease HtrA2 is regulated by Parkinson's disease-associated kinase PINK1. *Nat. Cell Biol.* 9, 1243–1252.

Politis, M., and Lindvall, O. (2012). Clinical application of stem cell therapy in Parkinson's disease. *BMC Med.* 10, 1.

Prosser, H.M., Koike-Yusa, H., Cooper, J.D., Law, F.C., and Bradley, A. (2011). A resource of vectors and ES cells for targeted deletion of microRNAs in mice. *Nat. Biotechnol.* 29, 840–845.

Pu, J., Jiang, H., Zhang, B., and Feng, J. (2012). Redefining Parkinson's disease research using induced pluripotent stem cells. *Curr. Neurol. Neurosci. Rep.* 12, 392–398.

Puelles, E., Annino, A., Tuorto, F., Usiello, A., Acampora, D., Czerny, T., Brodski, C., Ang, S.-L., Wurst, W., and Simeone, A. (2004). *Otx2* regulates the extent, identity and fate of neuronal progenitor domains in the ventral midbrain. *Development* 131, 2037–2048.

Qi, Z., Miller, G.W., and Voit, E.O. (2008). Computational systems analysis of dopamine metabolism. *PLoS One* 3, e2444.

Rao, M., and Shetty, A. (2004). Efficacy of doublecortin as a marker to analyse the absolute number and dendritic growth of newly generated neurons in the adult dentate gyrus. *Eur. J. Neurosci.* 19.

Rascol, O., Payoux, P., and Ory, F. (2003). Limitations of current Parkinson's disease therapy. *Ann. ...* 3–15.

Reyes, S., Fu, Y., Double, K., Thompson, L., Kirik, D., Paxinos, G., and Halliday, G.M. (2012). GIRK2 expression in dopamine neurons of the

substantia nigra and ventral tegmental area. *J. Comp. Neurol.* *520*, 2591–2607.

Rhee, J.-K., Kim, K., Chae, H., Evans, J., Yan, P., Zhang, B.-T., Gray, J., Spellman, P., Huang, T.H.-M., Nephew, K.P., et al. (2013). Integrated analysis of genome-wide DNA methylation and gene expression profiles in molecular subtypes of breast cancer. *Nucleic Acids Res.* *41*, 8464–8474.

Richardson, R.M., Kells, A.P., Rosenbluth, K.H., Salegio, E.A., Fiandaca, M.S., Larson, P.S., Starr, P. a, Martin, A.J., Lonser, R.R., Federoff, H.J., et al. (2011). Interventional MRI-guided putaminal delivery of AAV2-GDNF for a planned clinical trial in Parkinson's disease. *Mol. Ther.* *19*, 1048–1057.

Robel, S., Berninger, B., and Götz, M. (2011). The stem cell potential of glia: lessons from reactive gliosis. *Nat. Rev. Neurosci.* *12*, 88–104.

Roessler, R., Boddeke, E., and Copray, S. (2013). Induced pluripotent stem cell technology and direct conversion: new possibilities to study and treat Parkinson's disease. *Stem Cell Rev.* *9*, 505–513.

Rolletschek, a, Chang, H., Guan, K., Czyz, J., Meyer, M., and Wobus, a M. (2001). Differentiation of embryonic stem cell-derived dopaminergic neurons is enhanced by survival-promoting factors. *Mech. Dev.* *105*, 93–104.

Ron-Bigger, S., Bar-Nur, O., Isaac, S., Bocker, M., Lyko, F., and Eden, A. (2010). Aberrant epigenetic silencing of tumor suppressor genes is reversed by direct reprogramming. *Stem Cells* *28*, 1349–1354.

Ross, G.W., Petrovitch, H., Abbott, R.D., Nelson, J., Markesbery, W., Davis, D., Hardman, J., Launer, L., Masaki, K., Tanner, C.M., et al. (2004). Parkinsonian signs and substantia nigra neuron density in decedents elders without PD. *Ann. Neurol.* *56*, 532–539.

Rössler, R., Boddeke, E., and Copray, S. (2010). Differentiation of non-mesencephalic neural stem cells towards dopaminergic neurons. *Neuroscience* *170*, 417–428.

Rouaux, C., and Arlotta, P. (2013). Direct lineage reprogramming of post-mitotic callosal neurons into corticofugal neurons in vivo. *Nat. Cell Biol.* 15, 214–221.

Roybon, L., Hjalt, T., Christophersen, N.S., Li, J.-Y., and Brundin, P. (2008). Effects on differentiation of embryonic ventral midbrain progenitors by *Lmx1a*, *Msx1*, *Ng2*, and *Pitx3*. *J. Neurosci.* 28, 3644–3656.

Sacchetti, P., Mitchell, T.R., Granneman, J.G., and Bannon, M.J. (2001). *Nurr1* enhances transcription of the human dopamine transporter gene through a novel mechanism. *J. Neurochem.* 76, 1565–1572.

Salomon, B., Maury, S., and Loubiere, L. (1995). A truncated herpes simplex virus thymidine kinase phosphorylates thymidine and nucleoside analogs and does not cause sterility in transgenic mice. ... *Cell. Biol.* 15, 5322–5328.

Di Salvio, M., Di Giovannantonio, L.G., Acampora, D., Prosperi, R., Omodei, D., Prakash, N., Wurst, W., and Simeone, A. (2010). *Otx2* controls neuron subtype identity in ventral tegmental area and antagonizes vulnerability to MPTP. *Nat. Neurosci.* 13, 1481–1488.

Sánchez-Danés, a, Consiglio, a, Richaud, Y., Rodríguez-Pizà, I., Dehay, B., Edel, M., Bové, J., Memo, M., Vila, M., Raya, a, et al. (2012). Efficient generation of A9 midbrain dopaminergic neurons by lentiviral delivery of *LMX1A* in human embryonic stem cells and induced pluripotent stem cells. *Hum. Gene Ther.* 23, 56–69.

Saucedo-Cardenas, O., QUINTANA-HAU*, J.D., LE†, W.-D., SMIDT‡, M.P., COX‡, J.J., MAYO*, F. DE, BURBACH‡, J.P.H., and CONNEELY*, A.O.M. (1998). *Nurr1* is essential for the induction of the dopaminergic phenotype and the survival of ventral mesencephalic late dopaminergic precursor neurons. *Proc. ...* 95, 4013–4018.

Schimmang, T. (2013). Transcription factors that control inner ear development and their potential for transdifferentiation and reprogramming. *Hear. Res.* 297, 84–90.

Schlaeger, T.M., Daheron, L., Brickler, T.R., Entwisle, S., Chan, K., Cianci, A., DeVine, A., Ettenger, A., Fitzgerald, K., Godfrey, M., et al. (2014). A comparison of non-integrating reprogramming methods. *Nat. Biotechnol.*

Schröder, M., and Kaufman, R.J. (2005). ER stress and the unfolded protein response. *Mutat. Res.* 569, 29–63.

Seiler, A., Schneider, M., Förster, H., Roth, S., Wirth, E.K., Culmsee, C., Plesnila, N., Kremmer, E., Rådmark, O., Wurst, W., et al. (2008). Glutathione peroxidase 4 senses and translates oxidative stress into 12/15-lipoxygenase dependent- and AIF-mediated cell death. *Cell Metab.* 8, 237–248.

Sgadò, P., Albéri, L., Gherbassi, D., Galasso, S.L., Ramakers, G.M.J., Alavian, K.N., Smidt, M.P., Dyck, R.H., and Simon, H.H. (2006). Slow progressive degeneration of nigral dopaminergic neurons in postnatal *Engrailed* mutant mice. *Proc.*

Shao, L., Feng, W., Sun, Y., Bai, H., Liu, J., Currie, C., Kim, J., Gama, R., Wang, Z., Qian, Z., et al. (2009). Generation of iPS cells using defined factors linked via the self-cleaving 2A sequences in a single open reading frame. *Cell Res.* 19, 296–306.

Sheng, C., Zheng, Q., Wu, J., Xu, Z., Sang, L., Wang, L., Guo, C., Zhu, W., Tong, M., Liu, L., et al. (2012). Generation of dopaminergic neurons directly from mouse fibroblasts and fibroblast-derived neural progenitors. *Cell Res.* 22, 769–772.

Shenoy, A., and Blelloch, R. (2012). microRNA induced transdifferentiation. *F1000 Biol. Rep.* 4, 3.

Shiba-Fukushima, K., Inoshita, T., Hattori, N., and Imai, Y. (2014). PINK1-mediated phosphorylation of Parkin boosts Parkin activity in *Drosophila*. *PLoS Genet.* 10, e1004391.

Shilatifard, A. (2006). Chromatin modifications by methylation and ubiquitination: implications in the regulation of gene expression. *Annu. Rev. Biochem.* 75, 243–269.

Shim, J.-W., Park, C.-H., Bae, Y.-C., Bae, J.-Y., Chung, S., Chang, M.-Y., Koh, H.-C., Lee, H.-S., Hwang, S.-J., Lee, K.-H., et al. (2007). Generation of functional dopamine neurons from neural precursor cells isolated from the subventricular zone and white matter of the adult rat brain using Nurr1 overexpression. *Stem Cells* 25, 1252–1262.

Simeone, A., Di Salvio, M., Di Giovannantonio, L.G., Acampora, D., Omodei, D., and Tomasetti, C. (2011). The role of otx2 in adult mesencephalic-diencephalic dopaminergic neurons. *Mol. Neurobiol.* 43, 107–113.

Simon, H., and Saueressig, H. (2001). Fate of midbrain dopaminergic neurons controlled by the engrailed genes. *J. ...* 21, 3126–3134.

Smidt, M., Asbreuk, C., and Cox, J. (2000). A second independent pathway for development of mesencephalic dopaminergic neurons requires Lmx1b. *Nat. ...* 16, 337–341.

Smith, D.L., Woodman, B., Mahal, A., Sathasivam, K., Ghazi-Noori, S., Lowden, P. a S., Bates, G.P., and Hockly, E. (2003). Minocycline and doxycycline are not beneficial in a model of Huntington's disease. *Ann. Neurol.* 54, 186–196.

Son, E.Y., Ichida, J.K., Wainger, B.J., Toma, J.S., Rafuse, V.F., Wolf, C.J., and Eggan, K. (2011). Conversion of mouse and human fibroblasts into functional spinal motor neurons. *Cell Stem Cell* 9, 205–218.

Sonnier, L., Le Pen, G., Hartmann, A., Bizot, J.-C., Trovero, F., Krebs, M.-O., and Prochiantz, A. (2007). Progressive loss of dopaminergic neurons in the ventral midbrain of adult mice heterozygote for Engrailed1. *J. Neurosci.* 27, 1063–1071.

Literature

Soriano, P. (1999). Generalized lacZ expression with the ROSA26 Cre reporter strain. *Nat. Genet.* 21, 70–71.

Spillantini, M., Schmidt, M., and Lee, V. (1997). α -Synuclein in Lewy bodies. *Nature* 839–840.

Stanslowsky, N., Haase, A., Martin, U., Naujock, M., Leffler, A., Dengler, R., and Wegner, F. (2014). Functional differentiation of midbrain neurons from human cord blood-derived induced pluripotent stem cells. *Stem Cell Res. Ther.* 5, 35.

Stayte, S., and Vissel, B. (2014). Advances in non-dopaminergic treatments for Parkinson's disease. *Front. Neurosci.* 8, 113.

Stott, S.R.W., Metzakopian, E., Lin, W., Kaestner, K.H., Hen, R., and Ang, S.-L. (2013). *Foxa1* and *foxa2* are required for the maintenance of dopaminergic properties in ventral midbrain neurons at late embryonic stages. *J. Neurosci.* 33, 8022–8034.

Studer, L., Csete, M., Lee, S.H., Kabbani, N., Walikonis, J., Wold, B., and McKay, R. (2000). Enhanced proliferation, survival, and dopaminergic differentiation of CNS precursors in lowered oxygen. *J. Neurosci.* 20, 7377–7383.

Su, Z., Niu, W., Liu, M.-L., Zou, Y., and Zhang, C.-L. (2014). In vivo conversion of astrocytes to neurons in the injured adult spinal cord. *Nat. Commun.* 5, 3338.

Sun, X., Fu, X., Han, W., Zhao, Y., and Liu, H. (2010). Can controlled cellular reprogramming be achieved using microRNAs? *Ageing Res. Rev.* 9, 475–483.

Sundberg, M., Bogetofte, H., and Lawson, T. (2013). Improved Cell Therapy Protocols for Parkinson's Disease Based on Differentiation Efficiency and Safety of hESC-, hiPSC-, and Non-Human Primate iPSC-. ... *Cells* 1548–1562.

Swistowski, A., Peng, J., Liu, Q., Mali, P., Rao, M.S., Cheng, L., and Zeng, X. (2010). Efficient generation of functional dopaminergic neurons from human induced pluripotent stem cells under defined conditions. *Stem Cells* 28, 1893–1904.

Takagi, Y., Takahashi, J., Saiki, H., Morizane, A., Hayashi, T., Kishi, Y., Fukuda, H., Okamoto, Y., Koyanagi, M., Ideguchi, M., et al. (2005). Dopaminergic neurons generated from monkey embryonic stem cells function in a Parkinson primate model. *J. Clin. Invest.* 115, 102–109.

Tarazi, F.I., Sahli, Z.T., Wolny, M., and Mousa, S. a (2014). Emerging therapies for Parkinson's disease: From bench to bedside. *Pharmacol. Ther.*

Tate, P.H., and Bird, A.P. (1993). Effects of DNA methylation on DNA-binding proteins and gene expression. *Curr. Opin. Genet. Dev.* 3, 226–231.

Tchorz, J.S., Suply, T., Ksiazek, I., Giachino, C., Cloëtta, D., Danzer, C.-P., Doll, T., Isken, A., Lemaistre, M., Taylor, V., et al. (2012). A modified RMCE-compatible Rosa26 locus for the expression of transgenes from exogenous promoters. *PLoS One* 7, e30011.

Theka, I., Caiazzo, M., and Dvoretzkova, E. (2013). Rapid generation of functional dopaminergic neurons from human induced pluripotent stem cells through a single-step procedure using cell lineage. *Stem Cells Transl. ...* 1, 473–479.

Thier, M., Wörsdörfer, P., Lakes, Y.B., Gorris, R., Herms, S., Opitz, T., Seiferling, D., Quandel, T., Hoffmann, P., Nöthen, M.M., et al. (2012). Direct conversion of fibroblasts into stably expandable neural stem cells. *Cell Stem Cell* 10, 473–479.

Tian, C., Wang, Y., Sun, L., Ma, K., and Zheng, J. (2011). Reprogrammed mouse astrocytes retain a “memory” of tissue origin and possess more tendencies for neuronal differentiation than reprogrammed mouse embryonic. *Protein Cell* 2, 128–140.

Toledo, F., Liu, C.-W., Lee, C.J., and Wahl, G.M. (2006). RMCE-ASAP: a gene targeting method for ES and somatic cells to accelerate phenotype analyses. *Nucleic Acids Res.* *34*, e92.

Torper, O., Pfisterer, U., Wolf, D. a, Pereira, M., Lau, S., Jakobsson, J., Björklund, A., Grealish, S., and Parmar, M. (2013). Generation of induced neurons via direct conversion in vivo. *Proc. Natl. Acad. Sci. U. S. A.* *110*, 7038–7043.

Tronche, F., Kellendonk, C., Kretz, O., Gass, P., Anlag, K., Orban, P.C., Bock, R., Klein, R., and Schütz, G. (1999). Disruption of the glucocorticoid receptor gene in the nervous system results in reduced anxiety. *Nat. Genet.* *23*, 99–103.

Turan, S., Zehe, C., Kuehle, J., Qiao, J., and Bode, J. (2013). Recombinase-mediated cassette exchange (RMCE) - a rapidly-expanding toolbox for targeted genomic modifications. *Gene* *515*, 1–27.

Ueno, T., Tomita, J., Tanimoto, H., Endo, K., Ito, K., Kume, S., and Kume, K. (2012). Identification of a dopamine pathway that regulates sleep and arousal in *Drosophila*. *Nat. Neurosci.* *15*, 1516–1523.

Varlakhanova, N., Cotterman, R., Wilhelmine N. deVries, Morgan, J., Donahue, L.R., Murray, S., Knowles, B.B., and Knoepfler, P. (2010). *myc* maintains embryonic stem cell pluripotency and self-renewal. *Differentiation* *80*, 9–19.

Veenvliet, J. V, Dos Santos, M.T.M.A., Kouwenhoven, W.M., von Oerthel, L., Lim, J.L., van der Linden, A.J. a, Koerkamp, M.J. a G., Holstege, F.C.P., and Smidt, M.P. (2013). Specification of dopaminergic subsets involves interplay of *En1* and *Pitx3*. *Development* *140*, 3373–3384.

Vernay, B., Koch, M., Vaccarino, F., Briscoe, J., Simeone, A., Kageyama, R., and Ang, S.-L. (2005). *Otx2* regulates subtype specification and neurogenesis in the midbrain. *J. Neurosci.* *25*, 4856–4867.

Verrou, C., Zhang, Y., Zürn, C., Schamel, W.W., and Reth, M. (1999). Comparison of the tamoxifen regulated chimeric Cre recombinases MerCreMer and CreMer. *Biol. Chem.* 380, 1435–1438.

Victor, M.B., Richner, M., Hermansteyne, T.O., Ransdell, J.L., Sobieski, C., Deng, P.-Y., Klyachko, V.A., Nerbonne, J.M., and Yoo, A.S. (2014). Generation of Human Striatal Neurons by MicroRNA-Dependent Direct Conversion of Fibroblasts. *Neuron* 84, 311–323.

Vierbuchen, T., Ostermeier, A., Pang, Z.P., Kokubu, Y., Südhof, T.C., and Wernig, M. (2010). Direct conversion of fibroblasts to functional neurons by defined factors. *Nature* 463, 1035–1041.

Wang, X., and Michaelis, E.K. (2010). Selective neuronal vulnerability to oxidative stress in the brain. *Front. Aging Neurosci.* 2, 12.

Wernig, M., Tucker, K.L., Gornik, V., Schneiders, A., Buschwald, R., Wiestler, O.D., Barde, Y.-A., and Brüstle, O. (2002). Tau EGFP embryonic stem cells: an efficient tool for neuronal lineage selection and transplantation. *J. Neurosci. Res.* 69, 918–924.

Wilson, B.E., Mochon, E., and Boxer, L.M. (1996). Induction of bcl -2 Expression by Phosphorylated CREB Proteins during B-Cell Activation and Rescue from Apoptosis. *Mol. Cell. Biol.* 16, 5546–5556.

Wislet-Gendebien, S., Leprince, P., Moonen, G., and Rogister, B. (2003). Regulation of neural markers nestin and GFAP expression by cultivated bone marrow stromal cells. *J. Cell Sci.* 116, 3295–3302.

Witta, J., Baffi, J.S., Palkovits, M., Mezey, É., Castillo, S.O., and Nikodem, V.M. (2000). Nigrostriatal innervation is preserved in Nurr1-null mice, although dopaminergic neuron precursors are arrested from terminal differentiation. *Mol. Brain Res.* 84, 67–78.

Wong, E.T., Kolman, J.L., Li, Y.C., Mesner, L.D., Hillen, W., Berens, C., and Wahl, G.M. (2005). Reproducible doxycycline-inducible transgene expression

at specific loci generated by Cre-recombinase mediated cassette exchange. *Nucleic Acids Res.* *33*, 1–13.

Woods, N., Muessig, A., Schmidt, M., Flygare, J., Olsson, K., Salmon, P., Trono, D., Kalle, C. von, and Karlsson, S. (2003). Lentiviral vector transduction of NOD/SCID repopulating cells results in multiple vector integrations per transduced cell: risk of insertional mutagenesis. *Gene Ther.* *101*, 1284–1289.

Wu, J., and Kaufman, R.J. (2006). From acute ER stress to physiological roles of the Unfolded Protein Response. *Cell Death Differ.* *13*, 374–384.

Wurst, W., Auerbach, A., and Joyner, A. (1994). Multiple developmental defects in *Engrailed-1* mutant mice: an early mid-hindbrain deletion and patterning defects in forelimbs and sternum. *Development* *2075*, 2065–2075.

Xu, C., Bailly-maitre, B., and Reed, J.C. (2005). Endoplasmic reticulum stress : cell life and death decisions. *J. Clin. Invest.* *115*.

Xue, Y., Ouyang, K., Huang, J., Zhou, Y., Ouyang, H., Li, H., Wang, G., Wu, Q., Wei, C., Bi, Y., et al. (2013). Direct conversion of fibroblasts to neurons by reprogramming PTB-regulated microRNA circuits. *Cell* *152*, 82–96.

Yan, C.H., Levesque, M., Claxton, S., Johnson, R.L., and Ang, S.-L. (2011). *Lmx1a* and *Lmx1b* function cooperatively to regulate proliferation, specification, and differentiation of midbrain dopaminergic progenitors. *J. Neurosci.* *31*, 12413–12425.

Yan, Y., Yang, D., Zarnowska, E.D., Du, Z., Werbel, B., Valliere, C., Pearce, R. a, Thomson, J. a, and Zhang, S.-C. (2005). Directed differentiation of dopaminergic neuronal subtypes from human embryonic stem cells. *Stem Cells* *23*, 781–790.

Yang, F., Liu, Y., Tu, J., Wan, J., Zhang, J., Wu, B., Chen, S., Zhou, J., Mu, Y., and Wang, L. (2014). Activated astrocytes enhance the dopaminergic

differentiation of stem cells and promote brain repair through bFGF. *Nat. Commun.* 5, 1–14.

Ying, Q.-L., Stavridis, M., Griffiths, D., Li, M., and Smith, A. (2003). Conversion of embryonic stem cells into neuroectodermal precursors in adherent monoculture. *Nat. Biotechnol.* 21, 183–186.

Yoo, A.S., Sun, A.X., Li, L., Shcheglovitov, A., Portmann, T., Li, Y., Lee-Messer, C., Dolmetsch, R.E., Tsien, R.W., and Crabtree, G.R. (2011). MicroRNA-mediated conversion of human fibroblasts to neurons. *Nature* 476, 228–231.

Yoshikawa, T., Samata, B., Ogura, A., Miyamoto, S., and Takahashi, J. (2013). Systemic administration of valproic acid and zonisamide promotes differentiation of induced pluripotent stem cell-derived dopaminergic neurons. *Front. Cell. Neurosci.* 7, 11.

Young, A.B. (2009). Four decades of neurodegenerative disease research: how far we have come! *J. Neurosci.* 29, 12722–12728.

Yu, P.B., Hong, C.C., Sachidanandan, C., Babitt, J.L., Donna, Y., Hoynig, S.A., Lin, H.Y., Bloch, K.D., and Peterson, R.T. (2009). Dorsomorphin inhibits BMP signals required for embryogenesis and iron metabolism. *Nat. Chem. Biol.* 4, 33–41.

Yuan, L.W., and Gambée, J.E. (2001). Histone acetylation by p300 is involved in CREB-mediated transcription on chromatin. *Biochim. Biophys. Acta - Mol. Cell Res.* 1541, 161–169.

Yue, F., Cui, L., Johkura, K., Ogiwara, N., and Sasaki, K. (2006). Induction of midbrain dopaminergic neurons from primate embryonic stem cells by coculture with sertoli cells. *Stem Cells* 24, 1695–1706.

Zeng, X., Cai, J., Chen, J., Luo, Y., and You, Z. (2004). Dopaminergic differentiation of human embryonic stem cells. *Stem ...* 925–940.

Literature

Zetoune, A.B., Fontanière, S., Magnin, D., Anczuków, O., Buisson, M., Zhang, C.X., and Mazoyer, S. (2008). Comparison of nonsense-mediated mRNA decay efficiency in various murine tissues. *BMC Genet.* 9, 83.

Zetterström, R., Solomin, L., Jansson, L., Hoffer, B.J., Olson, L., and Perlmann, T. (1997). Dopamine Neuron Agenesis in Nurr1-Deficient Mice. *Science* (80-). 276, 248–250.

Zhang, X.-B. (2013). Cellular reprogramming of human peripheral blood cells. *Genomics. Proteomics Bioinformatics* 11, 264–274.

Zhang, X.-Q., and Su-Chun, Z. and (2010). Differentiation of Neural Precursors and Dopaminergic Neurons from Human Embryonic Stem Cells. *Methods Mol Biol.* 584, 1–9.

Zhang, F., Gradinaru, V., Adamantidis, A.R., Durand, R., Airan, R.D., de Lecea, L., and Deisseroth, K. (2010). Optogenetic interrogation of neural circuits: technology for probing mammalian brain structures. *Nat. Protoc.* 5, 439–456.

Zhao, P., Luo, Z., Tian, W., Yang, J., Ibáñez, D.P., Huang, Z., Tortorella, M.D., Esteban, M. a, and Fan, W. (2014). Solving the puzzle of Parkinson's disease using induced pluripotent stem cells. *Exp. Biol. Med. (Maywood).* 239, 1421–1432.

Zhao, T., Zhang, Z.-N., Rong, Z., and Xu, Y. (2011). Immunogenicity of induced pluripotent stem cells. *Nature* 474, 212–215.

Zheng, K., Heydari, B., and Simon, D. (2003). A common NURR1 polymorphism associated with Parkinson disease and diffuse Lewy body disease. *Arch. Neurol.* 60, 11–14.

Zweigerdt, R., Burg, M., Willbold, E., Abts, H., and Ruediger, M. (2003). Generation of confluent cardiomyocyte monolayers derived from embryonic stem cells in suspension: a cell source for new therapies and screening strategies. *Cytotherapy* 5, 399–413.

8. Acknowledgements

This study was performed during 2010-2014 in Helmholtz Zentrum München.

Many people contributed in achieving the successful completion of this study. First and foremost, I would like to thank Prof. Dr. Wolfgang Wurst for giving me the opportunity to do my PhD at the institute of Developmental Genetics, which he is directing. I would also like to express my gratitude for his support and trust during our close collaboration and his willingness to assist me towards achieving my goals.

Next, I would like to thank Dr. Joel Schick for trusting me for the PhD position, as well as for interesting scientific discussions throughout all these years and critical reading of the current Thesis.

Special thanks to my Thesis Committee members, Prof. Dr. Magdalena Götz, Dr. Andrea Huber-Brösamle and Dr. Marcus Conrad for valuable feedback and very fruitful discussions. Thank you to all the members of the reprogramming team. I would like to specifically thank Prof. Dr. Magdalena Götz and Elisa Murenu for the helpful and friendly interaction during our common meetings and for the excellent collaboration during the stab wound experiment. Also, thanks to Dr. Giacomo Masserdotti for providing the *Tnap*^{TgCreERT2/+} mouse line.

I would like to express my gratitude to Dr. Nilima Prakash for always being so friendly and available for discussions, as well as for considerable scientific and spiritual support. Also, many thanks to Dr. Ralf Kühn for our frequent meetings and for critical feedback. I would also like to thank him and his team, Adrienne, Susi and Heidi for the blastocyst injections. Thanks also to Dr. Daniela Vogt-Weisenhorn for inspiring discussions and her critical feedback.

Many thanks to all the lab members, Susi, Basti, Kati, Irina, Lena, Manuel, Marc, Pedro, Bettina for creating a very pleasant and friendly environment in and out of the lab and for technical support from Susi who also

Acknowledgements

contributed in some technical aspects of the current study. Being part of such an interactive team contributed in converting difficulties into motivation. Also many thanks to Michi, who was always available to answer my questions regarding official matters.

Last but not least, I would like to express my gratitude to Konstantinos, for believing in me and whose patience, support and understanding kept me going throughout all these years and of course to my family without whose support and trust I wouldn't be standing in that position.